Traitement et analyse d'images IRM de diffusion pour l'estimation de l'architecture locale des tissus

Haz-Edine Assemlal

GREYC (CNRS UMR 6072), ÉQUIPE IMAGE, CAEN, FRANCE

Le 11 janvier 2010

Directeur de thèse : Luc Brun
Co-directeur de thèse : David Tschumperlé

Diffusion Magnetic Resonance Imaging

Figure: 3 Tesla MRI scanner.

Diffusion MRI: Brownian Motion

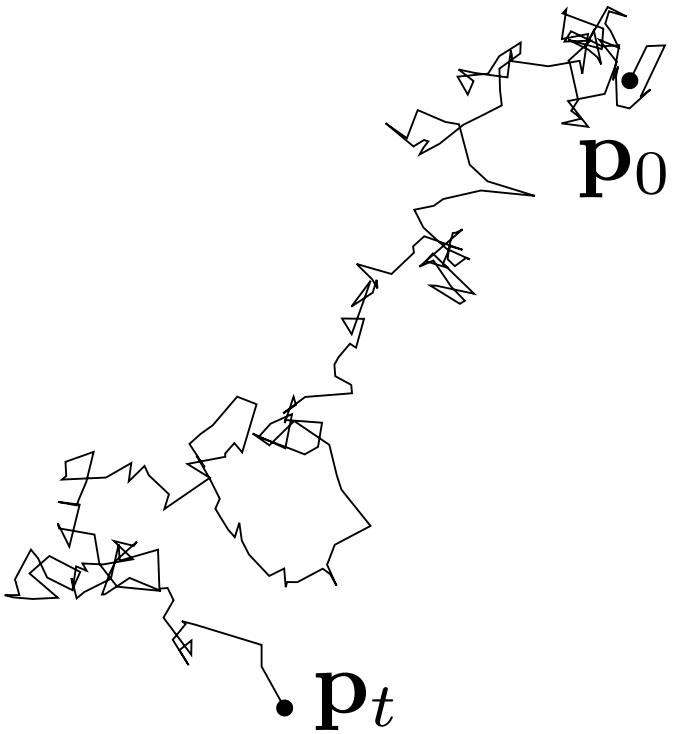

Figure: Brownian motion of water molecules.

Diffusion MRI: Brownian Motion

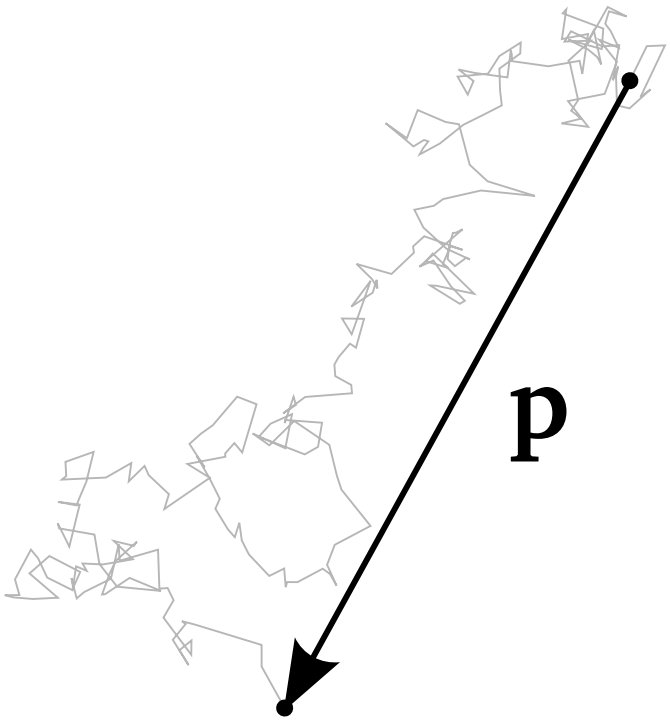

Figure: Diffusion: displacement during a time t.

Diffusion MRI: Brownian Motion

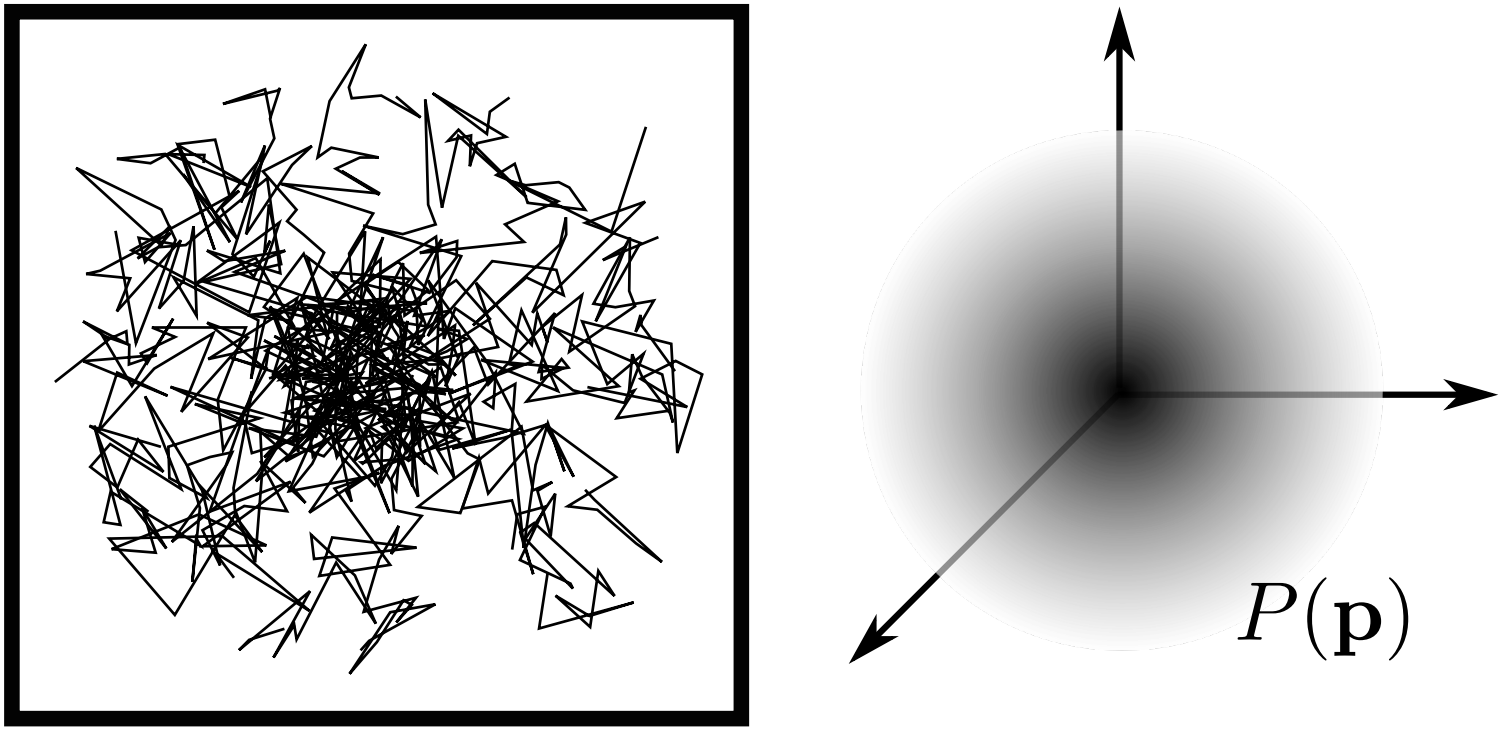

Figure: Free diffusion and its PDF [Einstein05].

Diffusion MRI: Brownian Motion

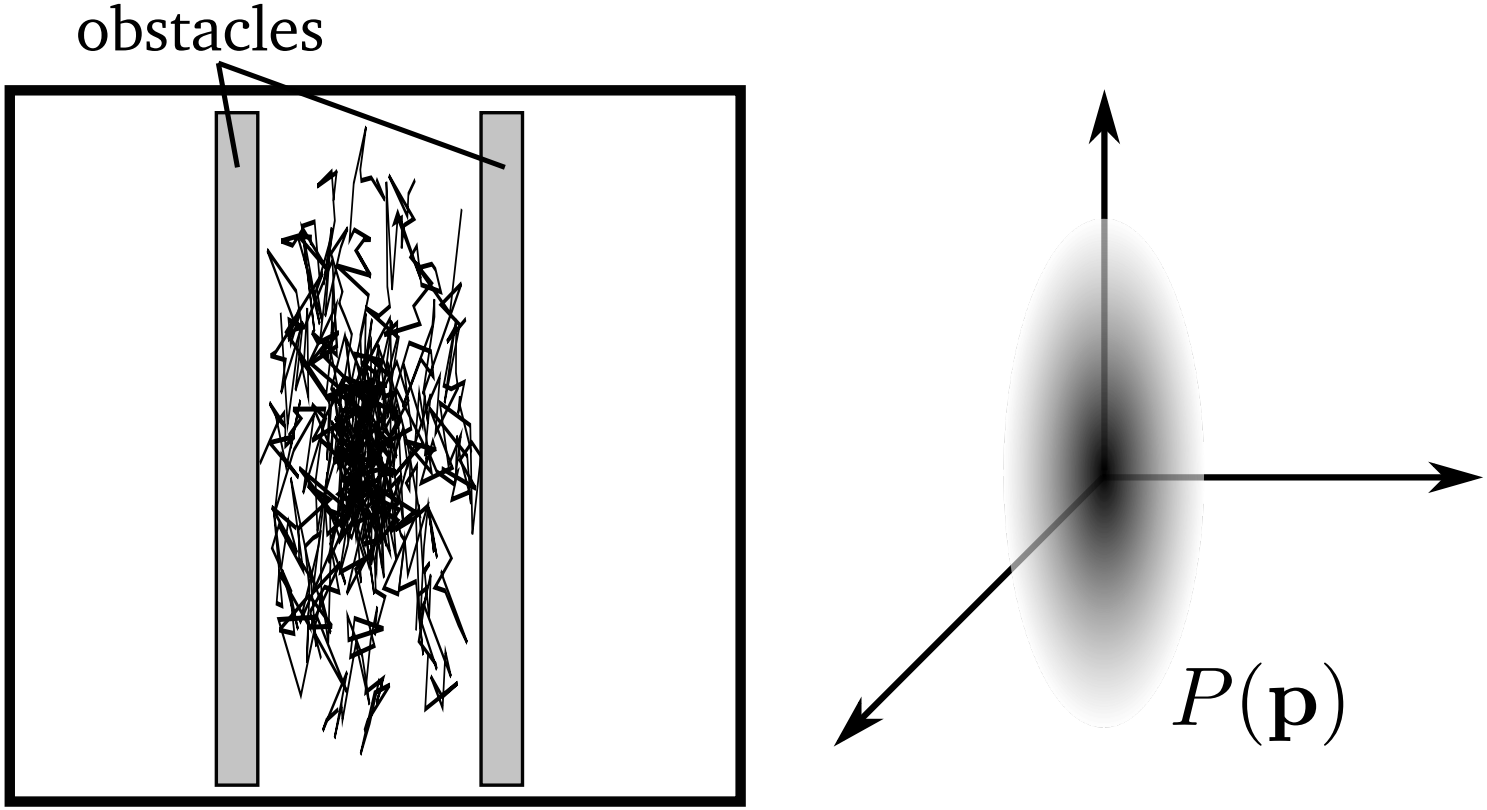

Figure: Restricted diffusion and its PDF [Lebihan85].

Diffusion MRI: Brownian Motion

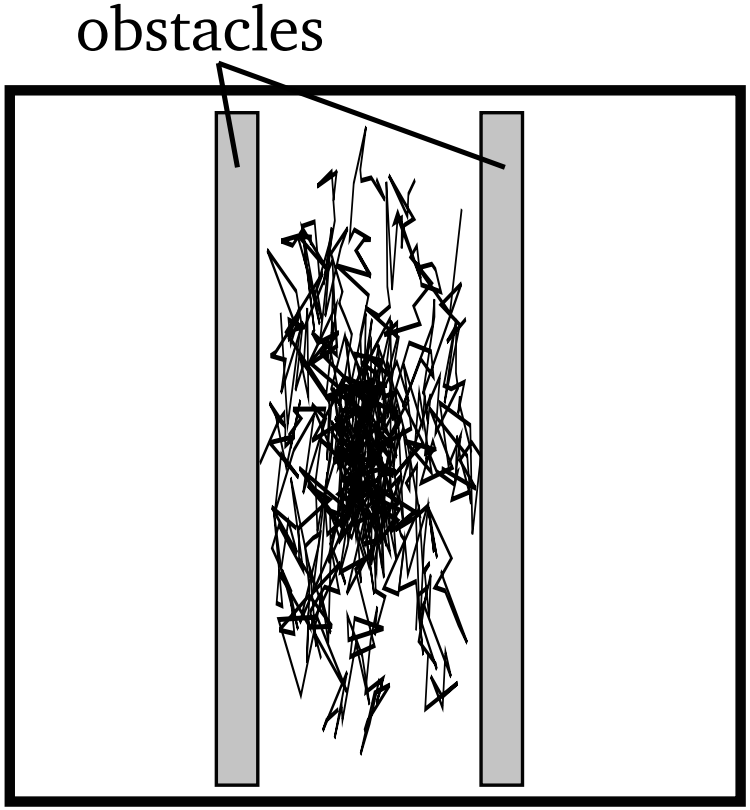

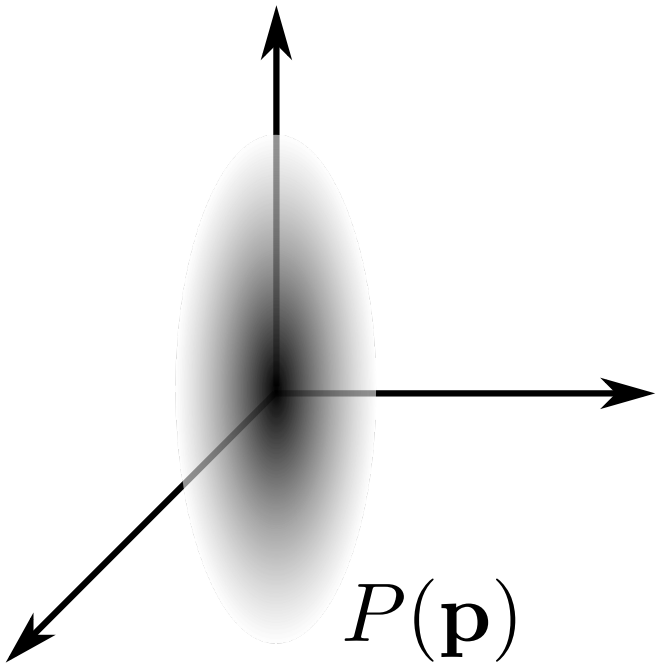

Figure: Restricted diffusion and its PDF [Lebihan

Diffusion image definition

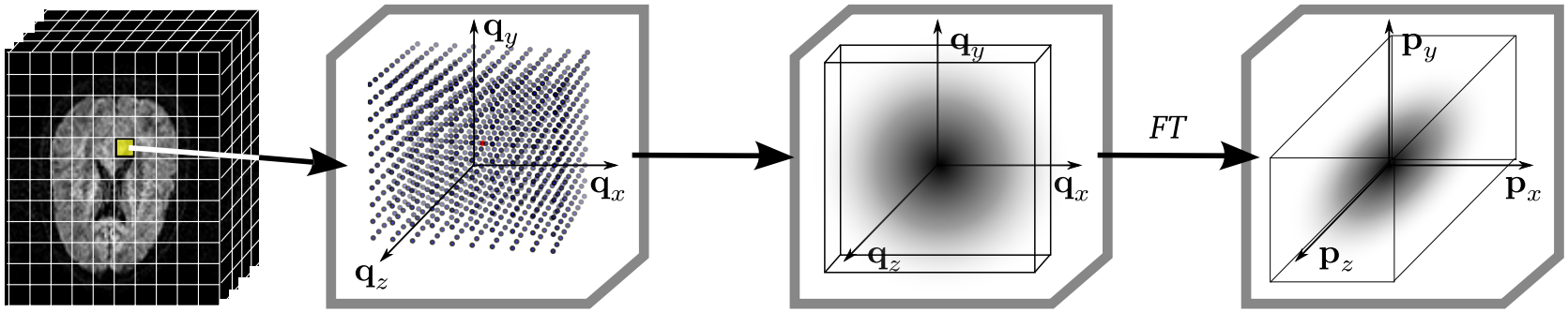

a) diffusion MRI of brain

b) q-space sampling

c) Approximation of diffusion profile E

d) Computation of diffusion propagator P

Diffusion image definition

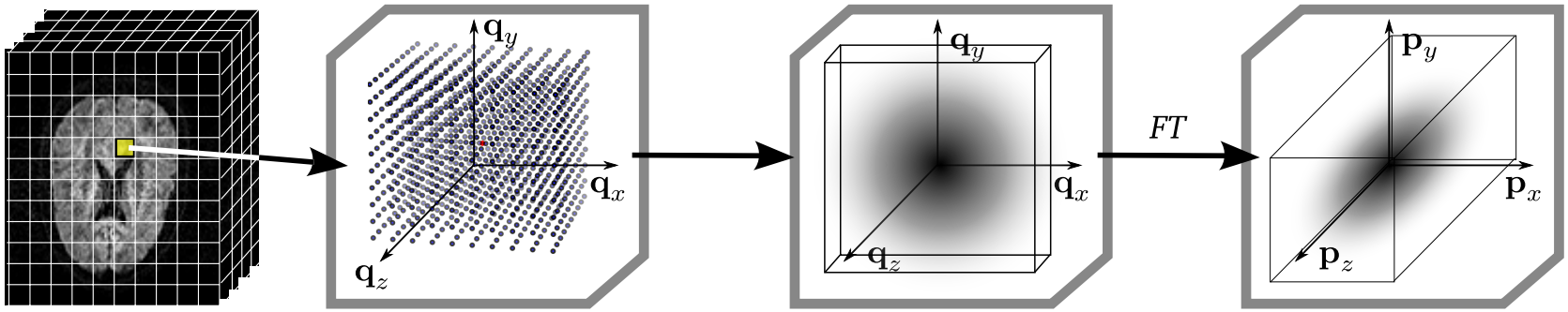

a) diffusion MRI of brain

b) q-space sampling

c) Approximation of diffusion profile E

d) Computation of diffusion propagator P

We define the acquired diffusion image as:

$$E : \left| \begin{array}{l} \Omega_x \times \Omega_q \rightarrow \mathbb{R} \\ (\mathbf{x}, \mathbf{q}) \rightarrow E(\mathbf{x}, \mathbf{q}) \end{array} \right.$$

Diffusion image definition

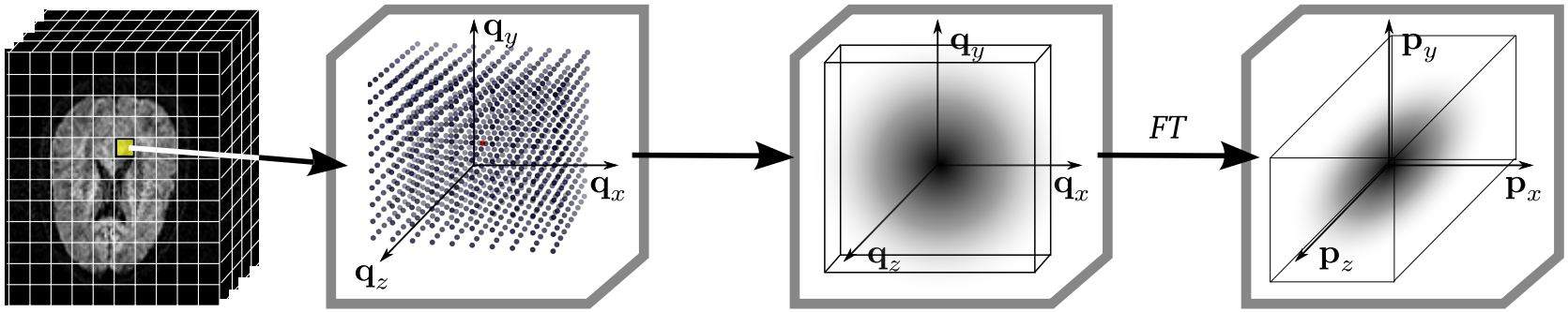

a) diffusion MRI of brain

b) q-space sampling

c) Approximation of diffusion profile E

d) Computation of diffusion propagator P

We define the acquired diffusion image as:

$$E : \left| \begin{array}{l} \Omega_x \times \Omega_q \rightarrow \mathbb{R} \\ (\mathbf{x}, \mathbf{q}) \rightarrow E(\mathbf{x}, \mathbf{q}) \end{array} \right.$$

The objective is to compute the diffusion PDF:

$$P : \left| \begin{array}{l} \Omega_x \times \Omega_p \rightarrow \mathbb{R} \\ (\mathbf{x}, \mathbf{p}) \rightarrow P(\mathbf{x}, \mathbf{p}) \end{array} \right.$$

Complete diffusion sampling

Diffusion Spectrum Imaging (DSI) - Fourier transform [Wedeen00]

$$P(\mathbf{p}) = \int_{\mathbf{q}} E(\mathbf{q}) \exp(-2\pi i \mathbf{q}^T \mathbf{p}) d\mathbf{q}$$

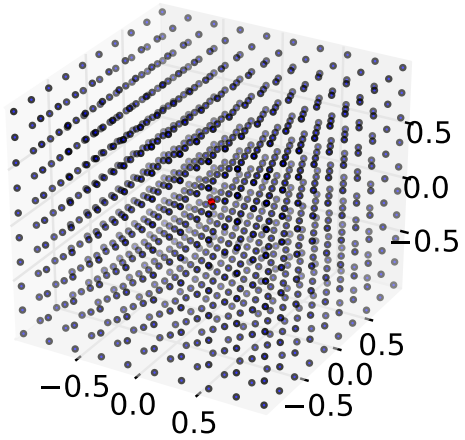

q-space sampling

Complete diffusion sampling

Diffusion Spectrum Imaging (DSI) - Fourier transform [Wedeen00]

$$P(\mathbf{p}) = \int_{\mathbf{q}} E(\mathbf{q}) \exp(-2\pi i \mathbf{q}^T \mathbf{p}) d\mathbf{q}$$

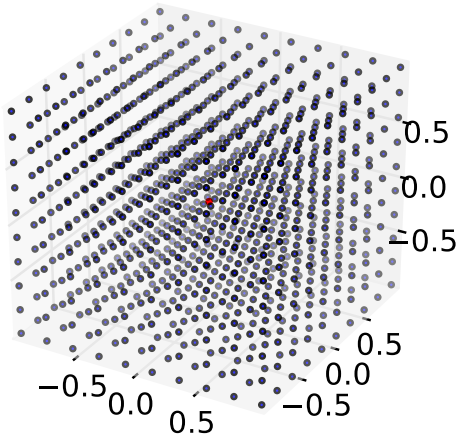

q-space sampling

Gaussian isotropic

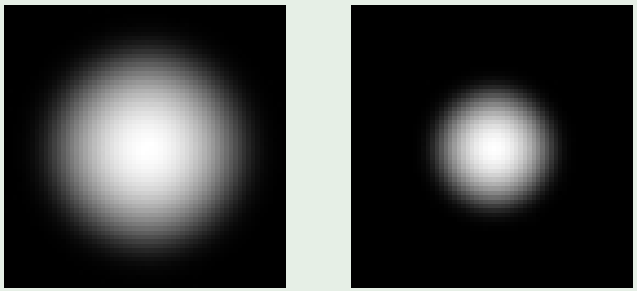

E P

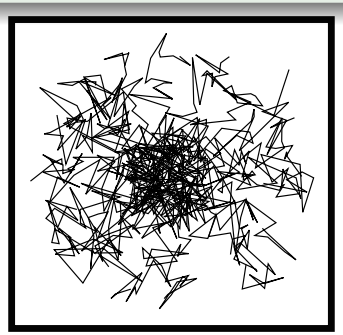

Complete diffusion sampling

Diffusion Spectrum Imaging (DSI) - Fourier transform [Wedeen00]

$$P(\mathbf{p}) = \int_{\mathbf{q}} E(\mathbf{q}) \exp(-2\pi i \mathbf{q}^T \mathbf{p}) d\mathbf{q}$$

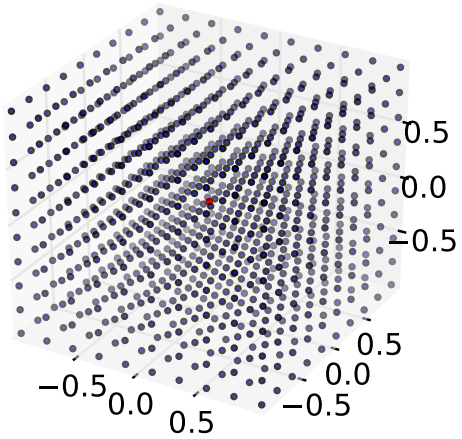

q-space sampling

Gaussian anisotropic

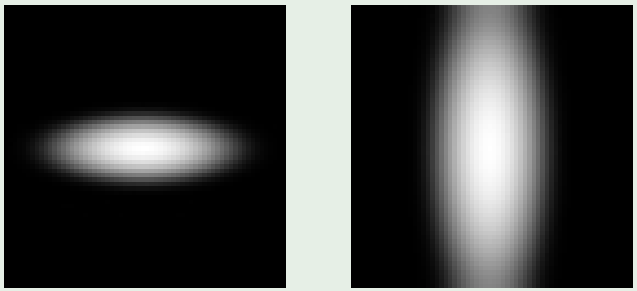

E P

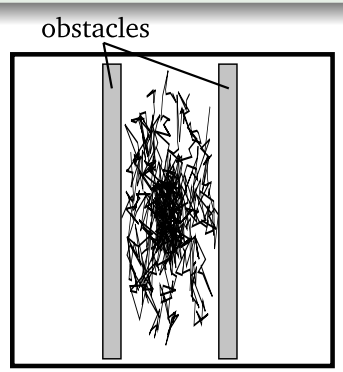

Complete diffusion sampling

Diffusion Spectrum Imaging (DSI) - Fourier transform [Wedeen00]

$$P(\mathbf{p}) = \int_{\mathbf{q}} E(\mathbf{q}) \exp(-2\pi i \mathbf{q}^T \mathbf{p}) d\mathbf{q}$$

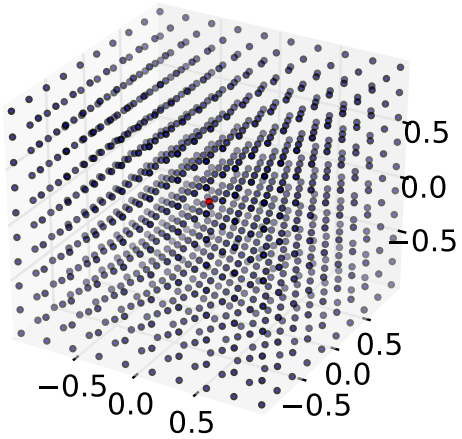

q-space sampling

Non-Gaussian angular

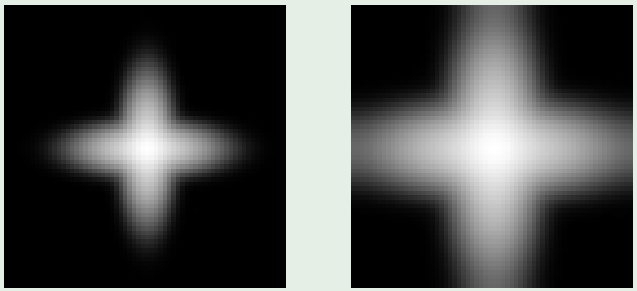

E P

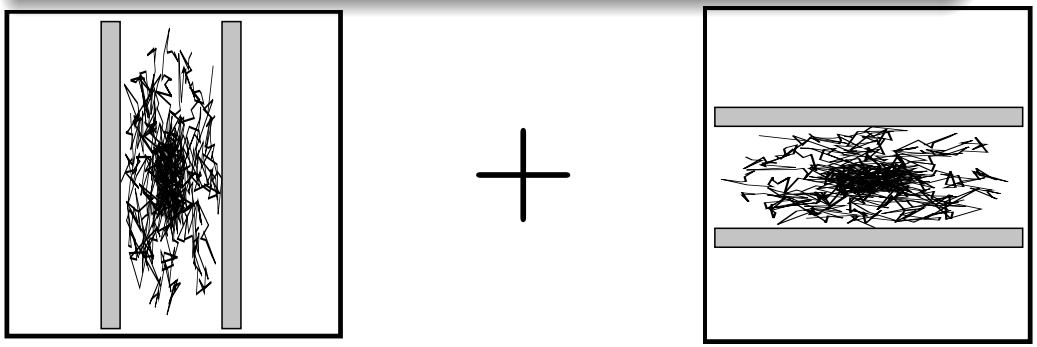

Complete diffusion sampling

Diffusion Spectrum Imaging (DSI) - Fourier transform [Wedeen00]

$$P(\mathbf{p}) = \int_{\mathbf{q}} E(\mathbf{q}) \exp(-2\pi i \mathbf{q}^T \mathbf{p}) d\mathbf{q}$$

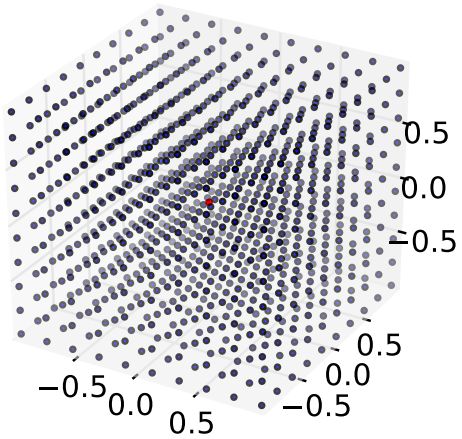

q-space sampling

Non-Gaussian radial

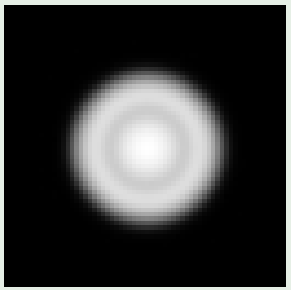

E

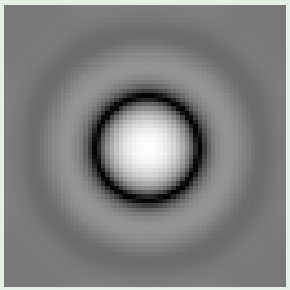

P

Complete diffusion sampling

Diffusion Spectrum Imaging (DSI) - Fourier transform [Wedeen00]

$$P(\mathbf{p}) = \int_{\mathbf{q}} E(\mathbf{q}) \exp(-2\pi i \mathbf{q}^T \mathbf{p}) d\mathbf{q}$$

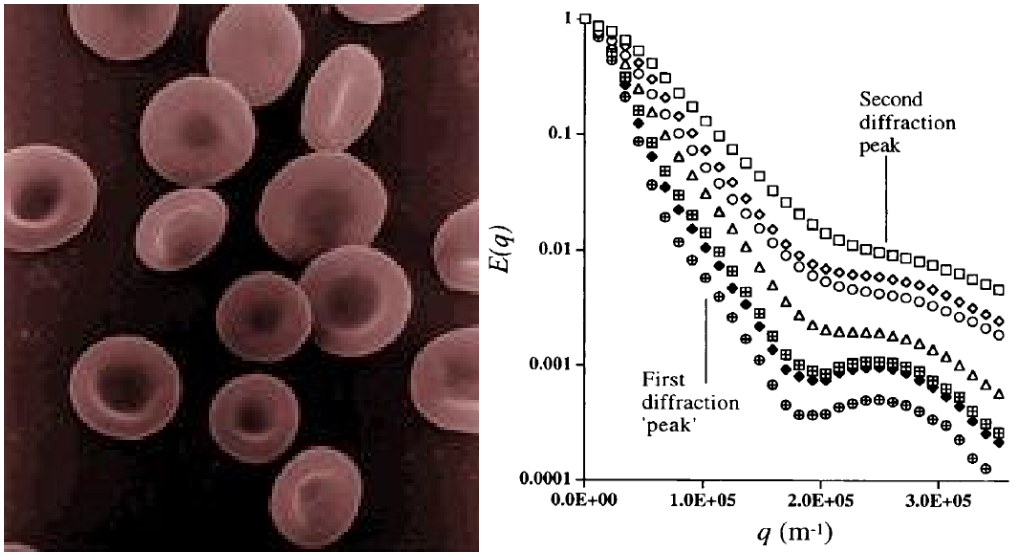

Figure: Human erythocytes rate for decreasing values of hematocrites [Kuchel97]. Observed in the human brain [Niendorf96].

Non-Gaussian radial

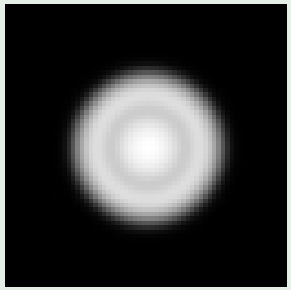

E

Complete diffusion sampling

Diffusion Spectrum Imaging (DSI) - Fourier transform [Wedeen00]

$$P(\mathbf{p}) = \int_{\mathbf{q}} E(\mathbf{q}) \exp(-2\pi i \mathbf{q}^T \mathbf{p}) d\mathbf{q}$$

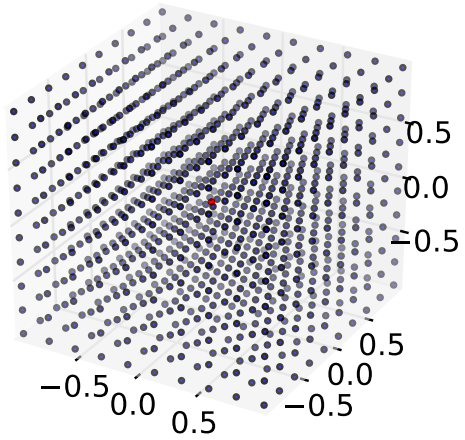

q-space sampling

Pro

- ☺ Complete diffusion (angular and radial profile)
- ☺ No *a priori* on the signal

Cons

- ☹ Very long acquisition time
- ☹ High gradients lead to magnetic field distortion

Low Angular Resolution Diffusion Imaging

Diffusion Tensor Imaging (DTI) - Gaussian assumption [Basser94]

$$E(\mathbf{q}) = \exp(-\mathbf{q}^{\mathrm{T}}\mathbf{D}\mathbf{q}) \quad \Rightarrow \quad P(\mathbf{p}) = \frac{1}{(|\mathbf{D}|(4\pi\tau)^3)^{1/2}} \exp\left(-\frac{\mathbf{p}^{\mathrm{T}}\mathbf{D}^{-1}\mathbf{p}}{4\tau}\right)$$

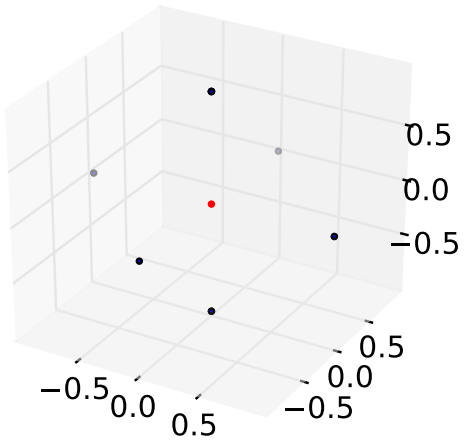

q-space sampling

Low Angular Resolution Diffusion Imaging

Diffusion Tensor Imaging (DTI) - Gaussian assumption [Basser94]

$$E(\mathbf{q}) = \exp(-\mathbf{q}^{\mathrm{T}}\mathbf{D}\mathbf{q}) \quad \Rightarrow \quad P(\mathbf{p}) = \frac{1}{(|\mathbf{D}|(4\pi\tau)^3)^{1/2}} \exp\left(-\frac{\mathbf{p}^{\mathrm{T}}\mathbf{D}^{-1}\mathbf{p}}{4\tau}\right)$$

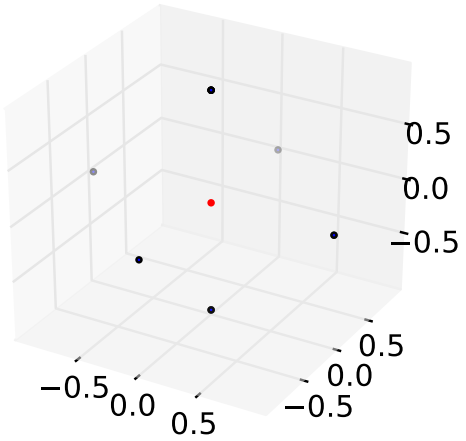

q-space sampling

Gaussian isotropic

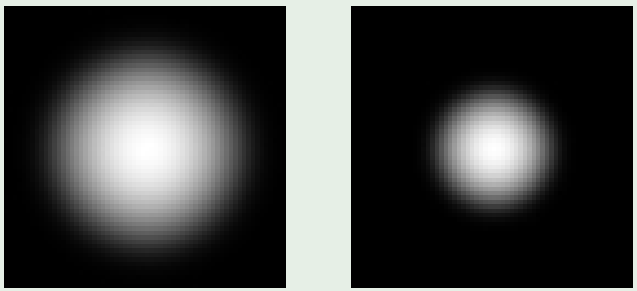

E P

Low Angular Resolution Diffusion Imaging

Diffusion Tensor Imaging (DTI) - Gaussian assumption [Basser94]

$$E(\mathbf{q}) = \exp(-\mathbf{q}^{\mathrm{T}}\mathbf{D}\mathbf{q}) \quad \Rightarrow \quad P(\mathbf{p}) = \frac{1}{(|\mathbf{D}|(4\pi\tau)^3)^{1/2}} \exp\left(-\frac{\mathbf{p}^{\mathrm{T}}\mathbf{D}^{-1}\mathbf{p}}{4\tau}\right)$$

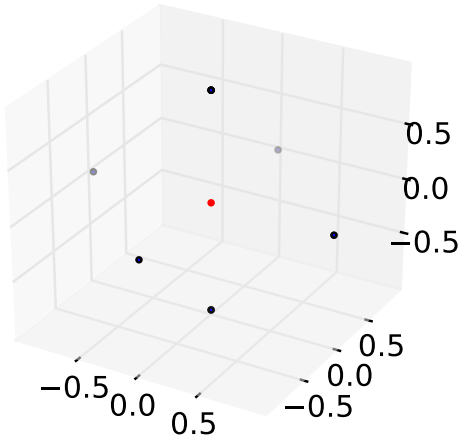

q-space sampling

Gaussian anisotropic

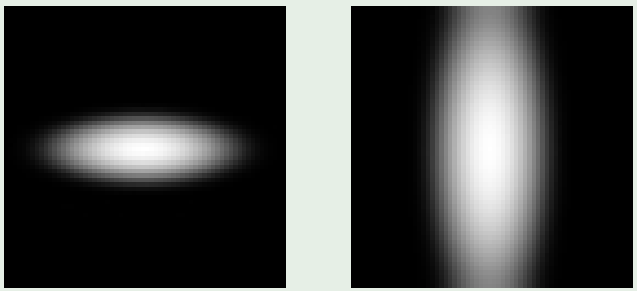

E P

Low Angular Resolution Diffusion Imaging

Diffusion Tensor Imaging (DTI) - Gaussian assumption [Basser94]

$$E(\mathbf{q}) = \exp(-\mathbf{q}^{\mathrm{T}}\mathbf{D}\mathbf{q}) \quad \Rightarrow \quad P(\mathbf{p}) = \frac{1}{(|\mathbf{D}|(4\pi\tau)^3)^{1/2}} \exp\left(-\frac{\mathbf{p}^{\mathrm{T}}\mathbf{D}^{-1}\mathbf{p}}{4\tau}\right)$$

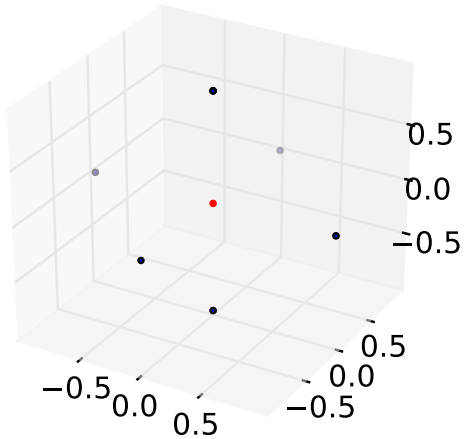

q-space sampling

Non-Gaussian angular

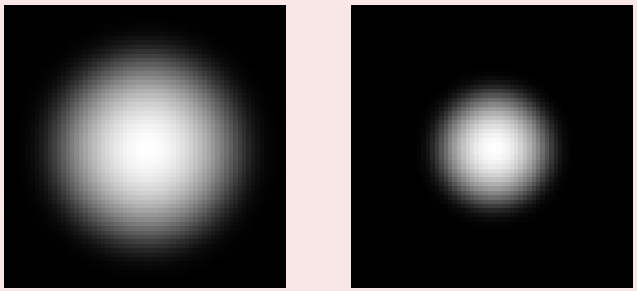

E P

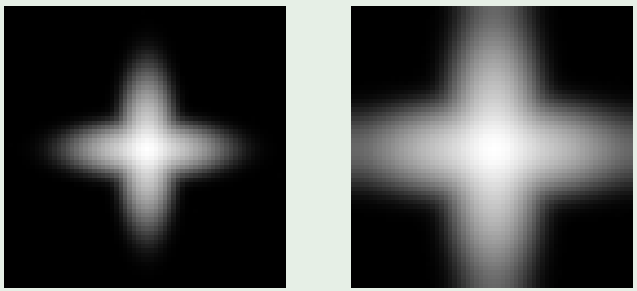

Low Angular Resolution Diffusion Imaging

Diffusion Tensor Imaging (DTI) - Gaussian assumption [Basser94]

$$E(\mathbf{q}) = \exp(-\mathbf{q}^{\mathrm{T}}\mathbf{D}\mathbf{q}) \quad \Rightarrow \quad P(\mathbf{p}) = \frac{1}{(|\mathbf{D}|(4\pi\tau)^3)^{1/2}} \exp\left(-\frac{\mathbf{p}^{\mathrm{T}}\mathbf{D}^{-1}\mathbf{p}}{4\tau}\right)$$

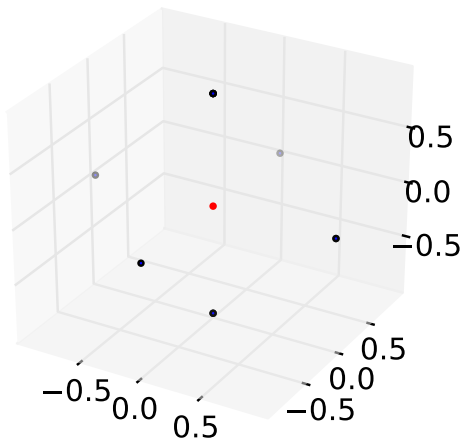

q-space sampling

Non-Gaussian radial

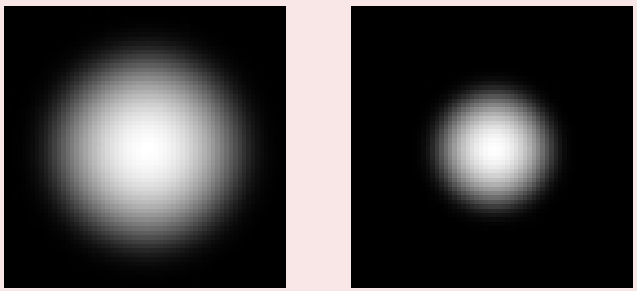

E P

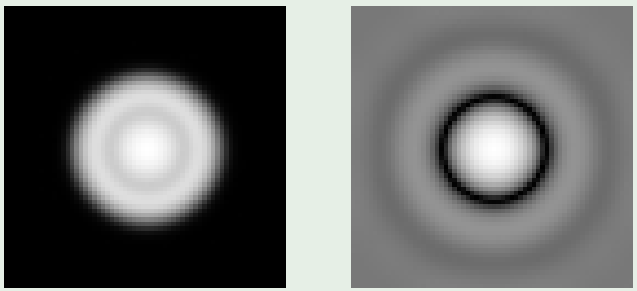

Low Angular Resolution Diffusion Imaging

Diffusion Tensor Imaging (DTI) - Gaussian assumption [Basser94]

$$E(\mathbf{q}) = \exp(-\mathbf{q}^{\mathrm{T}}\mathbf{D}\mathbf{q}) \quad \Rightarrow \quad P(\mathbf{p}) = \frac{1}{(|\mathbf{D}|(4\pi\tau)^3)^{1/2}} \exp\left(-\frac{\mathbf{p}^{\mathrm{T}}\mathbf{D}^{-1}\mathbf{p}}{4\tau}\right)$$

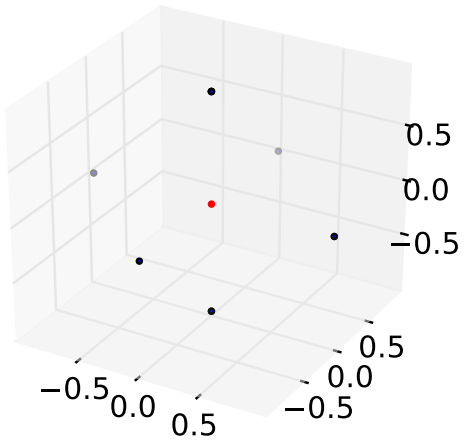

q-space sampling

Pro

- ☺ Very short acquisition time
- ☺ Well-established modality

Cons

- ☹ Inaccurate angular diffusion
- ☹ Simple *a priori* on the radial diffusion (Gaussian)

High Angular Resolution Diffusion Imaging [Tuch99]

Several methods

Q-Ball Imaging (QBI), Diffusion Orientation Transform (DOT), *etc.*

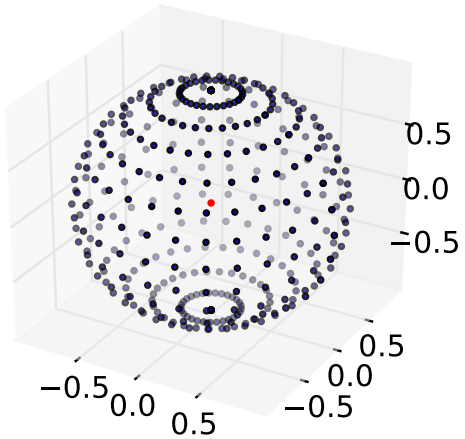

q-space sampling

High Angular Resolution Diffusion Imaging [Tuch99]

Several methods

Q-Ball Imaging (QBI), Diffusion Orientation Transform (DOT), *etc.*

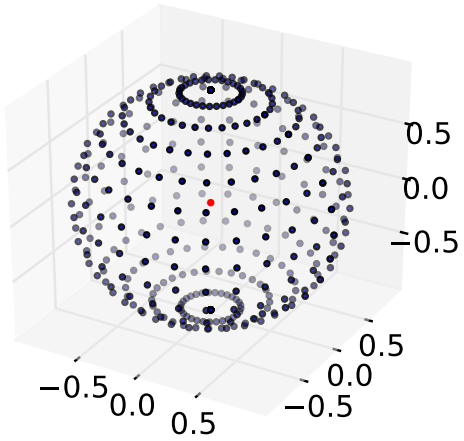

q-space sampling

Gaussian isotropic

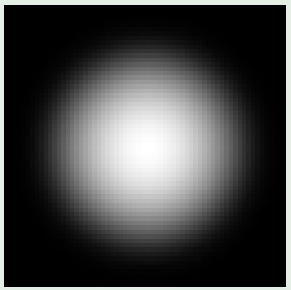

E

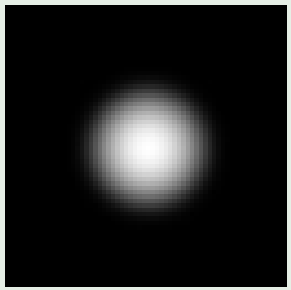

P

High Angular Resolution Diffusion Imaging [Tuch99]

Several methods

Q-Ball Imaging (QBI), Diffusion Orientation Transform (DOT), *etc.*

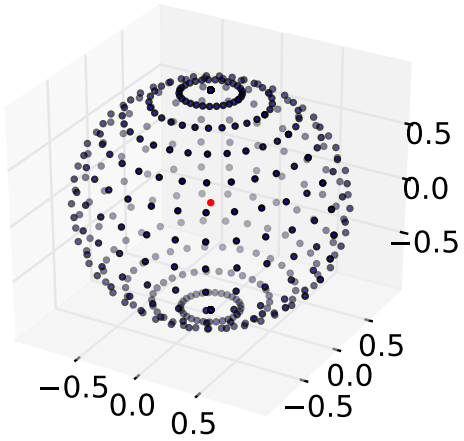

q-space sampling

Gaussian isotropic

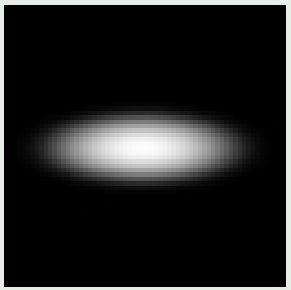

E

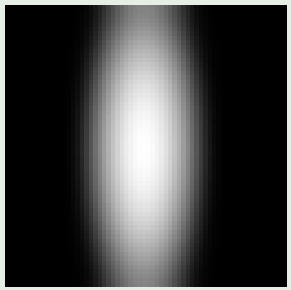

P

High Angular Resolution Diffusion Imaging [Tuch99]

Several methods

Q-Ball Imaging (QBI), Diffusion Orientation Transform (DOT), *etc.*

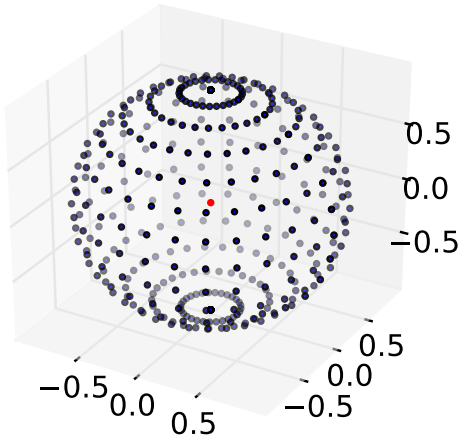

q-space sampling

Non-Gaussian angular

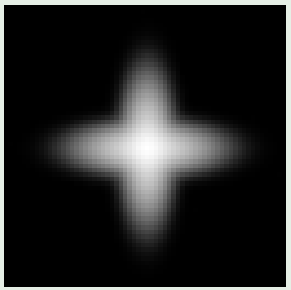

E

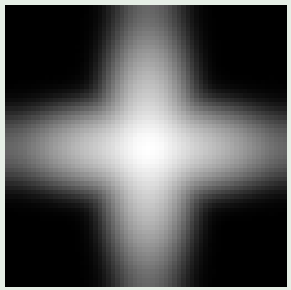

P

High Angular Resolution Diffusion Imaging [Tuch99]

Several methods

Q-Ball Imaging (QBI), Diffusion Orientation Transform (DOT), *etc.*

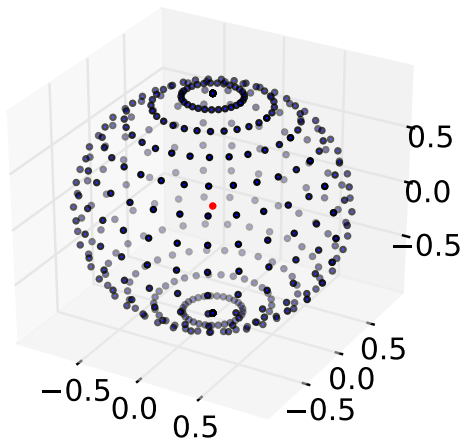

q-space sampling

Non-Gaussian radial

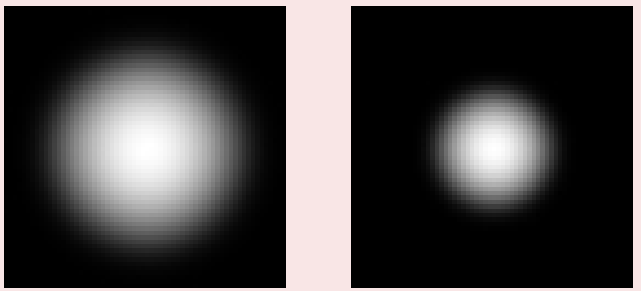

E P

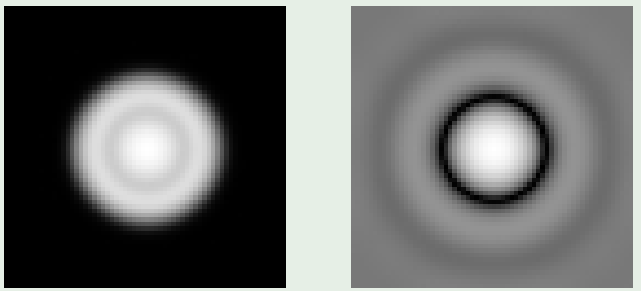

High Angular Resolution Diffusion Imaging [Tuch99]

Several methods

Q-Ball Imaging (QBI), Diffusion Orientation Transform (DOT), *etc.*

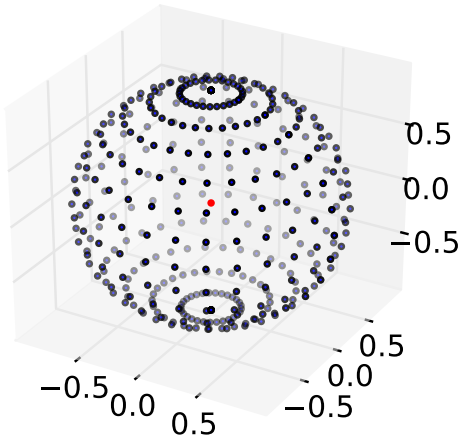

q-space sampling

Pro

- ☺ Reduced acquisition time
- ☺ Higher angular precision than DTI

Cons

- ☹ Simple *a priori* on the radial diffusion (Gaussian, Bessel, *etc.*)

Interest of Radial PDF

- Various brain tissues diffuses differently, which may reveal information on cells micro-structure that composed the organic tissue.

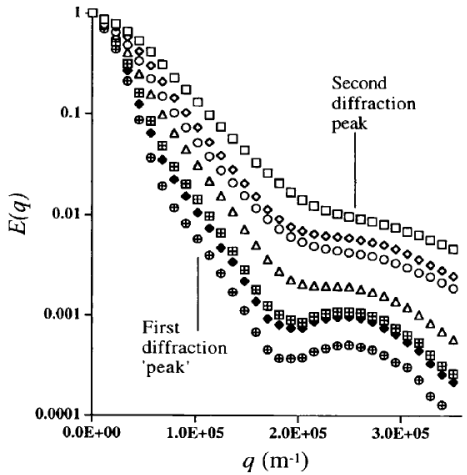

MR radial signal

- May increase detection of anomalies such as demyelination, a symptom of multiple sclerosis.

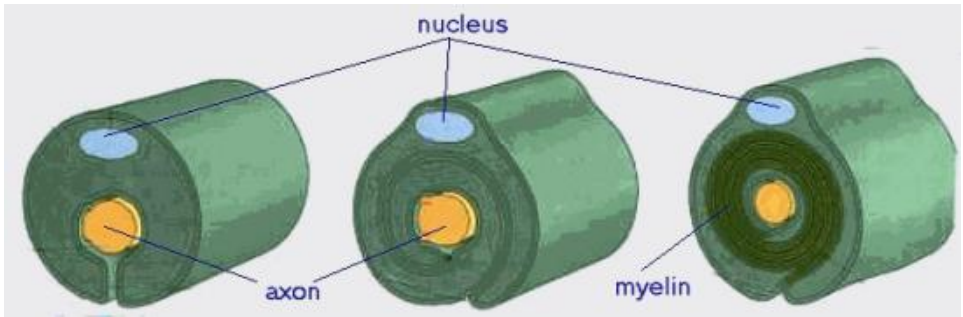

Figure: Myelination of an axone during the childhood [www.jdaross.cwc.net]

Our aim

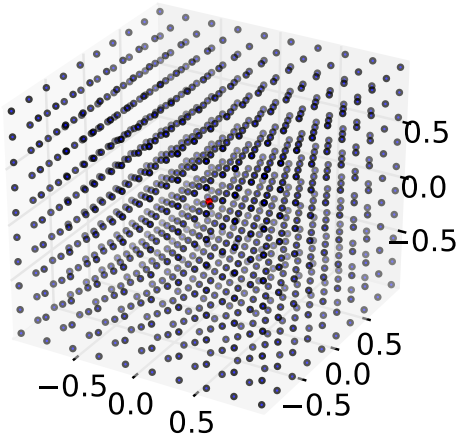

DSI

Pro

- Complete diffusion profile

Our aim

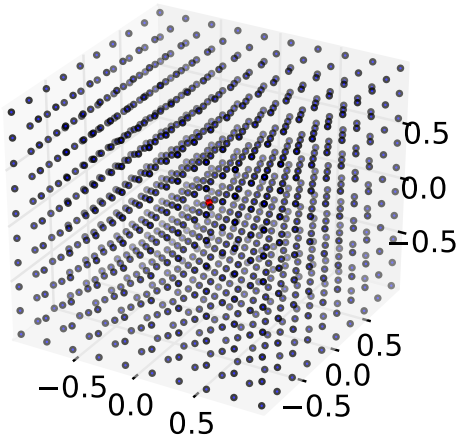

DSI

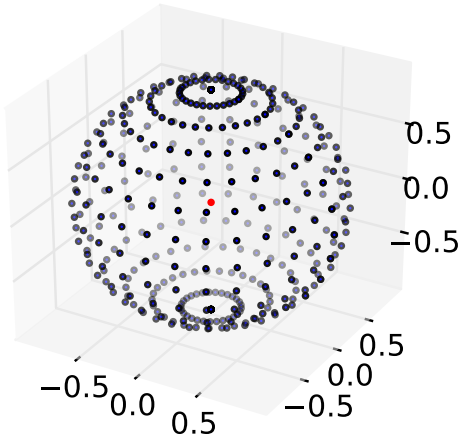

HARDI

Pro

- Complete diffusion profile

Pro

- Moderate acquisition time

Our aim

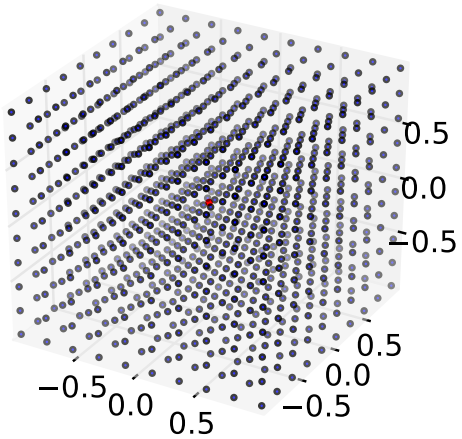

DSI

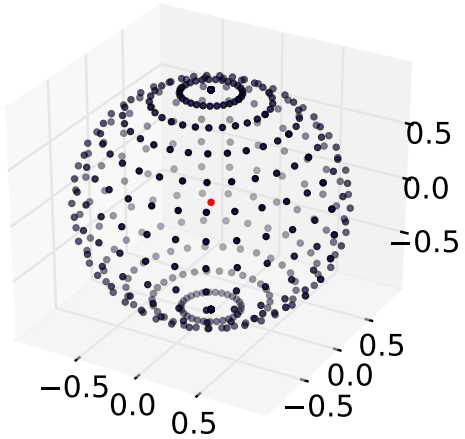

HARDI

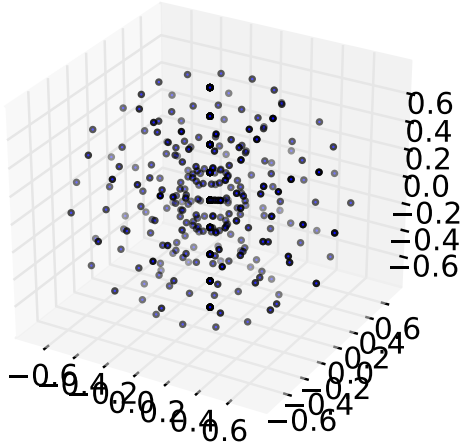

Sparse sampling

Pro

- Complete diffusion profile

Pro

- Moderate acquisition time

1. Diffusion signal estimation
   - Continuous representation of the signal
2. Extraction of various features of the PDF
   - Algorithm
   - Overview of proposed features
3. Robust extraction of diffusion features
   - Robustness to noise
   - Robustness to q-space sampling

1. Diffusion signal estimation
   - Continuous representation of the signal
2. Extraction of various features of the PDF
   - Algorithm
   - Overview of proposed features
3. Robust extraction of diffusion features
   - Robustness to noise
   - Robustness to q-space sampling

Continuous representation of the signal

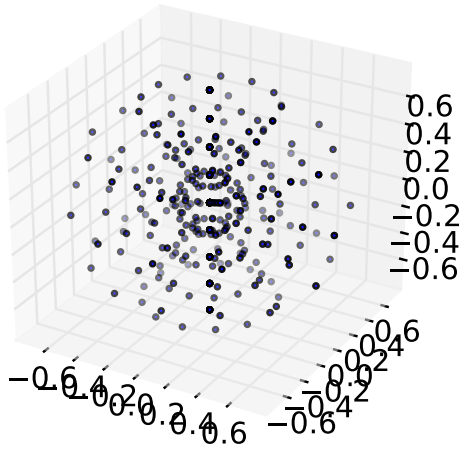

q-space sampling

Figure: A sparse sampling of the q-space.

Continuous representation of the signal

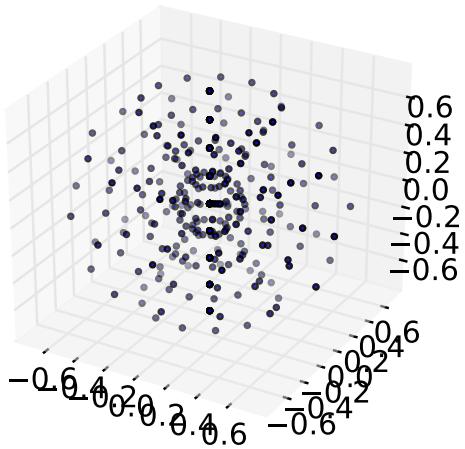

q-space sampling

Figure: A sparse sampling of the q-space.

Problem

Still insufficient number of samples for a Fourier transform. Which mathematical tool for the signal approximation ?

Continuous representation of the signal

Continuous representation of the MR signal E in the following basis (Spherical Polar Fourier SPF):

$$E(\mathbf{q}) = \sum_{n=0}^{\infty} \sum_{l=0}^{\infty} \sum_{m=-l}^{l} a_{nlm} R_n(||\mathbf{q}||) y_l^m \left(\frac{\mathbf{q}}{||\mathbf{q}||} \right) \quad (1)$$

where a_{nlm} expansion coefficients, R_n and y_l^m are respectively are radial and angular atoms.
The basis is *orthonormal* in spherical coordinates:

$$\int_{\mathbf{q} \in \mathbb{R}^3} \left[R_n(||\mathbf{q}||) y_l^m \left(\frac{\mathbf{q}}{||\mathbf{q}||} \right) \right] \cdot \left[R_{n'}(||\mathbf{q}||) y_{l'}^{m'} \left(\frac{\mathbf{q}}{||\mathbf{q}||} \right) \right] d\mathbf{q} = \delta_{nn'll'mm'} \quad (2)$$

Angular Atoms

$$y_l^m = \begin{cases} \sqrt{2}\,\Re(Y_l^m) & \text{if} \quad 0 < m \leq l \\ Y_l^0, & \text{if} \quad m = 0 \\ \sqrt{2}\,\Im(Y_l^{|m|}) & \text{if} \quad -l \leq m < 0 \end{cases} \qquad \text{with } l \in 2\mathbb{N} \tag{3}$$

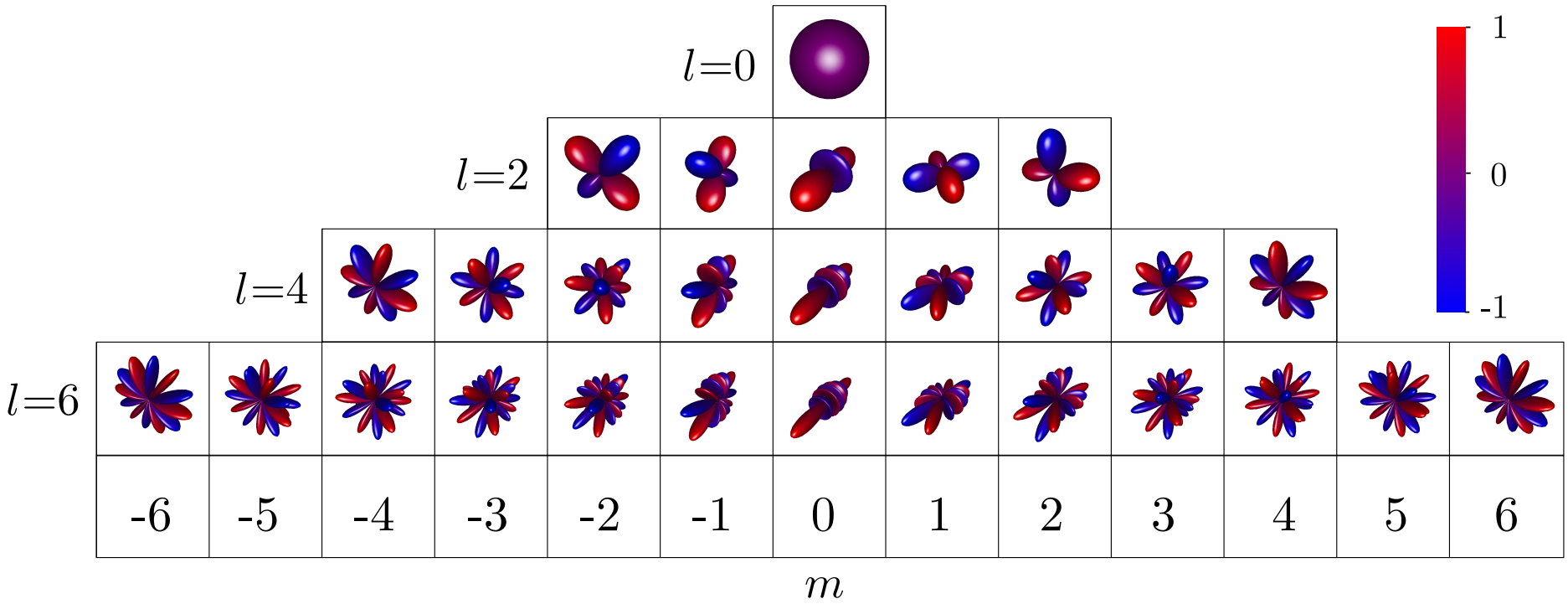

Figure: Real and symmetric spherical harmonics: first orders $l = 0, 2, 4, 6$. Blue indicates a negative value, whereas indicates red a positive value.

Angular Atoms

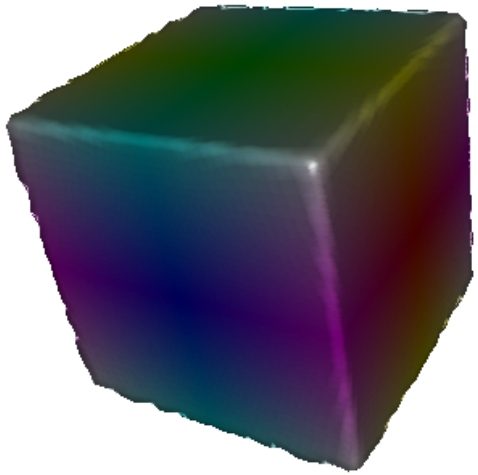

(a)

Figure: Square sampled along a 5-subdivided icosahedron.

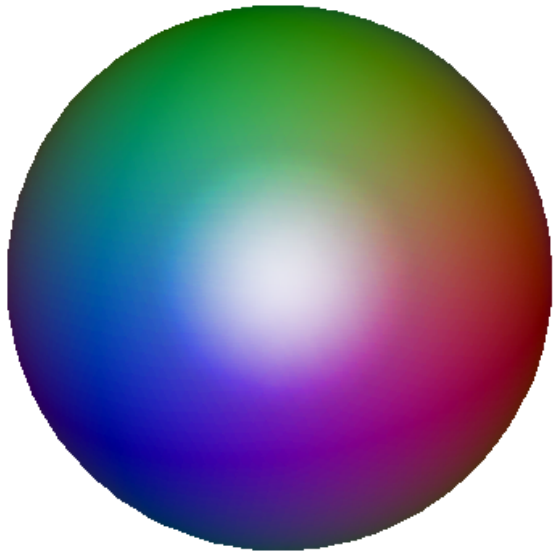

(a) 1 coefficients

Figure: Angular reconstruction along with increasing truncation order L.

Angular Atoms

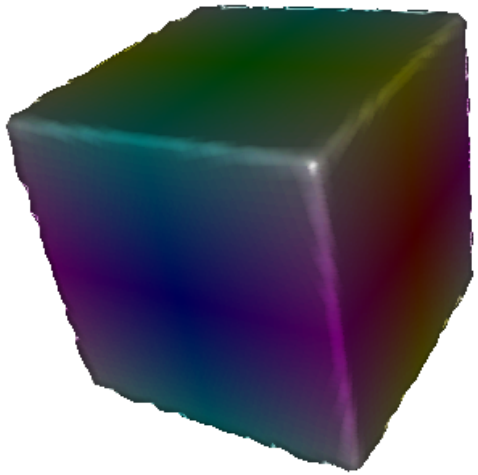

(a)

Figure: Square sampled along a 5-subdivided icosahedron.

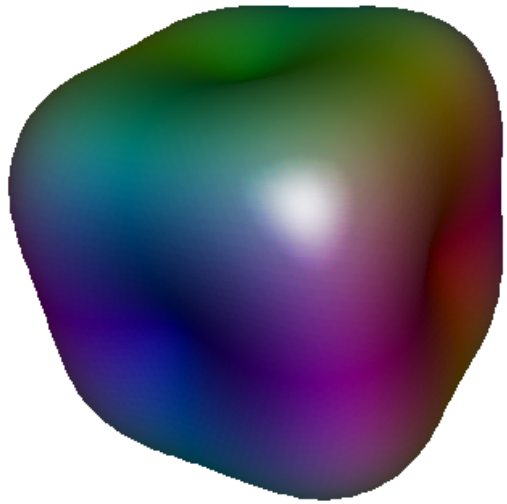

(a) 15 coefficients

Figure: Angular reconstruction along with increasing truncation order L.

Angular Atoms

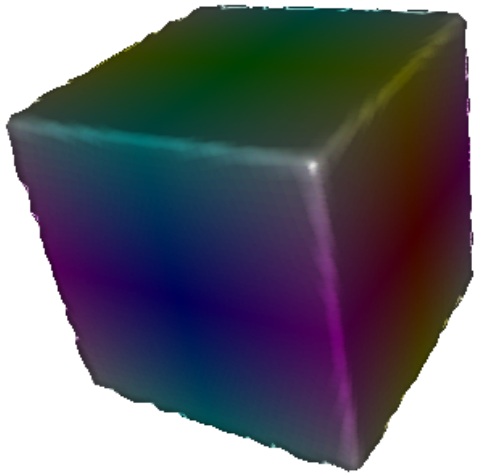

(a)

Figure: Square sampled along a 5-subdivided icosahedron.

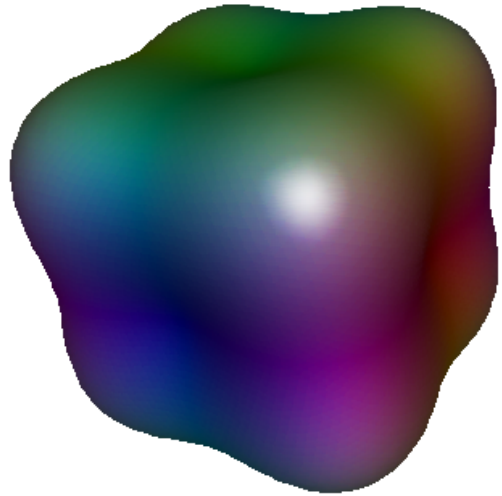

(a) 28 coefficients

Figure: Angular reconstruction along with increasing truncation order L.

Angular Atoms

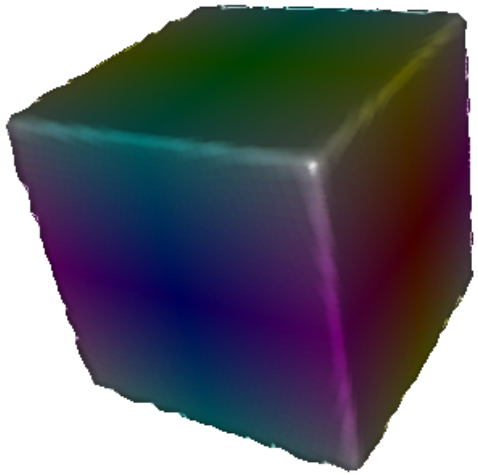

(a)

Figure: Square sampled along a 5-subdivided icosahedron.

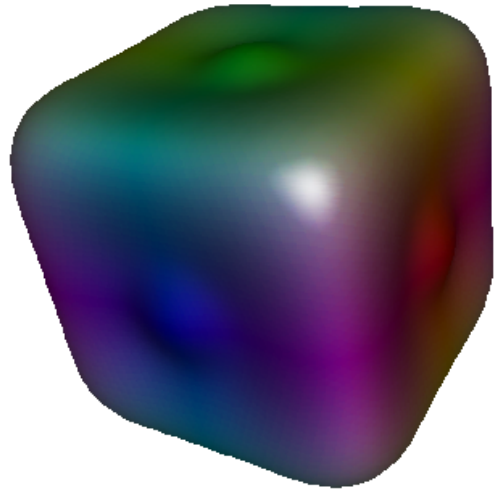

(a) 45 coefficients

Figure: Angular reconstruction along with increasing truncation order L.

Angular Atoms

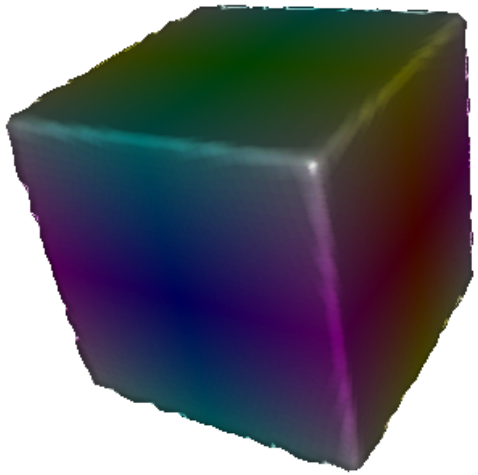

(a)

Figure: Square sampled along a 5-subdivided icosahedron.

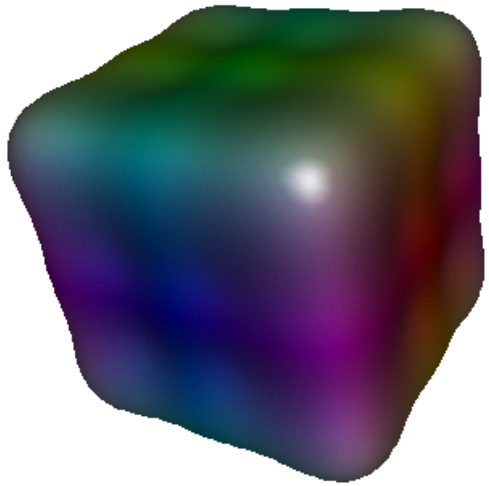

(a) 66 coefficients

Figure: Angular reconstruction along with increasing truncation order L.

Angular Atoms

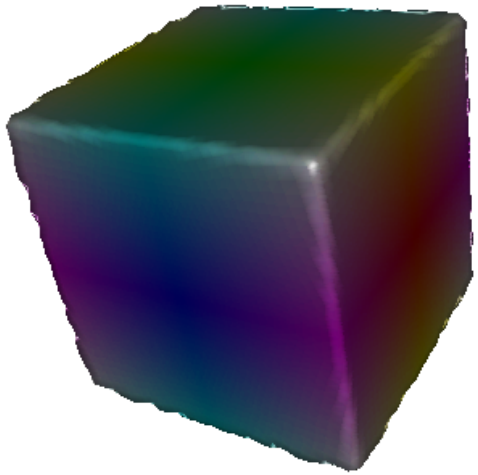

(a)

Figure: Square sampled along a 5-subdivided icosahedron.

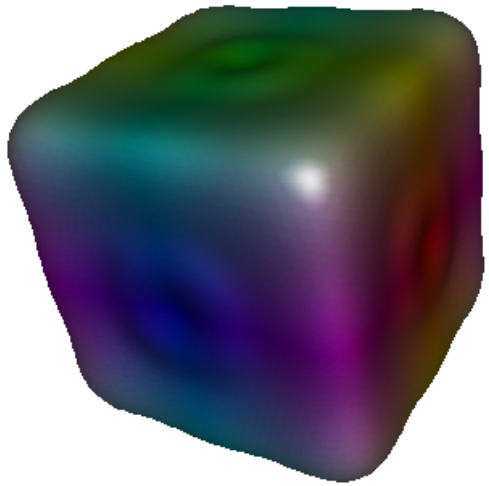

(a) 91 coefficients

Figure: Angular reconstruction along with increasing truncation order L.

Angular Atoms

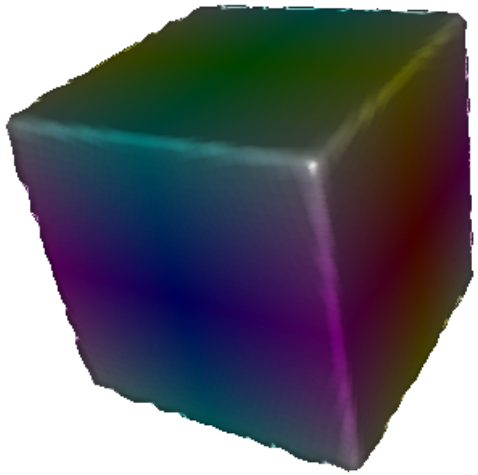

(a)

Figure: Square sampled along a 5-subdivided icosahedron.

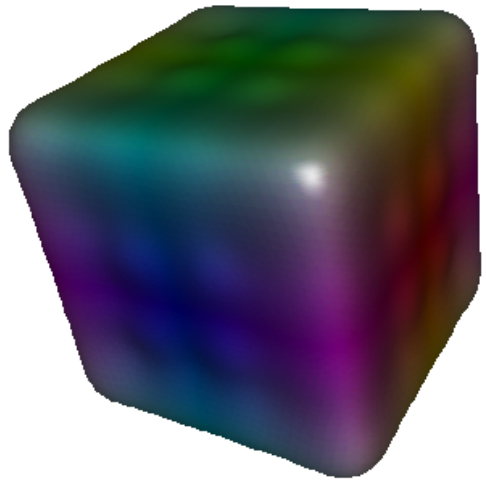

(a) 120 coefficients

Figure: Angular reconstruction along with increasing truncation order L.

Angular Atoms

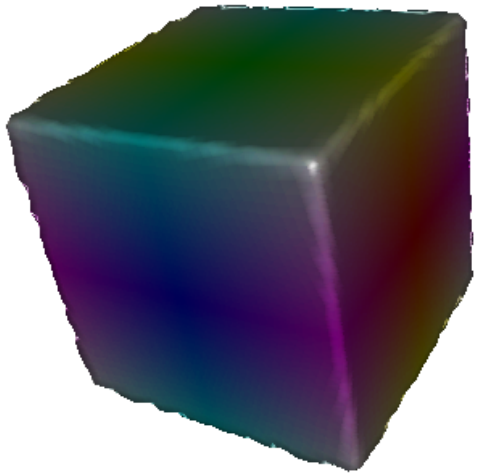

(a)

Figure: Square sampled along a 5-subdivided icosahedron.

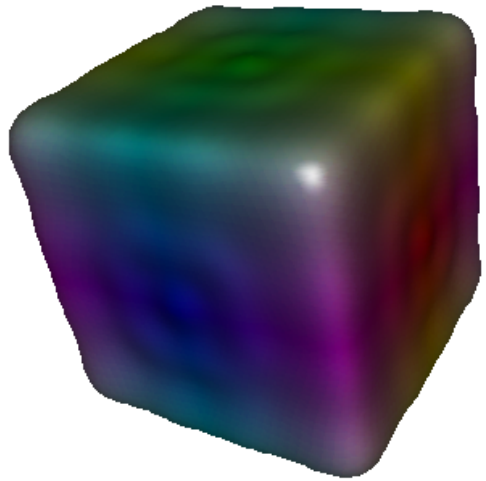

(a) 153 coefficients

Figure: Angular reconstruction along with increasing truncation order L.

Radial Atoms

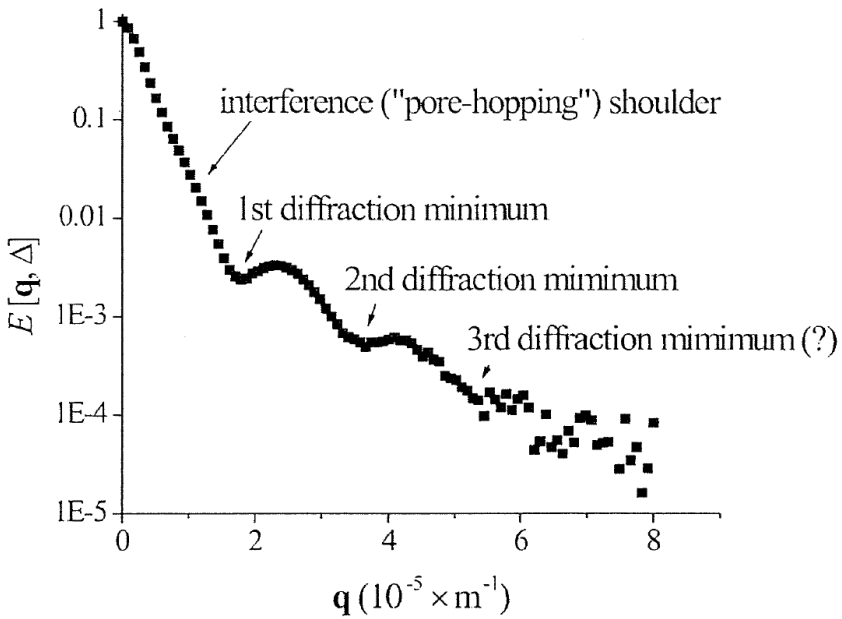

Figure: Experimental plot [Regan06]

Radial Atoms

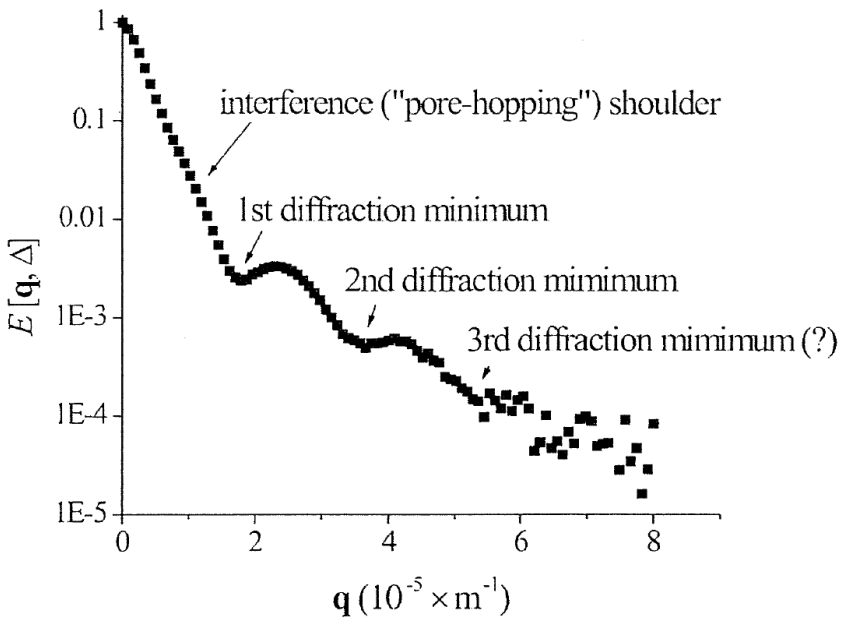

Figure: Experimental plot [Regan06]

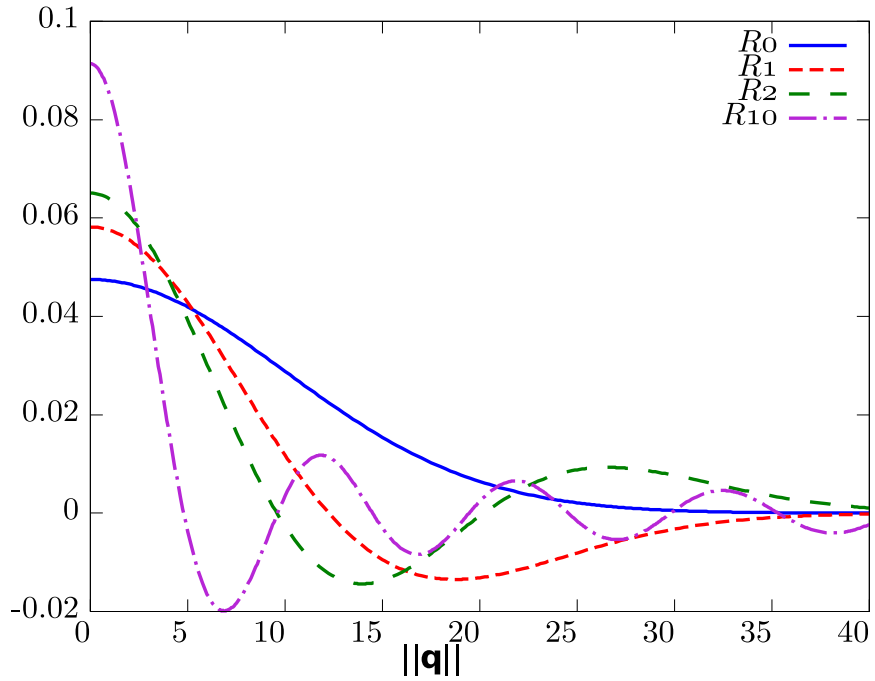

Figure: Some radial atoms R_n

Our proposition

$$R_n(||\mathbf{q}||) = \left[\frac{2}{\gamma^{3/2}}\frac{n!}{\Gamma(n+3/2)}\right]^{1/2} \exp\left(-\frac{||\mathbf{q}||^2}{2\gamma}\right) L_n^{1/2}\left(\frac{||\mathbf{q}||^2}{\gamma}\right)$$

Radial Atoms

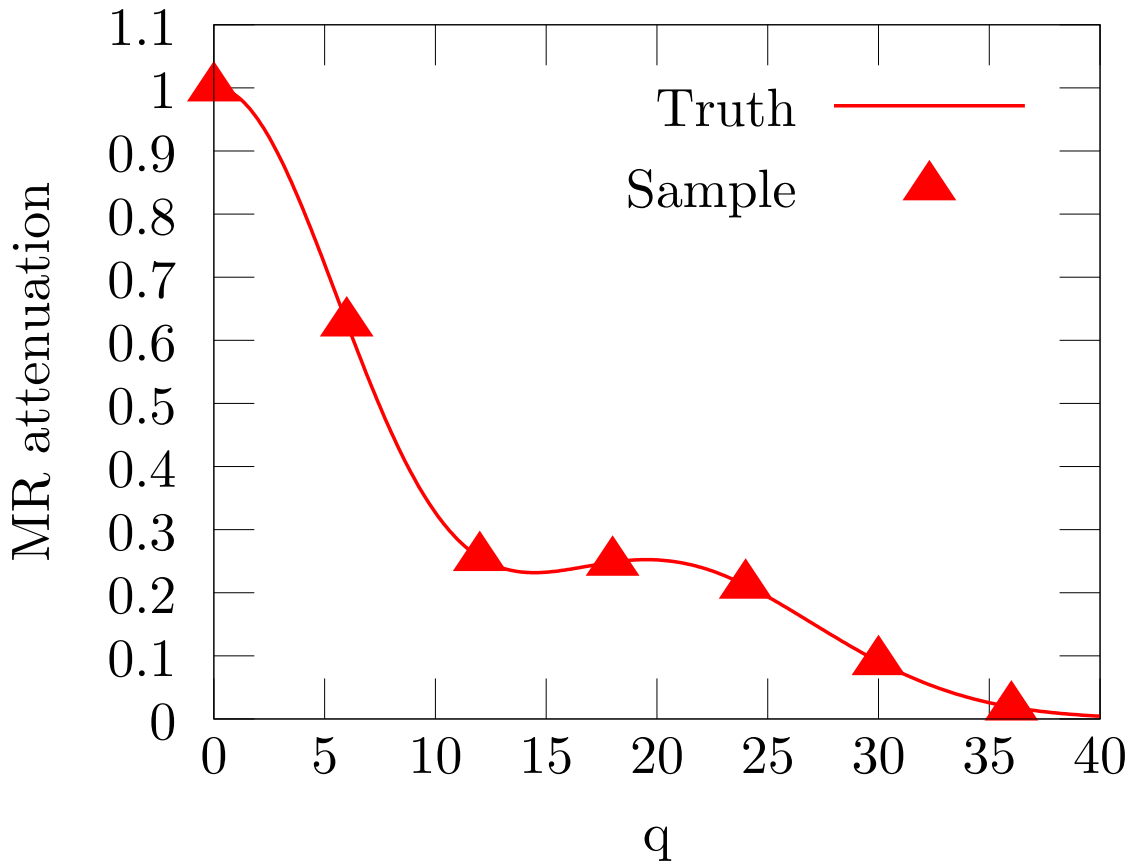

(a) Signal de diffusion

Figure: Radial reconstruction along with increasing truncation order N.

Radial Atoms

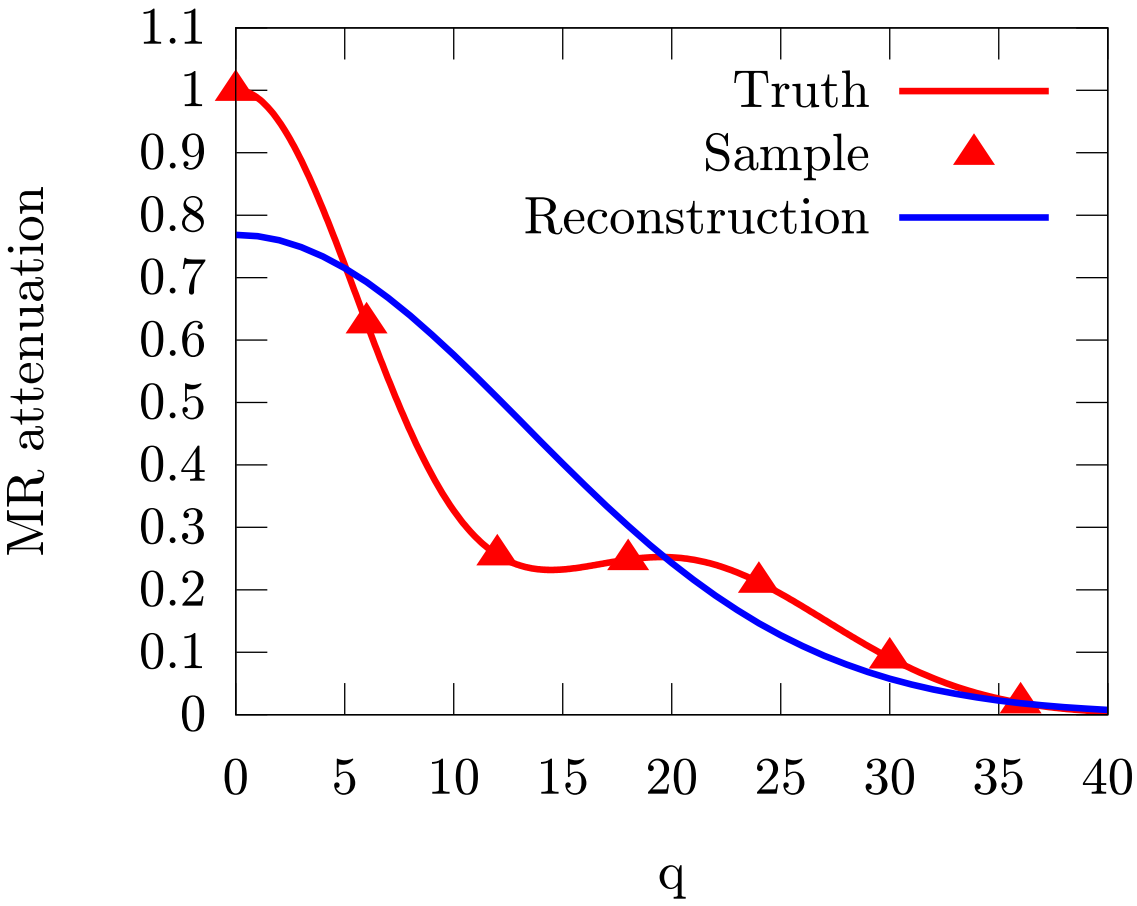

(a) 1 Coefficient

Figure: Radial reconstruction along with increasing truncation order N.

Radial Atoms

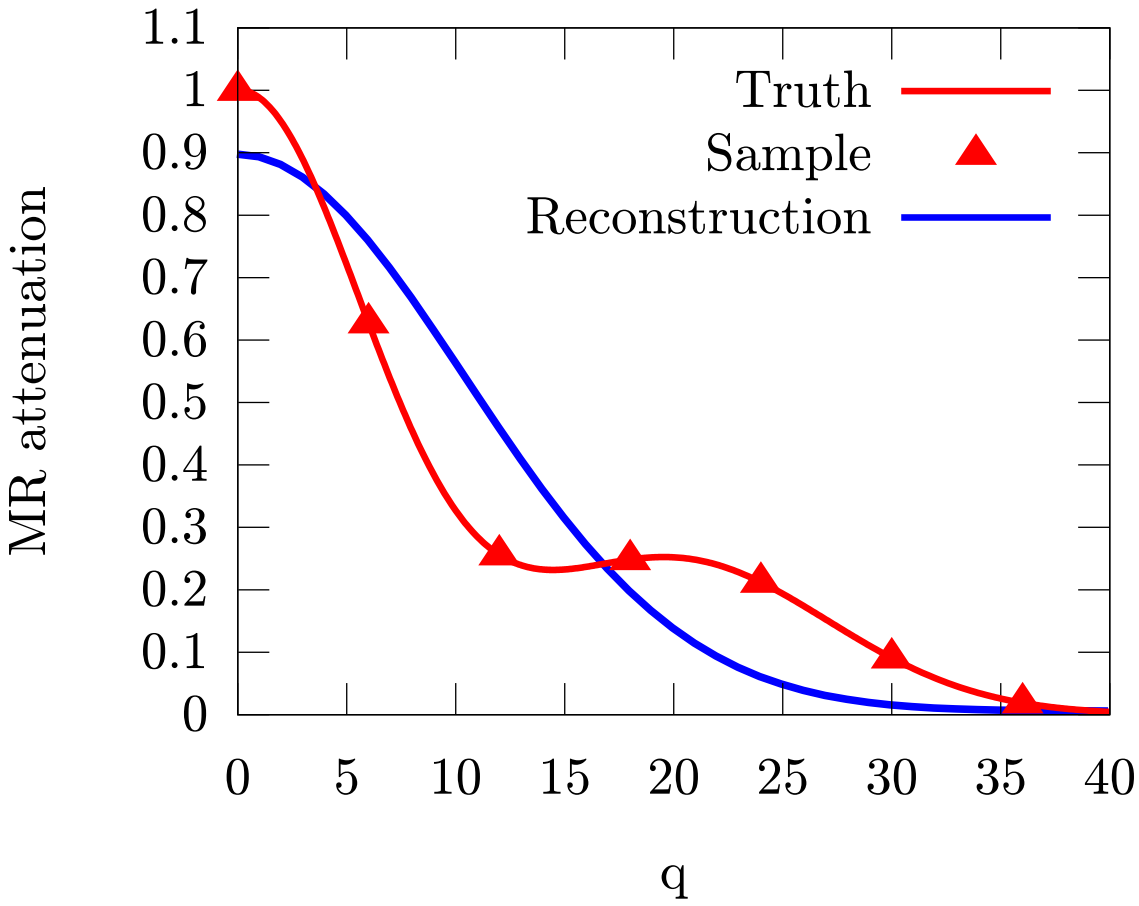

(a) 2 Coefficients

Figure: Radial reconstruction along with increasing truncation order N.

Radial Atoms

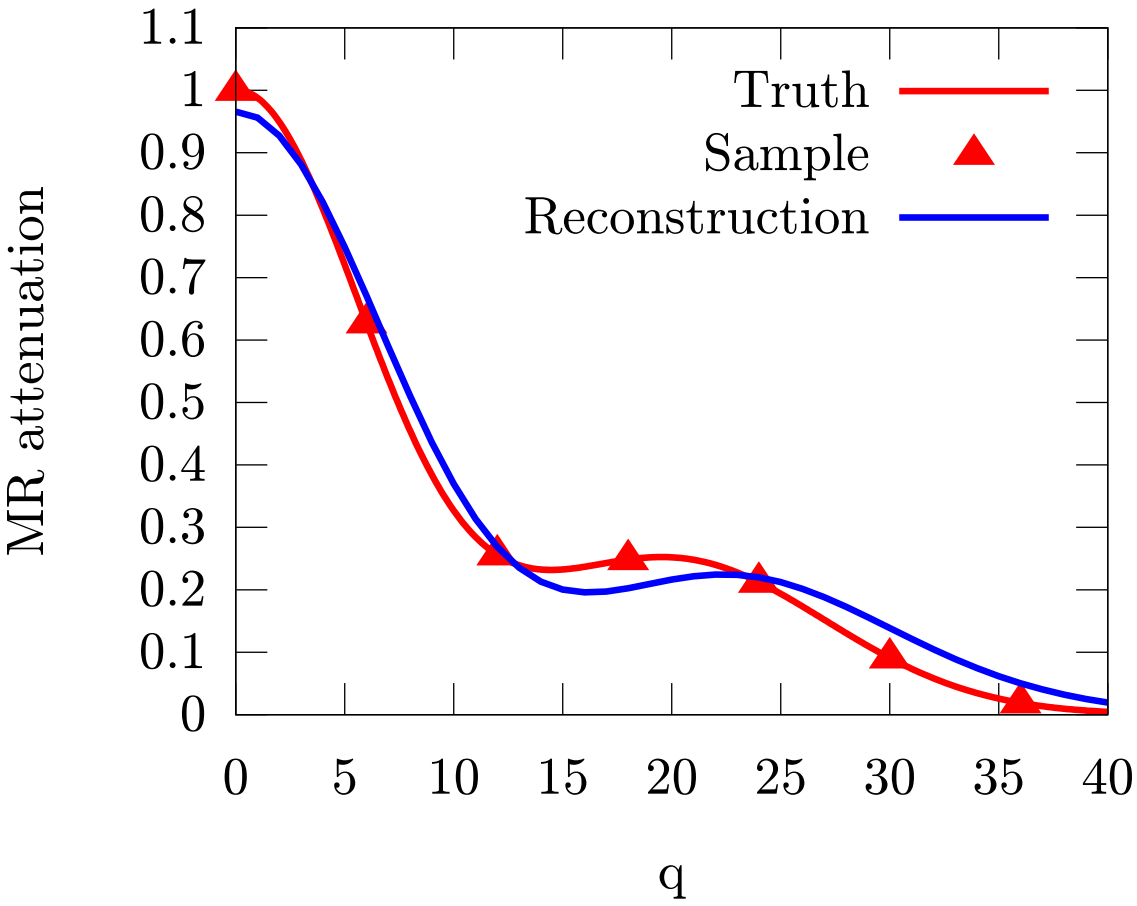

(a) 3 Coefficients

Figure: Radial reconstruction along with increasing truncation order N.

Radial Atoms

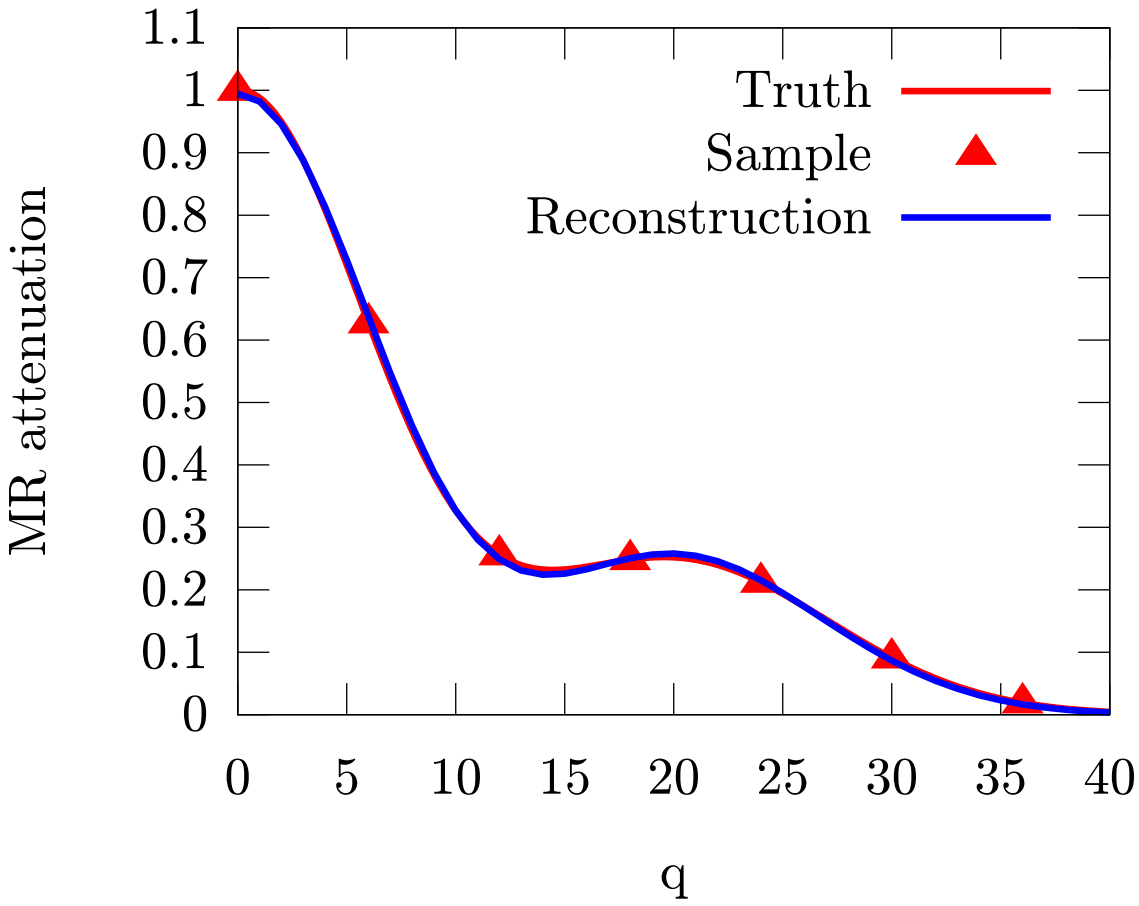

(a) 4 Coefficients

Figure: Radial reconstruction along with increasing truncation order N.

Radial Atoms

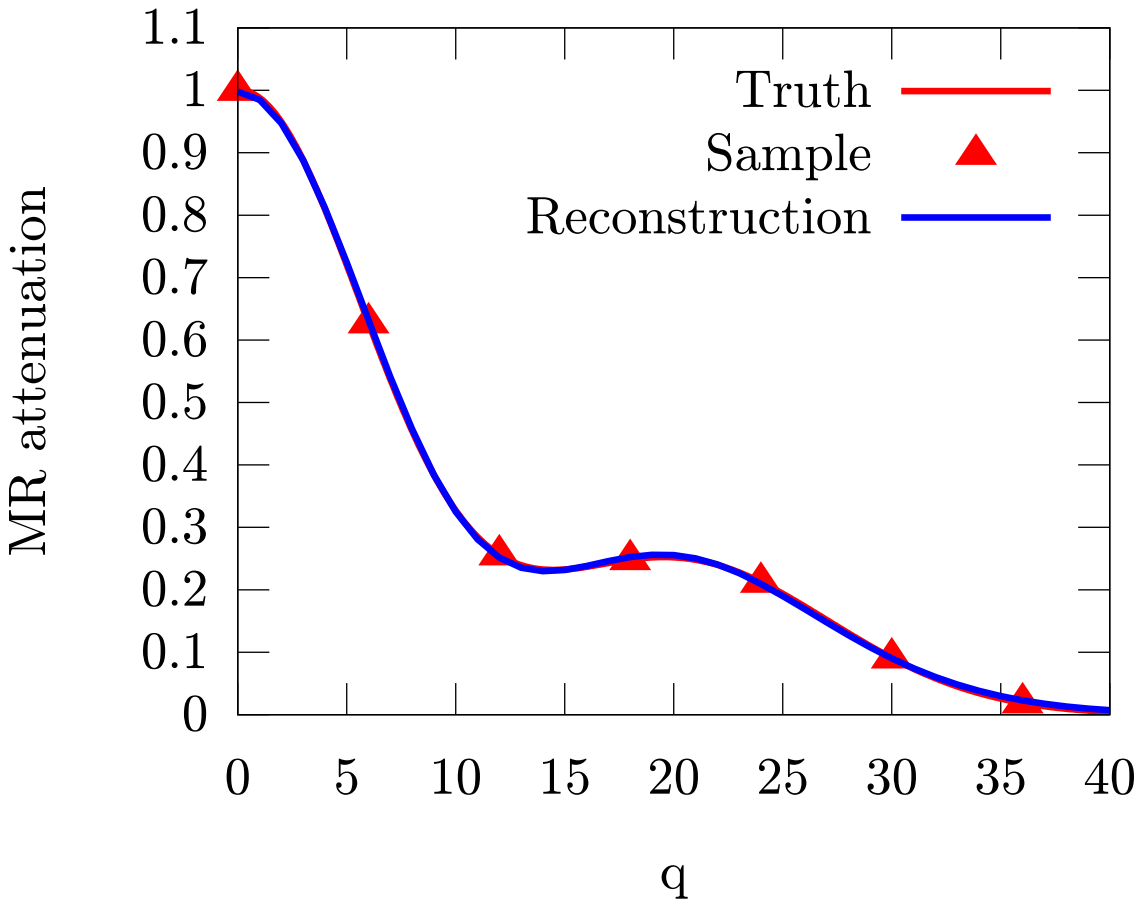

(a) 5 Coefficients

Figure: Radial reconstruction along with increasing truncation order N.

Linear signal estimation

The representation of the signal $\mathbf{E}$ as a coefficient vector $\mathbf{A}$ in the basis $\mathbf{M}$ is expressed as:

$$\mathbf{E} = \mathbf{M}\,\mathbf{A}$$

The coefficient estimation is computed by the linear damped least square method:

$$\begin{aligned} \Rightarrow \mathbf{A} &= \arg\min_{\mathbf{A}} ||\mathbf{E} - \mathbf{M}\mathbf{A}||^2 + \lambda_l ||\mathbf{L}||^2 + \lambda_n ||\mathbf{N}||^2 \\ &= (\mathbf{M}^T\mathbf{M} + \lambda_l \mathbf{L}^T\mathbf{L} + \lambda_n \mathbf{N}^T\mathbf{N})^{-1}\mathbf{M}^T\mathbf{E} \end{aligned}$$

where $\mathbf{M}$, $\mathbf{E}$, $\mathbf{A}$ stands for:

$$\mathbf{M} = \begin{bmatrix} R_0(||\mathbf{q}_1||) y_0^0\left(\frac{\mathbf{q}_1}{||\mathbf{q}_1||}\right) & \dots & R_N(||\mathbf{q}_1||) y_L^L\left(\frac{\mathbf{q}_1}{||\mathbf{q}_1||}\right) \\ \vdots & \ddots & \vdots \\ R_0(||\mathbf{q}_{n_s}||) y_0^0\left(\frac{\mathbf{q}_{n_s}}{||\mathbf{q}_{n_s}||}\right) & \dots & R_N(||\mathbf{q}_{n_s}||) y_L^L\left(\frac{\mathbf{q}_{n_s}}{||\mathbf{q}_{n_s}||}\right) \end{bmatrix},$$

$$\mathbf{E} = (E(\mathbf{q}_1), \dots, E(\mathbf{q}_{ns}))^T \quad \mathbf{A} = (a_{000}, \dots, a_{NLL})^T$$

Simulation: linear least square reconstruction

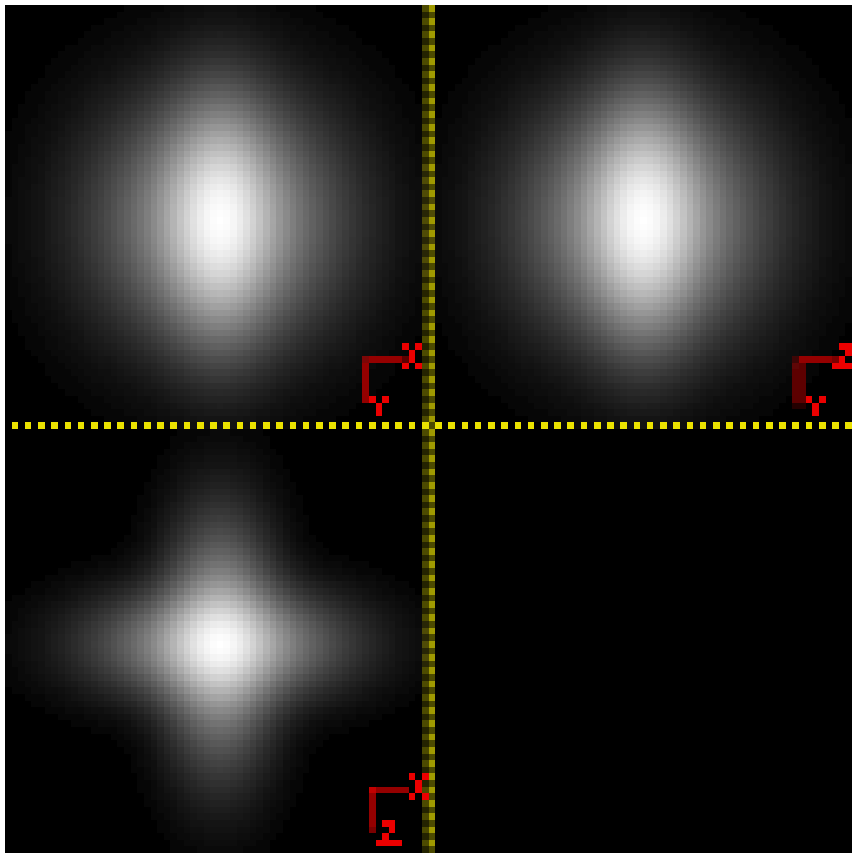

Figure: Original signal

Simulation: linear least square reconstruction

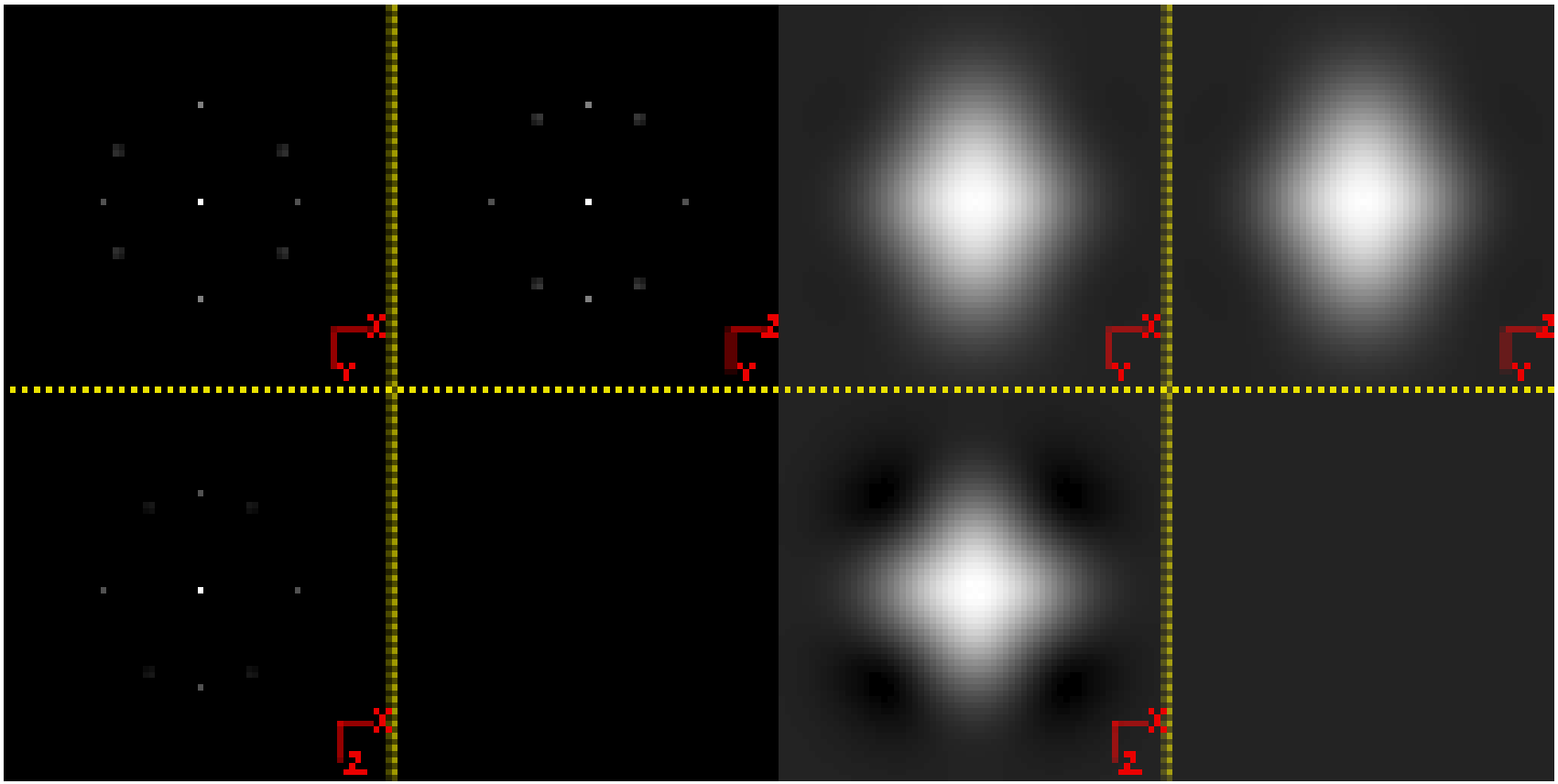

Figure: $N = 1$, $L = 4$, $\gamma = 100$,
1 sphere – 42 directions,
PSNR: 33.337902, 30 Coefficients

Simulation: linear least square reconstruction

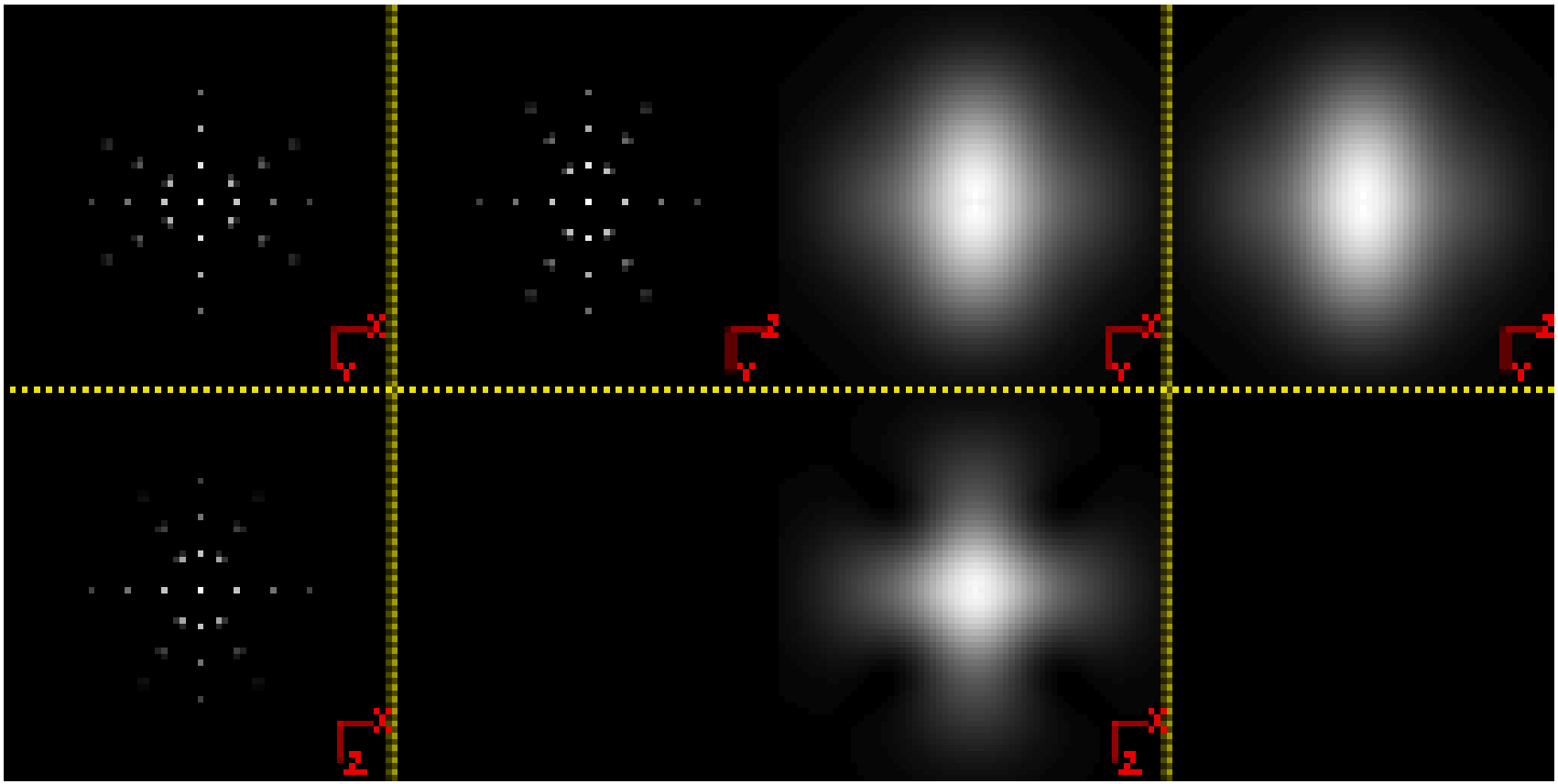

Figure: $N = 3$, $L = 4$, $\gamma = 70$,
3 spheres – 42 directions,
PSNR: 45.172752, 45 Coefficients

Simulation: linear least square reconstruction

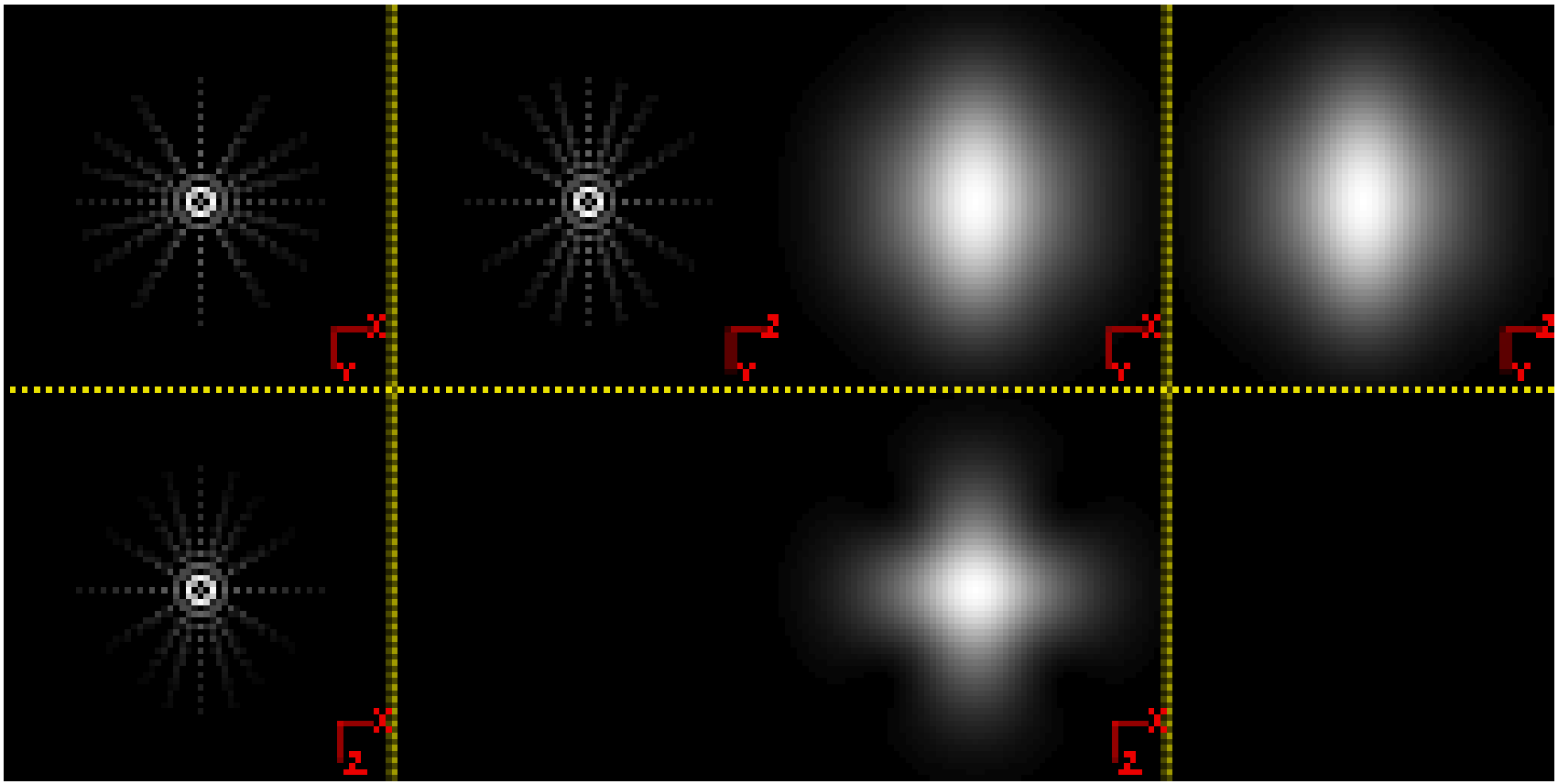

Figure: $N = 5$, $L = 6$, $\gamma = 50$,
10 spheres – 162 directions,
PSNR: 50.255381, 168 Coefficients

1. Diffusion signal estimation
   - Continuous representation of the signal

2. Extraction of various features of the PDF
   - Algorithm
   - Overview of proposed features

3. Robust extraction of diffusion features
   - Robustness to noise
   - Robustness to q-space sampling

1. Diffusion signal estimation
   - Continuous representation of the signal
2. Extraction of various features of the PDF
   - Algorithm
   - Overview of proposed features
3. Robust extraction of diffusion features
   - Robustness to noise
   - Robustness to q-space sampling

Features of the PDF

Now that we have a continuous reconstruction of the diffusion signal E, how do we compute the PDF ?

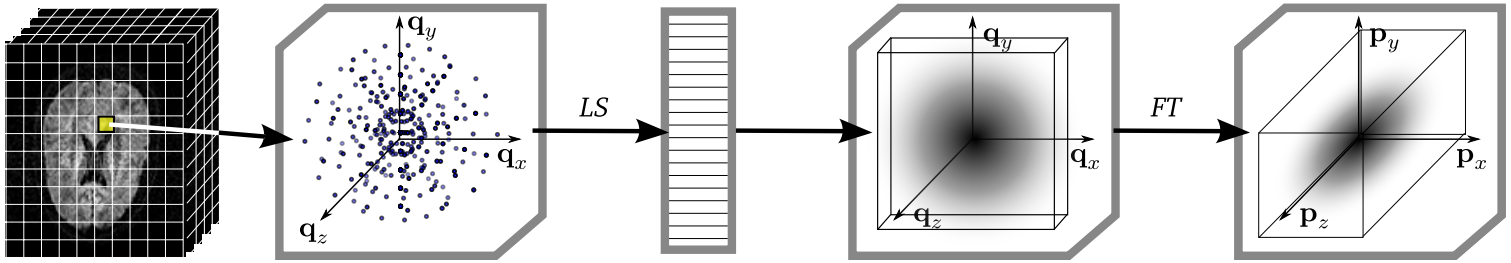

a) diffusion MRI of brain

b) q-space sampling

c) SPF coefficients of the diffusion profile E

d) Approximation of diffusion profile E

e) Computation of diffusion propagator P

Features of the PDF

Now that we have a continuous reconstruction of the diffusion signal E, how do we compute the PDF ?

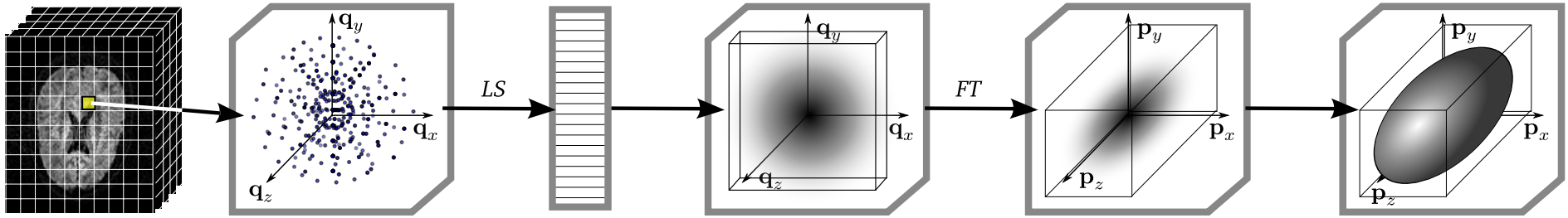

a) diffusion MRI of brain | b) q-space sampling | c) SPF coefficients of the diffusion profile E | d) Approximation of diffusion profile E | e) Computation of diffusion propagator P | f) Extraction of features

Features of the PDF

Now that we have a continuous reconstruction of the diffusion signal E, how do we compute the PDF ?

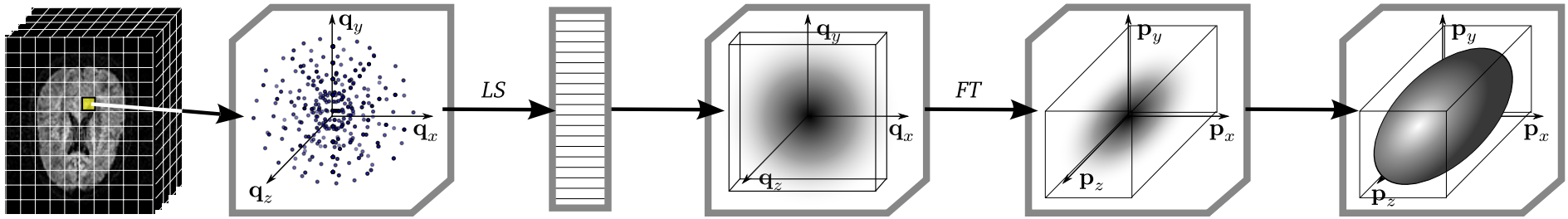

a) diffusion MRI of brain | b) q-space sampling | c) SPF coefficients of the diffusion profile E | d) Approximation of diffusion profile E | e) Computation of diffusion propagator P | f) Extraction of features

Proposition

We are interesting in a data reduction suitable to display: *features* of the PDF.

$$\mathcal{G}(\mathbf{k}) = \int_{p \in \mathbb{R}^3} PDF(\mathbf{p})\, H_{\mathbf{k}}(\mathbf{p}) d\mathbf{p}$$

Features of the PDF: projection

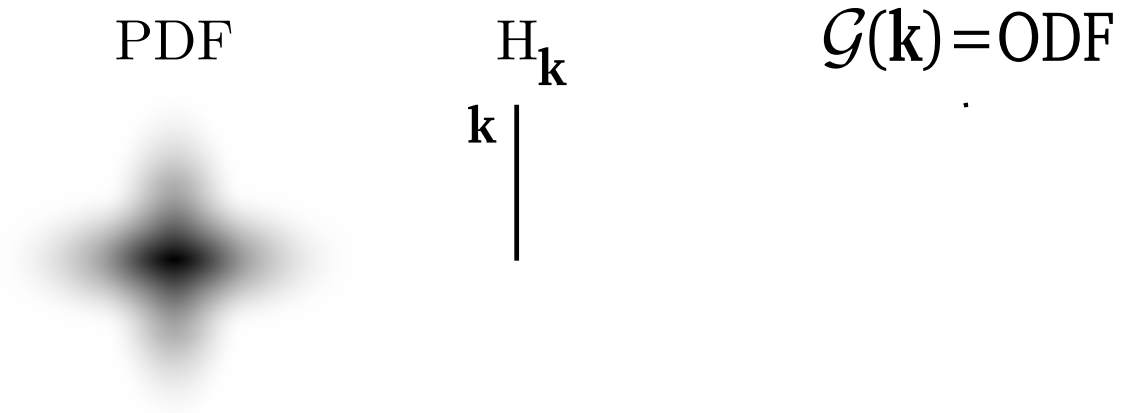

Figure: Example: ODF feature.

$$\mathcal{G}(\mathbf{k}) = \int_{p \in \mathbb{R}^3} PDF(\mathbf{p})\, H_{\mathbf{k}}(\mathbf{p}) d\mathbf{p} \tag{4}$$

Features of the PDF: projection

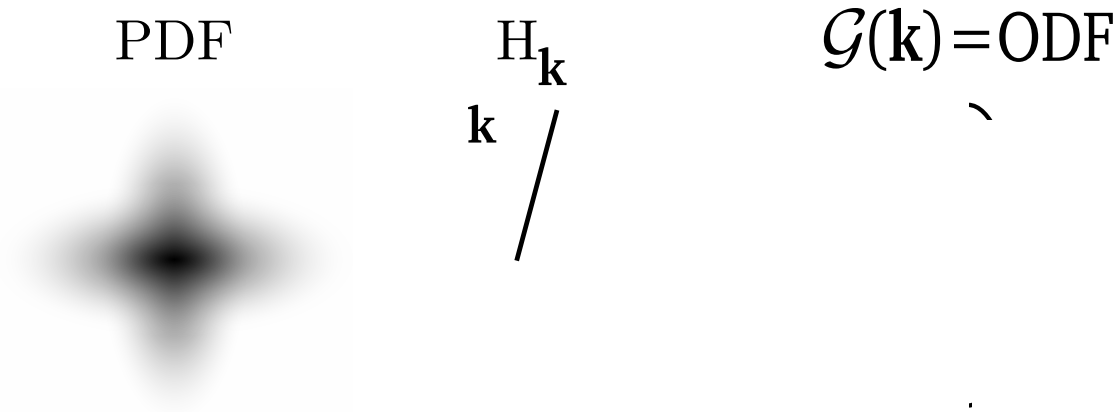

Figure: Example: ODF feature.

$$\mathcal{G}(\mathbf{k}) = \int_{p \in \mathbb{R}^3} PDF(\mathbf{p})\, H_{\mathbf{k}}(\mathbf{p}) d\mathbf{p} \tag{4}$$

Features of the PDF: projection

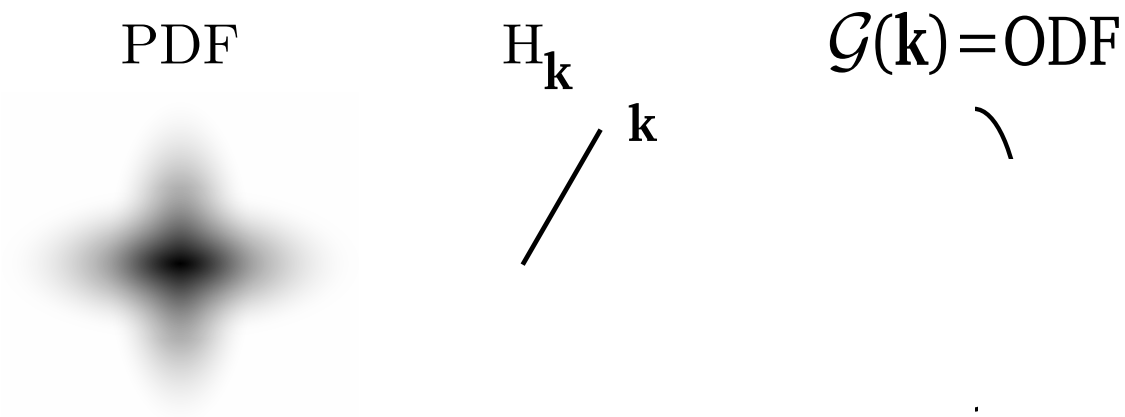

Figure: Example: ODF feature.

$$\mathcal{G}(\mathbf{k}) = \int_{p \in \mathbb{R}^3} PDF(\mathbf{p})\, H_{\mathbf{k}}(\mathbf{p}) d\mathbf{p} \tag{4}$$

Features of the PDF: projection

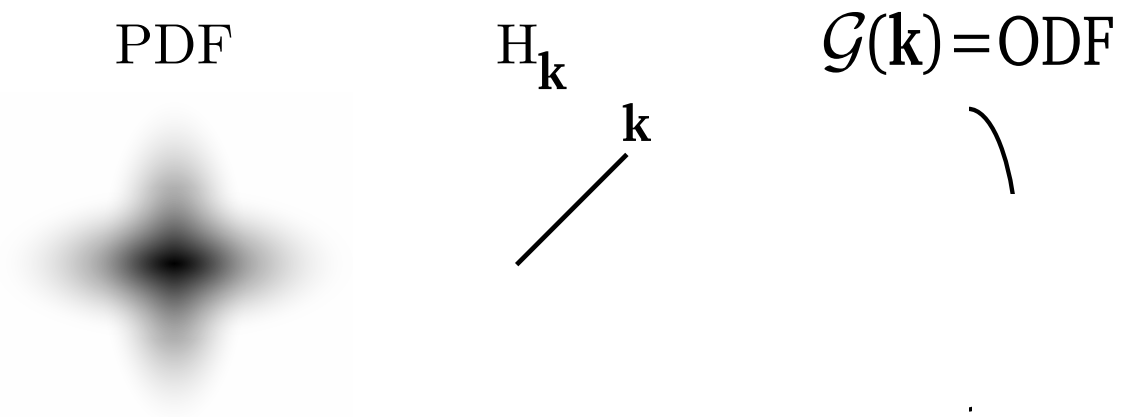

Figure: Example: ODF feature.

$$\mathcal{G}(\mathbf{k}) = \int_{p \in \mathbb{R}^3} PDF(\mathbf{p})\, H_{\mathbf{k}}(\mathbf{p}) d\mathbf{p} \tag{4}$$

Features of the PDF: projection

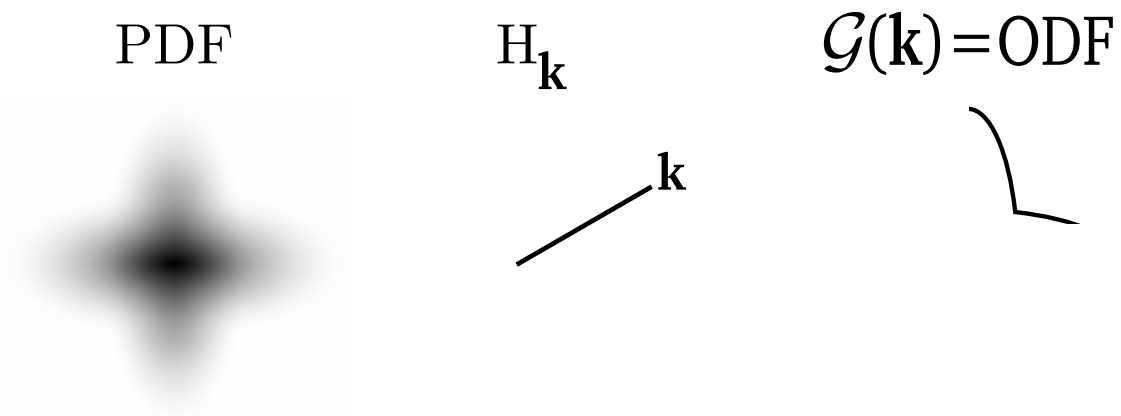

Figure: Example: ODF feature.

$$\mathcal{G}(\mathbf{k}) = \int_{p \in \mathbb{R}^3} PDF(\mathbf{p})\, H_{\mathbf{k}}(\mathbf{p}) d\mathbf{p} \tag{4}$$

Features of the PDF: projection

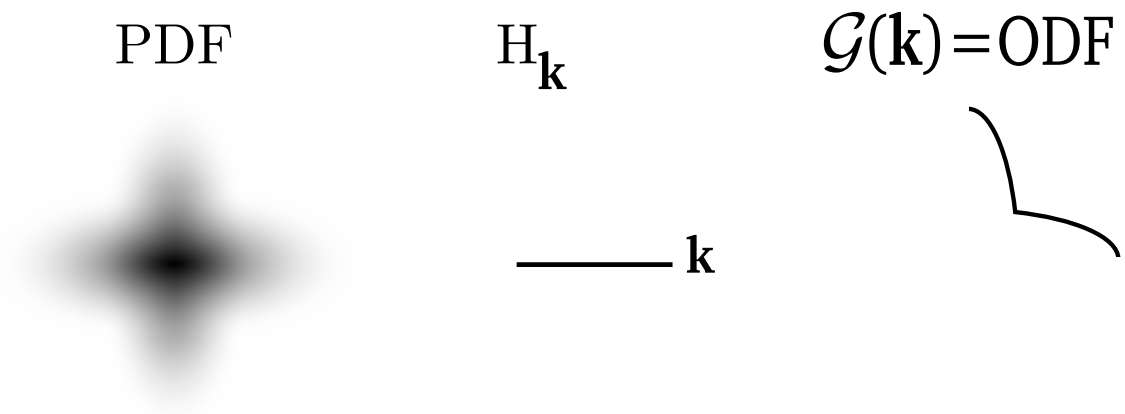

Figure: Example: ODF feature.

$$\mathcal{G}(\mathbf{k}) = \int_{p \in \mathbb{R}^3} PDF(\mathbf{p})\, H_{\mathbf{k}}(\mathbf{p}) d\mathbf{p} \tag{4}$$

Features of the PDF: projection

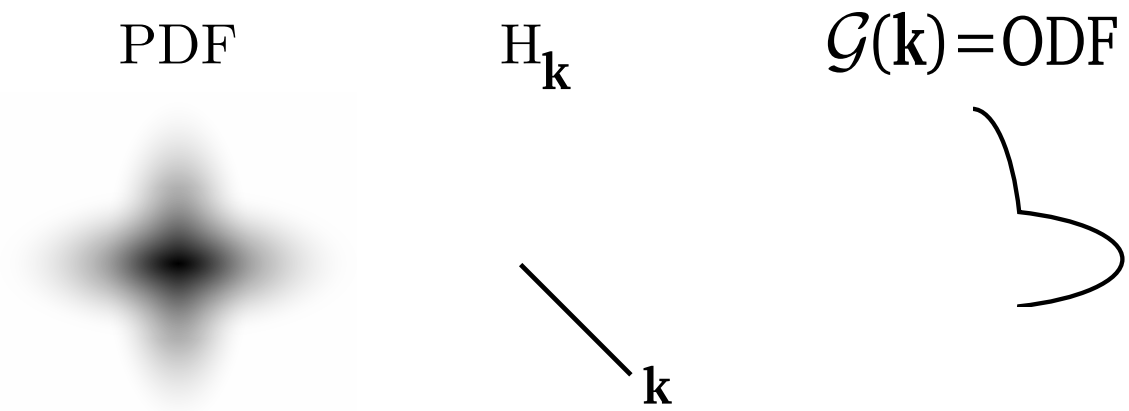

Figure: Example: ODF feature.

$$\mathcal{G}(\mathbf{k}) = \int_{p \in \mathbb{R}^3} PDF(\mathbf{p})\, H_{\mathbf{k}}(\mathbf{p}) d\mathbf{p} \tag{4}$$

Features of the PDF: projection

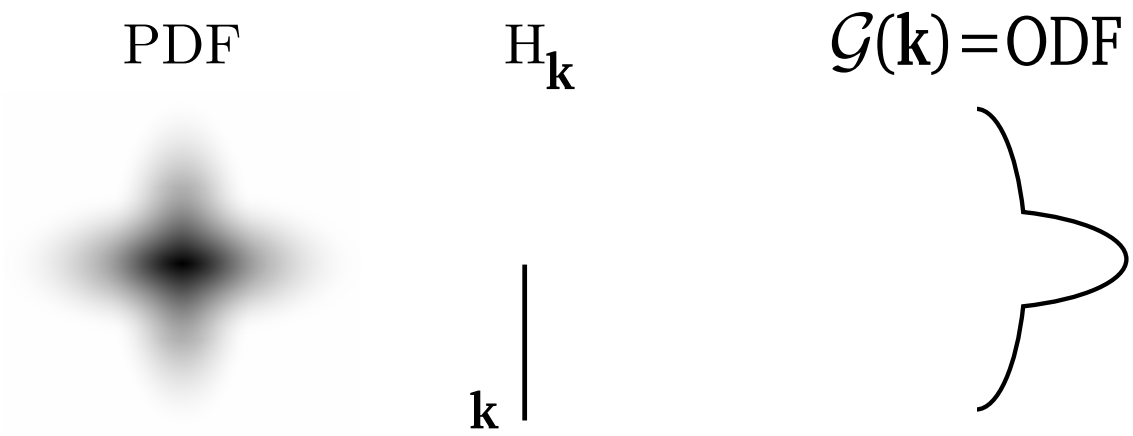

Figure: Example: ODF feature.

$$\mathcal{G}(\mathbf{k}) = \int_{p \in \mathbb{R}^3} PDF(\mathbf{p})\, H_{\mathbf{k}}(\mathbf{p}) d\mathbf{p} \tag{4}$$

Features of the PDF: projection

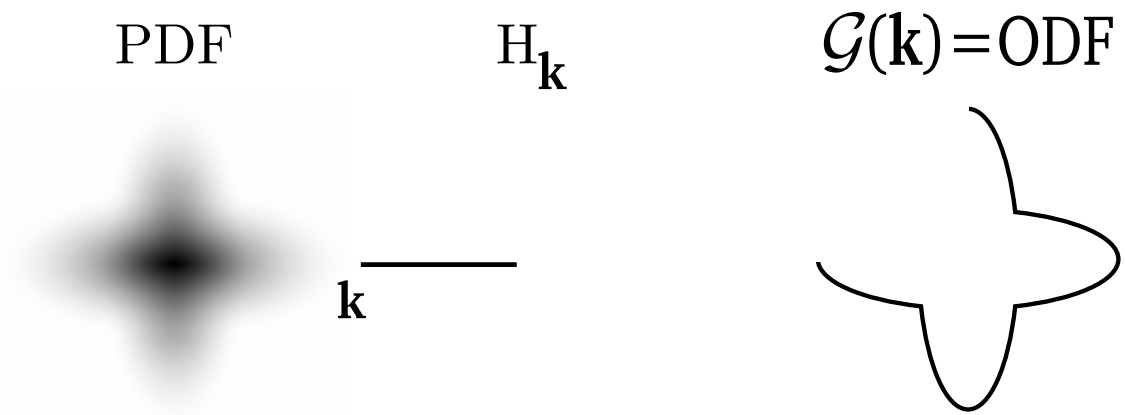

Figure: Example: ODF feature.

$$\mathcal{G}(\mathbf{k}) = \int_{p \in \mathbb{R}^3} PDF(\mathbf{p})\, H_{\mathbf{k}}(\mathbf{p}) d\mathbf{p} \tag{4}$$

Features of the PDF: projection

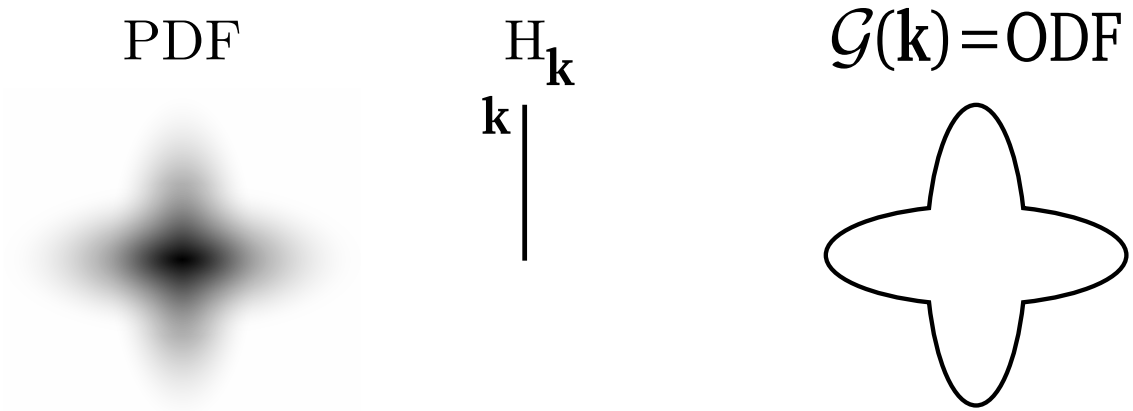

Figure: Example: ODF feature.

$$\mathcal{G}(\mathbf{k}) = \int_{p \in \mathbb{R}^3} PDF(\mathbf{p})\, H_{\mathbf{k}}(\mathbf{p}) d\mathbf{p} \tag{4}$$

Features of the PDF: projection

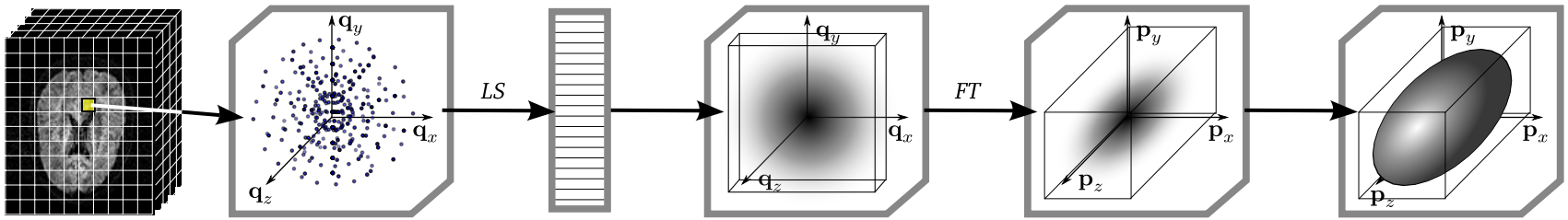

$$\mathcal{G}(\mathbf{k}) = \int_{p \in \mathbb{R}^3} PDF(\mathbf{p})\, H_{\mathbf{k}}(\mathbf{p}) d\mathbf{p}$$

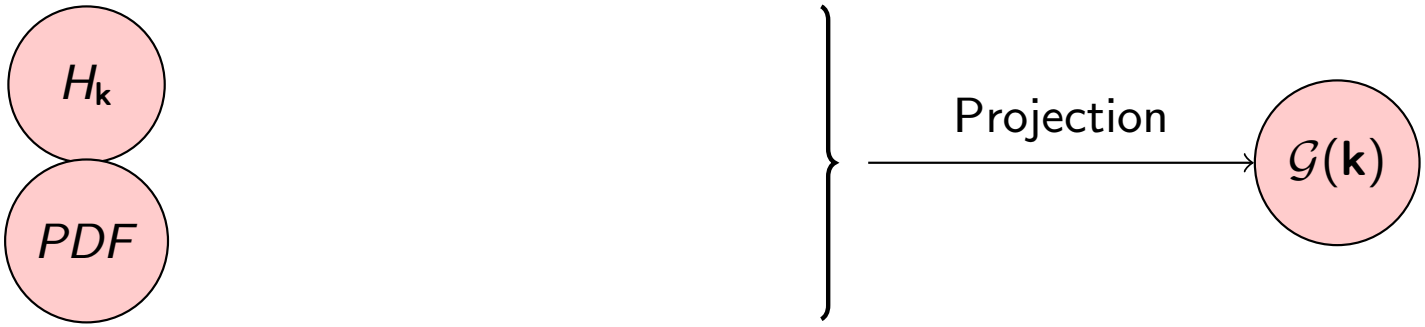

Figure: Overview of the algorithm for the *fast computation* of a PDF feature $\mathcal{G}$ at point $\mathbf{k}$

Features of the PDF: projection

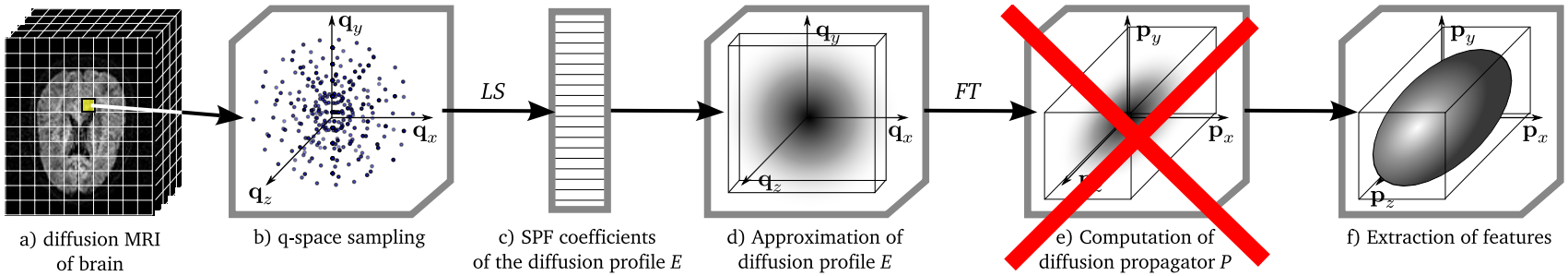

$$\mathcal{G}(\mathbf{k}) = \int_{p \in \mathbb{R}^3} PDF(\mathbf{p})\, H_{\mathbf{k}}(\mathbf{p}) d\mathbf{p}$$

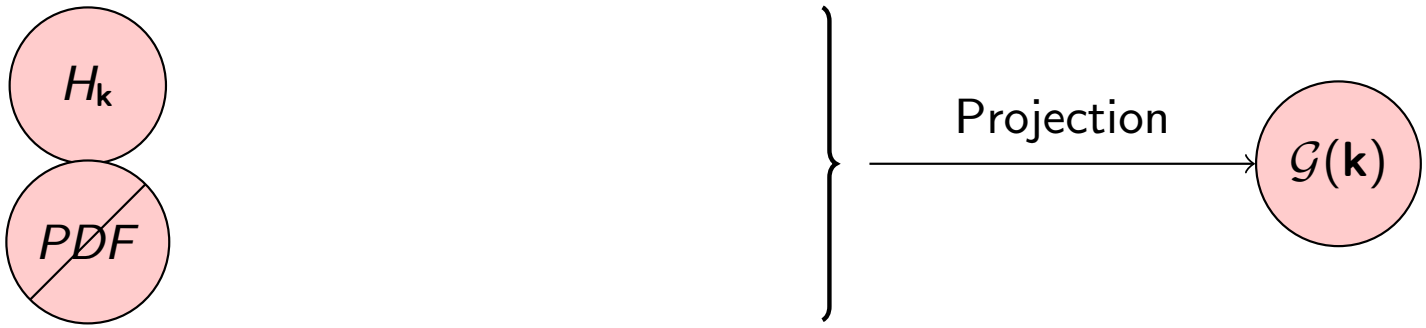

Figure: Overview of the algorithm for the *fast computation* of a PDF feature $\mathcal{G}$ at point $\mathbf{k}$

Features of the PDF: projection

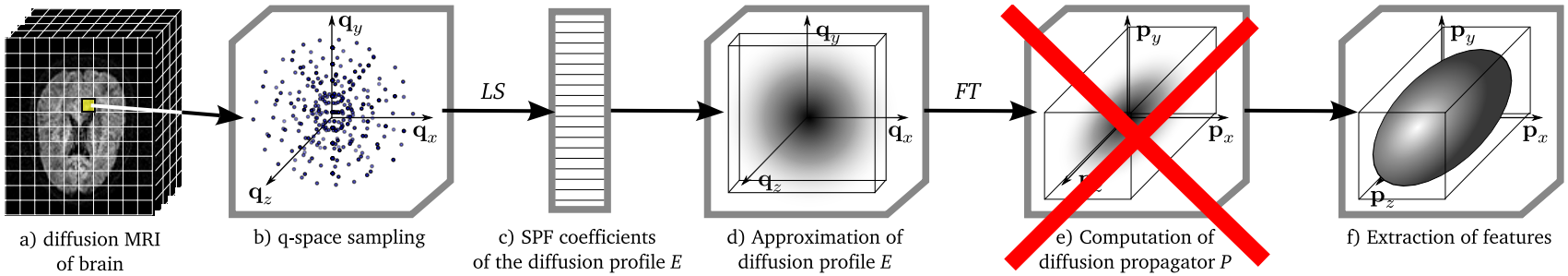

$$\mathcal{G}(\mathbf{k}) = \int_{q \in \mathbb{R}^3} E(\mathbf{q})\, h_{\mathbf{k}}(\mathbf{q}) d\mathbf{q}$$

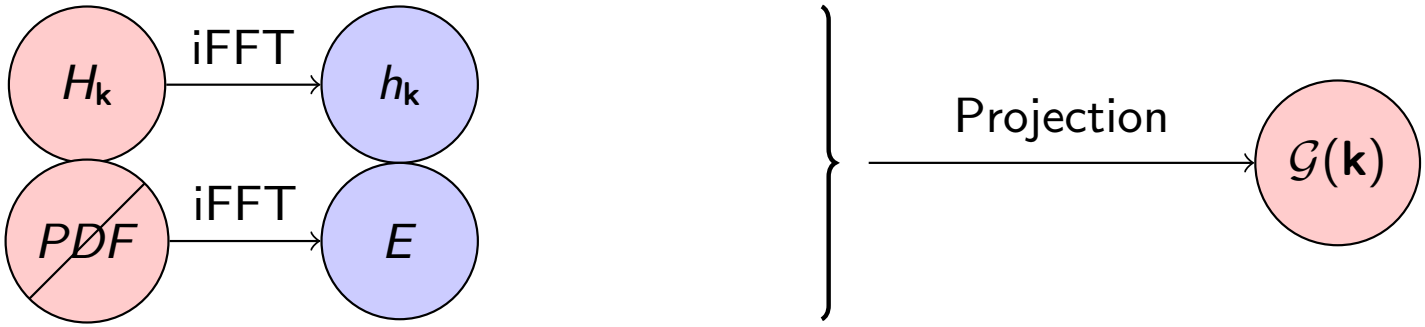

Figure: Overview of the algorithm for the *fast computation* of a PDF feature $\mathcal{G}$ at point $\mathbf{k}$

Features of the PDF: projection

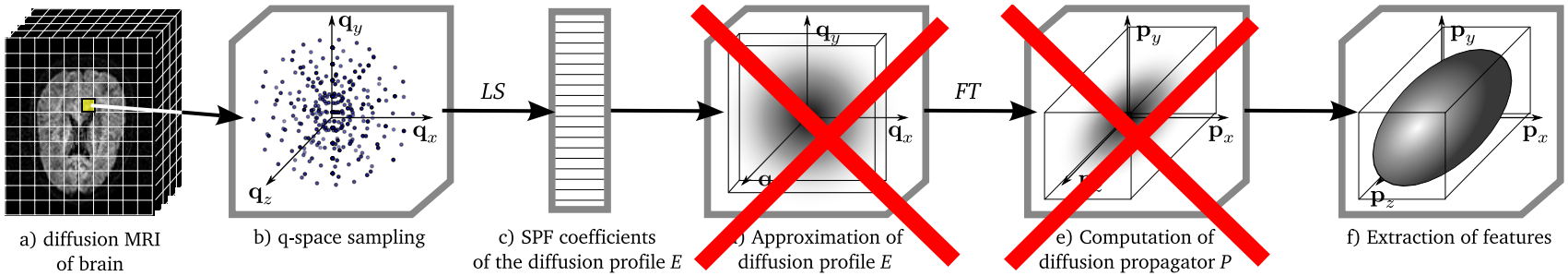

$$\mathcal{G}(\mathbf{k}) = \int_{q \in \mathbb{R}^3} E(\mathbf{q})\, h_{\mathbf{k}}(\mathbf{q}) d\mathbf{q}$$

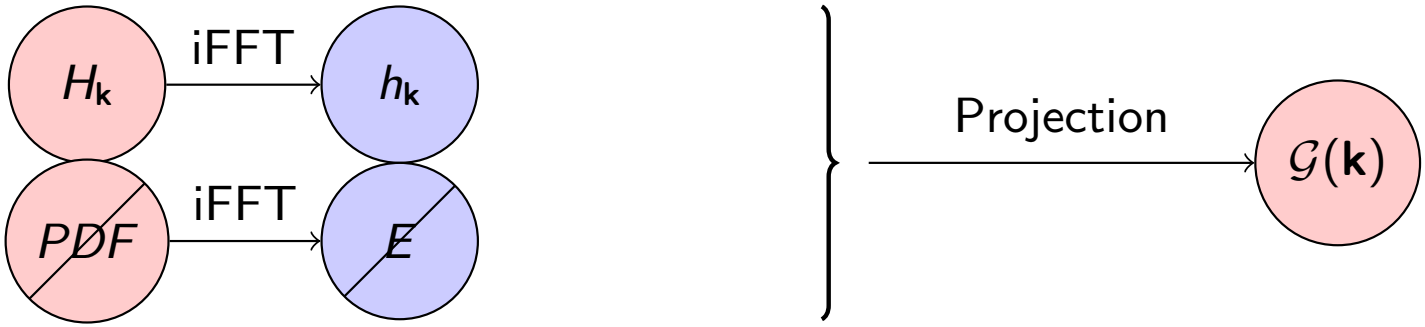

Figure: Overview of the algorithm for the *fast computation* of a PDF feature $\mathcal{G}$ at point $\mathbf{k}$

Features of the PDF: projection

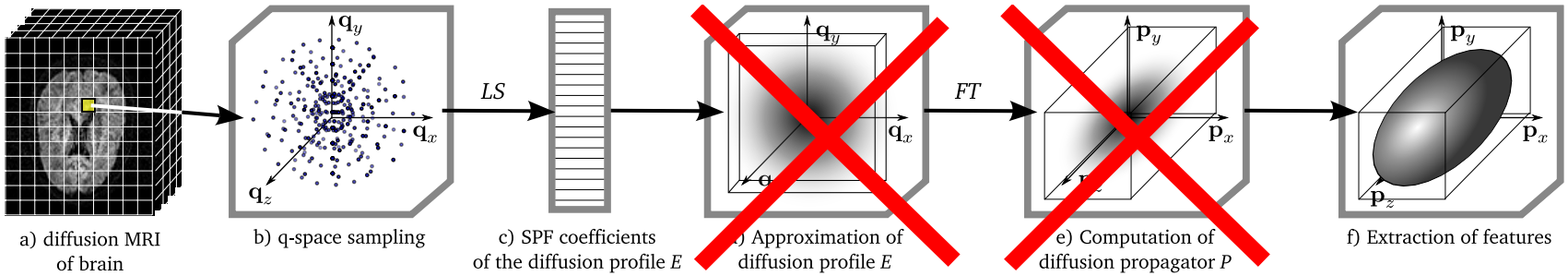

$$\mathcal{G}(\mathbf{k}) = \sum_{n,l,m}^{\infty} a_{nlm} h^{\mathbf{k}}_{nlm}$$

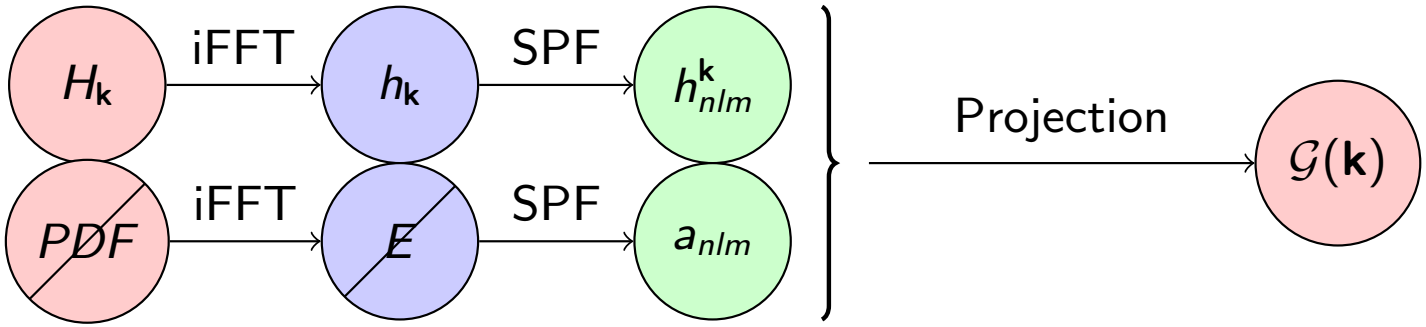

Figure: Overview of the algorithm for the *fast computation* of a PDF feature $\mathcal{G}$ at point $\mathbf{k}$

1. Diffusion signal estimation
   - Continuous representation of the signal
2. Extraction of various features of the PDF
   - Algorithm
   - Overview of proposed features
3. Robust extraction of diffusion features
   - Robustness to noise
   - Robustness to q-space sampling

Features of the PDF

Features $\mathcal{G}$	Domain $\mathcal{M}$
Moments	–
Return to zero	–
Anisotropy	–
Mean radial diffusion	$\mathbb{R}$
Funk-Radon Transform (FRT)	$\mathcal{S}^2$
Orientation Density Function (ODF)	$\mathcal{S}^2$
Isoradius (ISO)	$\mathcal{S}^2$
Displacement PDF	$\mathbb{R}^3$
Diffusion signal E	$\mathbb{R}^3$

Table: Overview of proposed features $\mathcal{G}$ of the PDF.

Moments

Moments of the diffusion PDF of order $a+b+c$ are expressed as the scalar product between P and H^{abc}:

$$\mathcal{G}_{abc} = \int_{\mathbf{p}\in\mathbb{R}^3} P(\mathbf{p}) H^{abc}(\mathbf{p}) \mathrm{d}\mathbf{p} \quad \text{avec} \quad H^{abc}(\mathbf{p}) = p_x^a p_y^b p_z^c$$

These moments can be grouped as a tensor of order $a+b+c$, so that the DTI is a special case with $a+b+c=2$.

$$\mathrm{DTI} = \begin{pmatrix} \mathcal{G}_{200} & \mathcal{G}_{110} & \mathcal{G}_{101} \\ \mathcal{G}_{110} & \mathcal{G}_{020} & \mathcal{G}_{011} \\ \mathcal{G}_{101} & \mathcal{G}_{011} & \mathcal{G}_{002} \end{pmatrix}$$

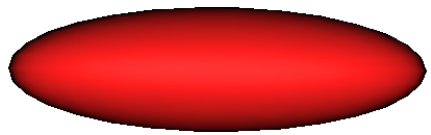

Funk-Radon Transform (FRT)

The Funk-Radon transform approximates the ODF. It is used by HARDI methods such as the Q-Ball Imaging.

The FRT feature is written as:

$$\mathcal{G}(\mathbf{k}) = \int_{\mathbf{p}\in\mathbb{R}^3} H_{\mathbf{k}}(\mathbf{p}) P(\mathbf{p}) \mathrm{d}\mathbf{p}$$

where $H_{\mathbf{k}}$ is the associated projection function at point $\mathbf{k} \in \mathcal{S}^2$. Let $q' \in \mathbb{R}$ be the sampling radius of the q-sphere and $\mathbf{p} = p\mathbf{r}$, so that [Tuch04]:

$$H_{\mathbf{k}}(\mathbf{p}) = 2\pi q' J_0(2\pi q' p) \delta\left(1 - \mathbf{r}\cdot\mathbf{k}\right)$$

Funk-Radon Transform (FRT)

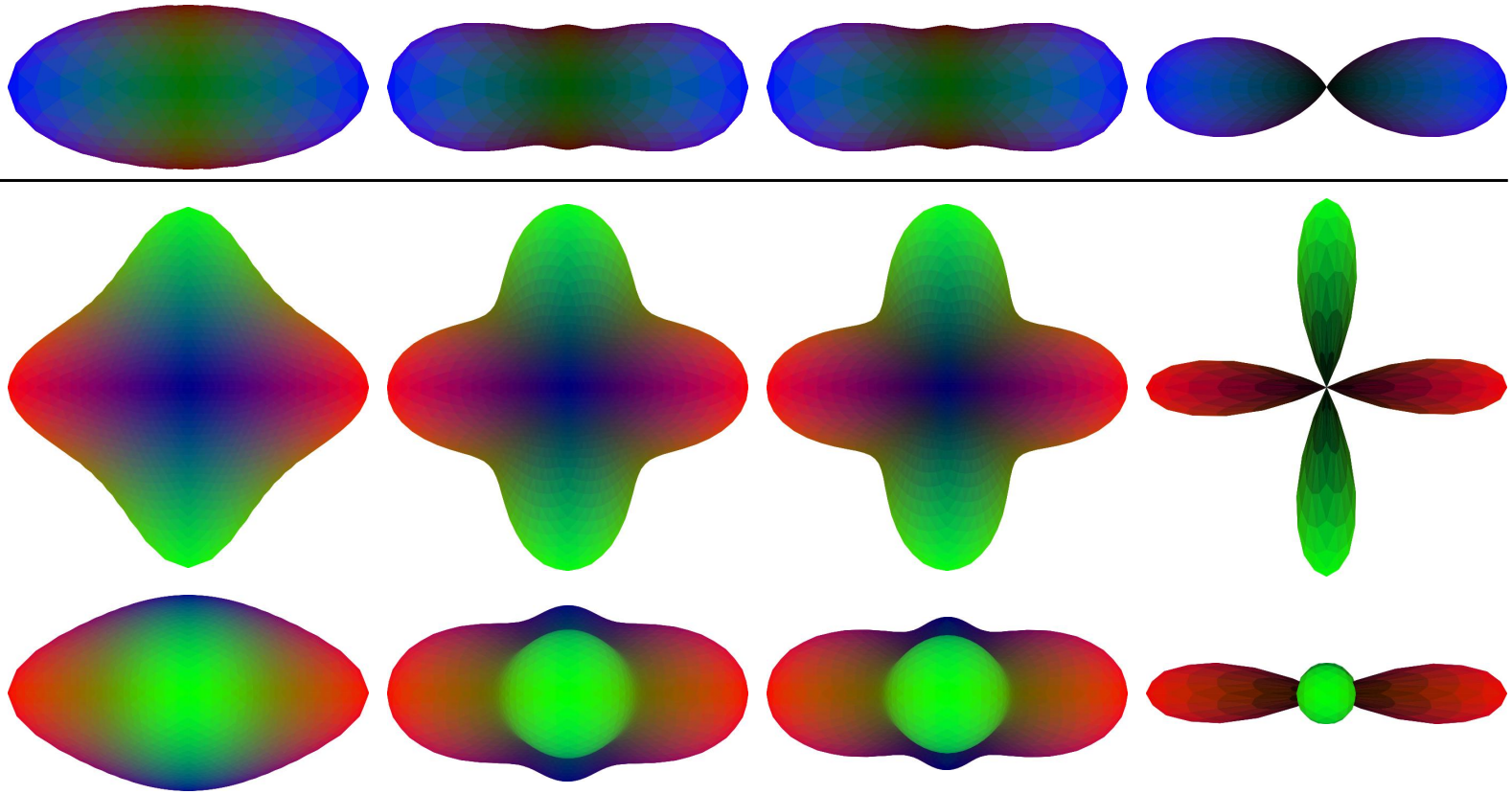

(a) ODF exacte	(b) QBI	(c) $\mathcal{G}$=FRT	(d) $\mathcal{G}$=FRT
–		Low resolution	

Figure: Reproduction of the QBI method by our approach.

ODF

The diffusion orientation density function (ODF) is the projection of the PDF on the unit sphere.
This feature is expressed as:

$$\mathcal{G}(\mathbf{k}) = \int_{\mathbf{p}\in\mathbb{R}^3} P(\mathbf{p}) H_{\mathbf{k}}(\mathbf{p}) \mathrm{d}\mathbf{p}$$

where $H_{\mathbf{k}}$ is

$$H_{\mathbf{k}}(\mathbf{p}) = \delta(1 - \mathbf{r}\cdot\mathbf{k})$$

ODF

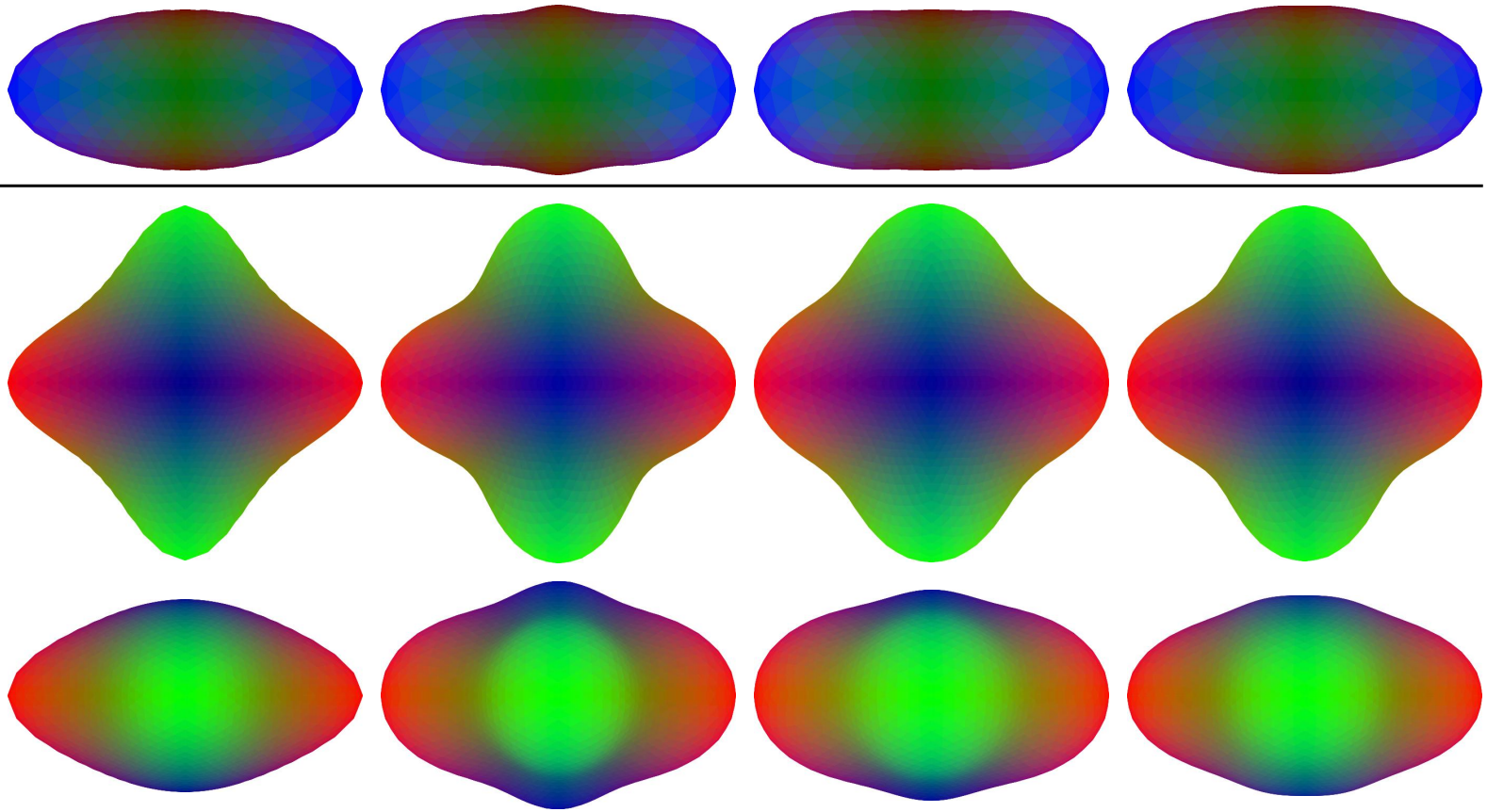

(a) True ODF	(b) $\mathcal{G}$=ODF	(c) $\mathcal{G}$=ODF	(d) $\mathcal{G}$=ODF
–	Low Res.	Med. Res.	High Res.

Figure: ODF approximation at low, medium and high resolution.

Results of *in-vivo* experiences

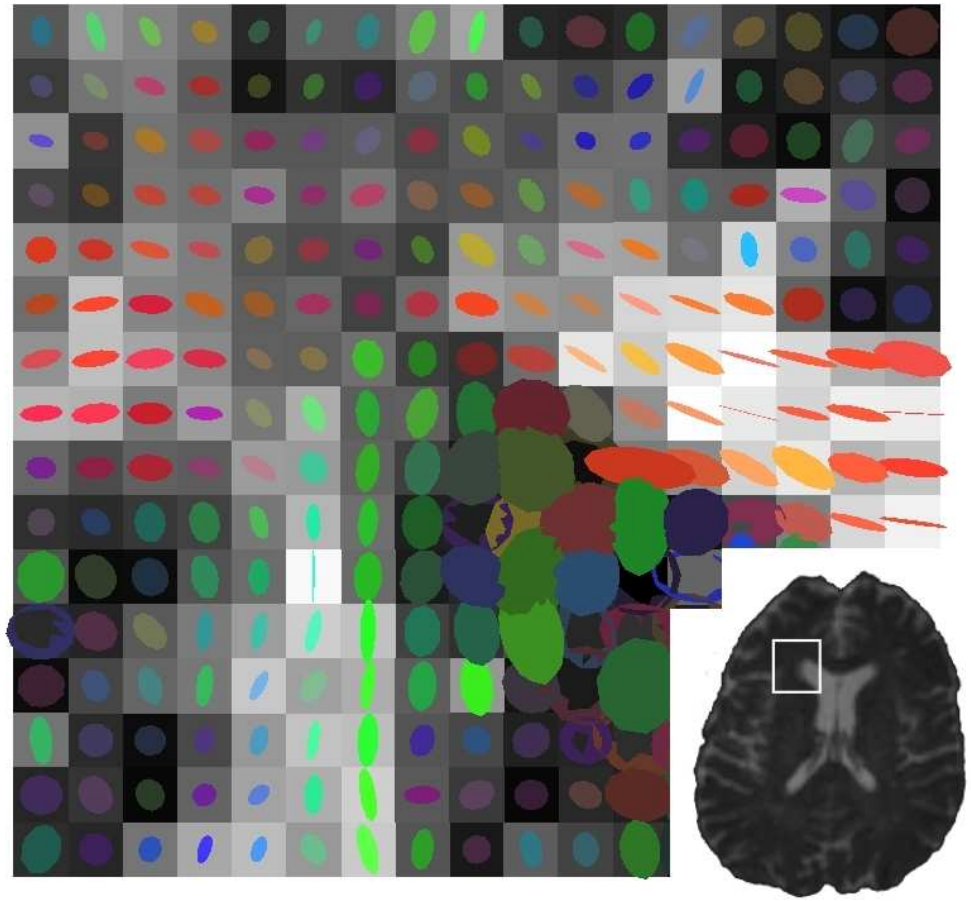

(a) DTI (Basser94)

Figure: Brain white matter: ODF overlayed on a GFA map.
DTI(a) and QBI(b) were computed with $b = 3000\,\mathrm{s/mm^2}$.
Our method (c) shows the obtained ODF with $b = 1000$ and $3000\mathrm{s/mm^2}$.

Results of *in-vivo* experiences

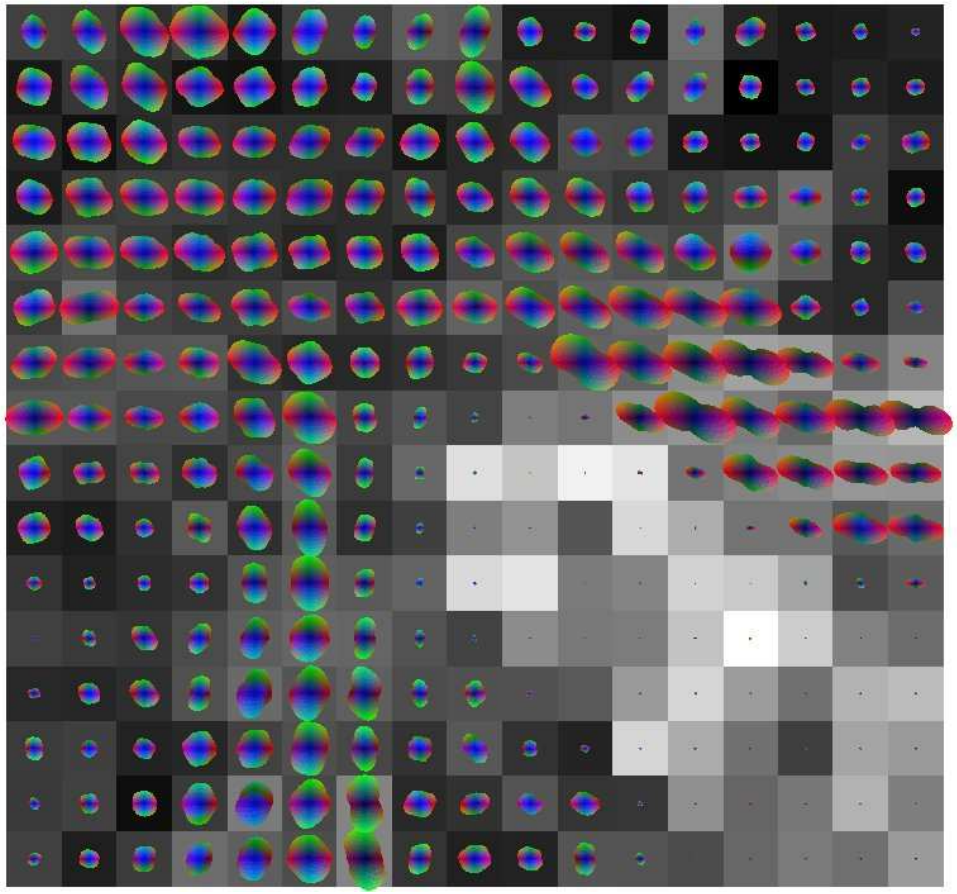

(a) QBI (Descoteaux07)

Figure: Brain white matter: ODF overlayed on a GFA map.
DTI(a) and QBI(b) were computed with $b = 3000\,\mathrm{s/mm^2}$.
Our method (c) shows the obtained ODF with $b = 1000$ and $3000\mathrm{s/mm^2}$.

Results of *in-vivo* experiences

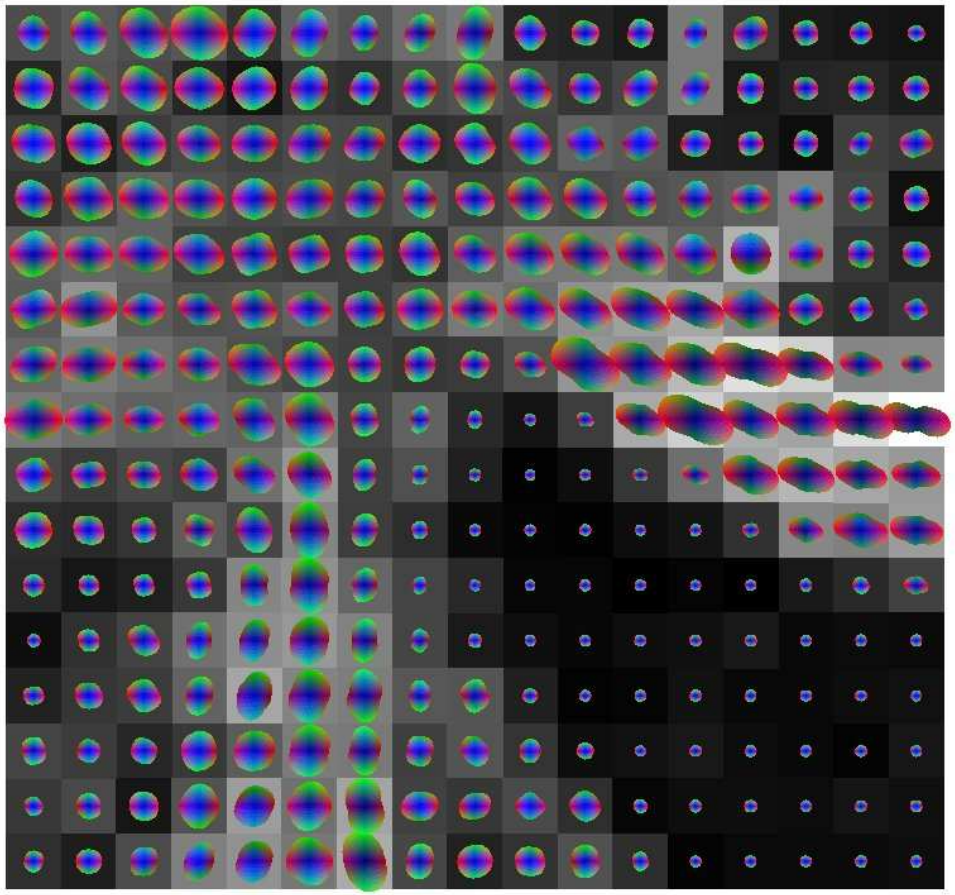

(a) Our method, $\mathcal{G}$=ODF

Figure: Brain white matter: ODF overlayed on a GFA map.
DTI(a) and QBI(b) were computed with $b = 3000\,\mathrm{s/mm^2}$.
Our method (c) shows the obtained ODF with $b = 1000$ and $3000\mathrm{s/mm^2}$.

Anisotropy

The anisotropy is a scalar measure which is useful to have hindsight on the wiring structure of the nerve fibers across the brain.

The generalized fractional anisotropy feature, which generalizes the fractional anisotropy (FA), is expressed as:

$$\mathrm{GFA}(\mathcal{G}) = \frac{\mathrm{std}(\mathcal{G})}{\mathrm{rms}(\mathcal{G})} = \sqrt{\frac{\int_{\mathbf{k}\in\boldsymbol{\mathcal{S}}^2}(\mathcal{G}(\mathbf{k}) - \langle\mathcal{G}\rangle)^2 \mathrm{d}\mathbf{k}}{\int_{\mathbf{k}\in\boldsymbol{\mathcal{S}}^2}\mathcal{G}(\mathbf{k})^2 \mathrm{d}\mathbf{k}}}$$

where $\mathcal{G} : \boldsymbol{\mathcal{S}}^2 \to \mathbb{R}$ is a spherical feature of the PDF (*e.g.* $\mathcal{G} =$ FRT,ODF,ISO, *etc.*).

Anisotropy

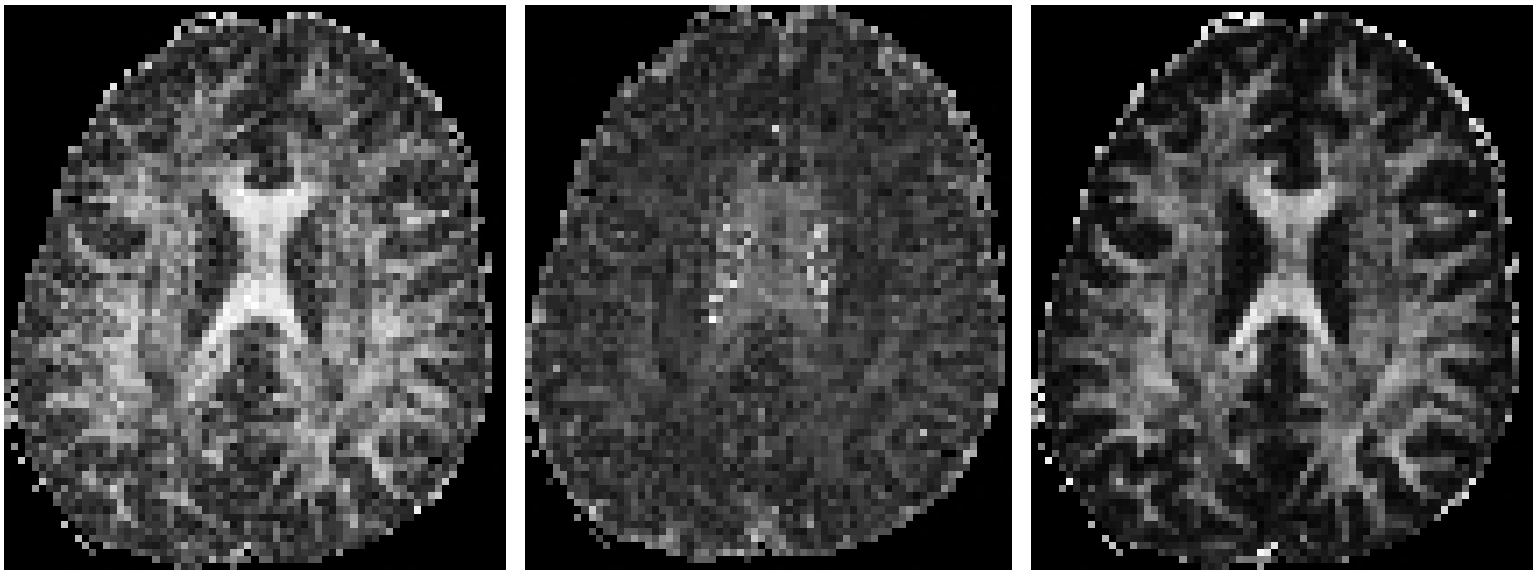

(a) FA sur DTI (b) GFA sur FRT (c) GFA sur ODF

Figure: Anisotropy of several spherical features. (a)-(c) Anisotropy based on the DTI, QBI et true ODF.

More details in the manuscript

Features $\mathcal{G}$	Domain $\mathcal{M}$
Moments	–
Return to zero	–
Anisotropy	–
Mean radial diffusion	$\mathbb{R}$
Funk-Radon Transform (FRT)	$\mathcal{S}^2$
Orientation Density Function (ODF)	$\mathcal{S}^2$
Isoradius (ISO)	$\mathcal{S}^2$
Displacement PDF	$\mathbb{R}^3$
Diffusion signal E	$\mathbb{R}^3$

Table: Overview of proposed features $\mathcal{G}$ of the PDF.

1. Diffusion signal estimation
   - Continuous representation of the signal
2. Extraction of various features of the PDF
   - Algorithm
   - Overview of proposed features
3. Robust extraction of diffusion features
   - Robustness to noise
   - Robustness to q-space sampling

1. Diffusion signal estimation
   - Continuous representation of the signal
2. Extraction of various features of the PDF
   - Algorithm
   - Overview of proposed features
3. Robust extraction of diffusion features
   - Robustness to noise
   - Robustness to q-space sampling

Robustness to noise

Problem

Acquisition noise not Gaussian but Rician.

Nontheless most methods use least square estimation !

$\Rightarrow$ **Bias especially at low SNR values (high b values).**

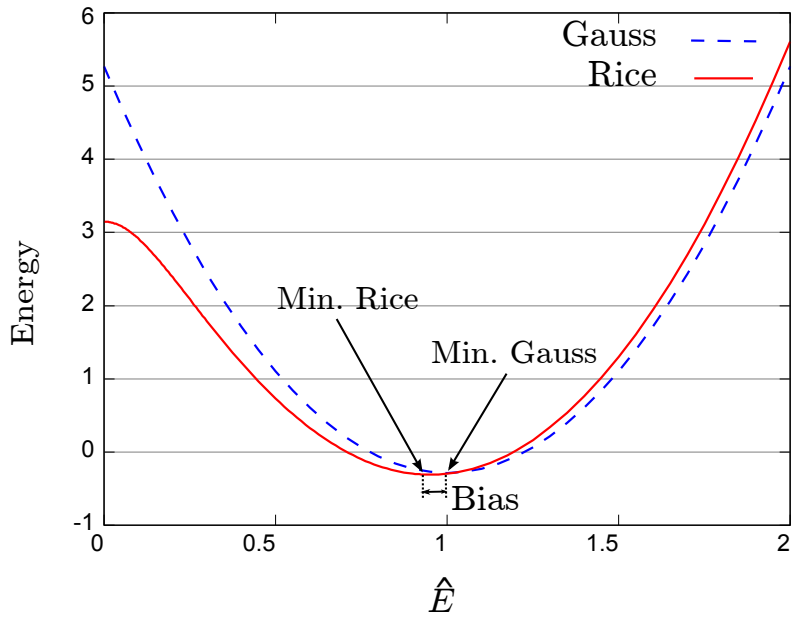

Variational framework

Robustly estimate and regularize the SPF coefficients by minimizing the functional energy:

$$\min_{A} \left\{ \int_{\Omega_E} \left[\sum_{k}^{n_s} \psi(\hat{\mathbf{E}}_k) \right] + \alpha_r \varphi(||\nabla \mathbf{A}||) d\Omega_E \right\}, \text{ with } \hat{\mathbf{E}} = \mathbf{MA} \tag{5}$$

The best fitting coefficients A are computed with a gradient descent coming from the Euler-Lagrange derivation of the energy. This leads to a set of *multi-valued* partial derivate equation.

$$\begin{cases} \mathbf{A}_{t=0} & = U_0 \\ \\ \frac{\partial \mathbf{A}_j}{\partial t} & = \sum_k^{n_s} \mathbf{M}_{k,j} \psi'(\hat{\mathbf{E}}_k) + \alpha_r \operatorname{div}(\varphi(||\nabla \mathbf{A}||)) \end{cases} \tag{6}$$

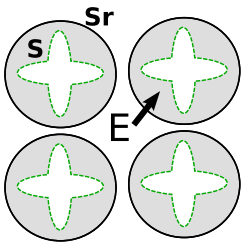

iteration 0

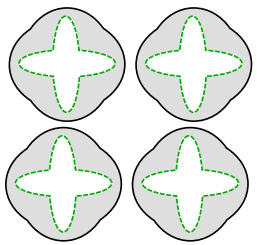

iteration 1

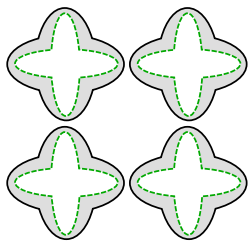

...

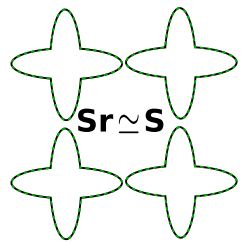

iteration n

Advantages: adaptive to noise distribution

- ψ-likelihood function adapted to MRI noise law:

The best ψ function is the one specific to MR scanners, ie. Rice distribution:

$$p(E|\hat{E},\sigma) = \frac{E}{\sigma^2} \exp\left(\frac{-(E^2+\hat{E}^2)}{2\sigma^2}\right) I_0\left(\frac{E\cdot\hat{E}}{\sigma^2}\right) \tag{7}$$

We seek $\hat{E}$ which maximizes a posteriori (MAP) the log-posterior probability [Basu06]

$$\log p(\hat{E}|E) = \log p(E|\hat{E}) + \log p(\hat{E}) - \log p(E) \tag{8}$$

Consequently the pointwise likelihood is

$$\log p(E|\hat{E},\sigma) = \log \frac{E}{\sigma^2} - \frac{(E^2+\hat{E}^2)}{2\sigma^2} + \log I_0\left(\frac{E\cdot\hat{E}}{\sigma^2}\right) = \psi(\hat{E}) \tag{9}$$

Advantages: regularity

- Ensure a global regularity of the SPF field:
  $\varphi(||\nabla \mathbf{A}||) = \varphi(\sum_{nlm} ||\nabla A_{nlm}||)$

φ is a contour preserving function, widely used in image processing.
Example of possible regularization function φ

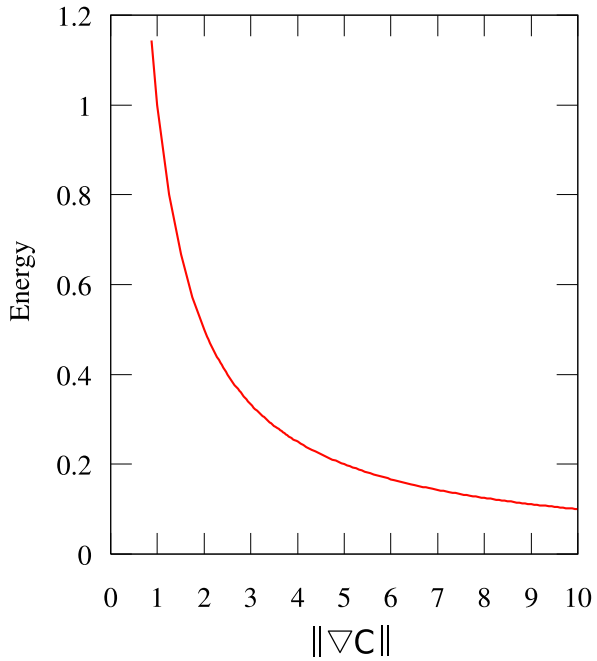

Simulation: validation on synthetical data (likelihood)

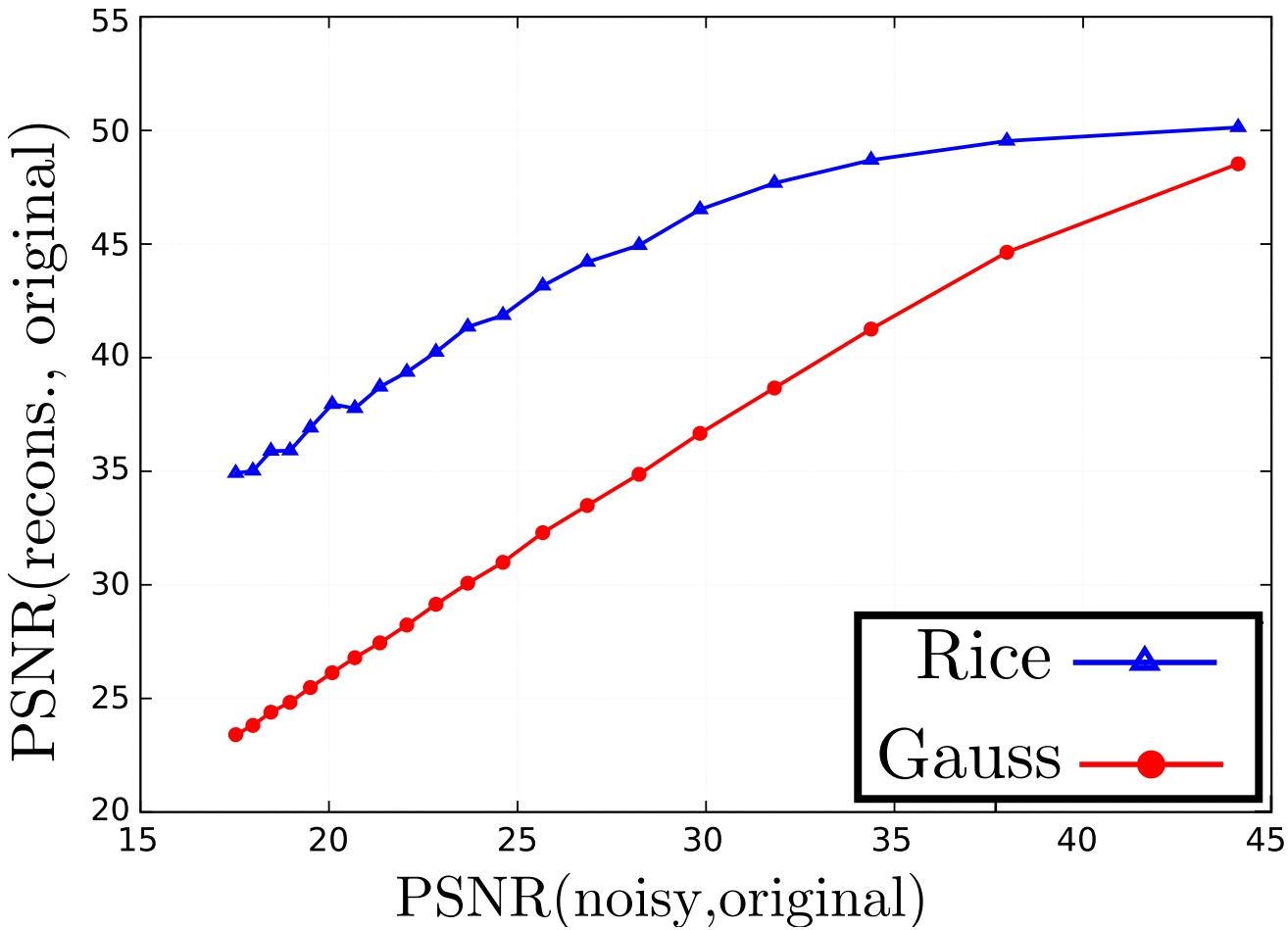

Figure: Synthetic phantom of networks of crossing fibers. Performances of likelihood functions on increasing levels of noise.

Simulation: Rician vs Gaussian likelihood function

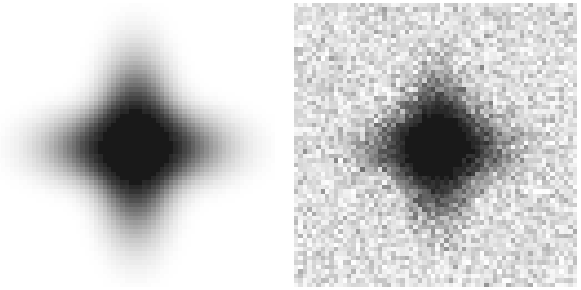

a) Truth b) Noisy

c) Gaussian d) Rician

$|Gauss - Truth|$ $|Rice - Truth|$

Simulation: energy minimization

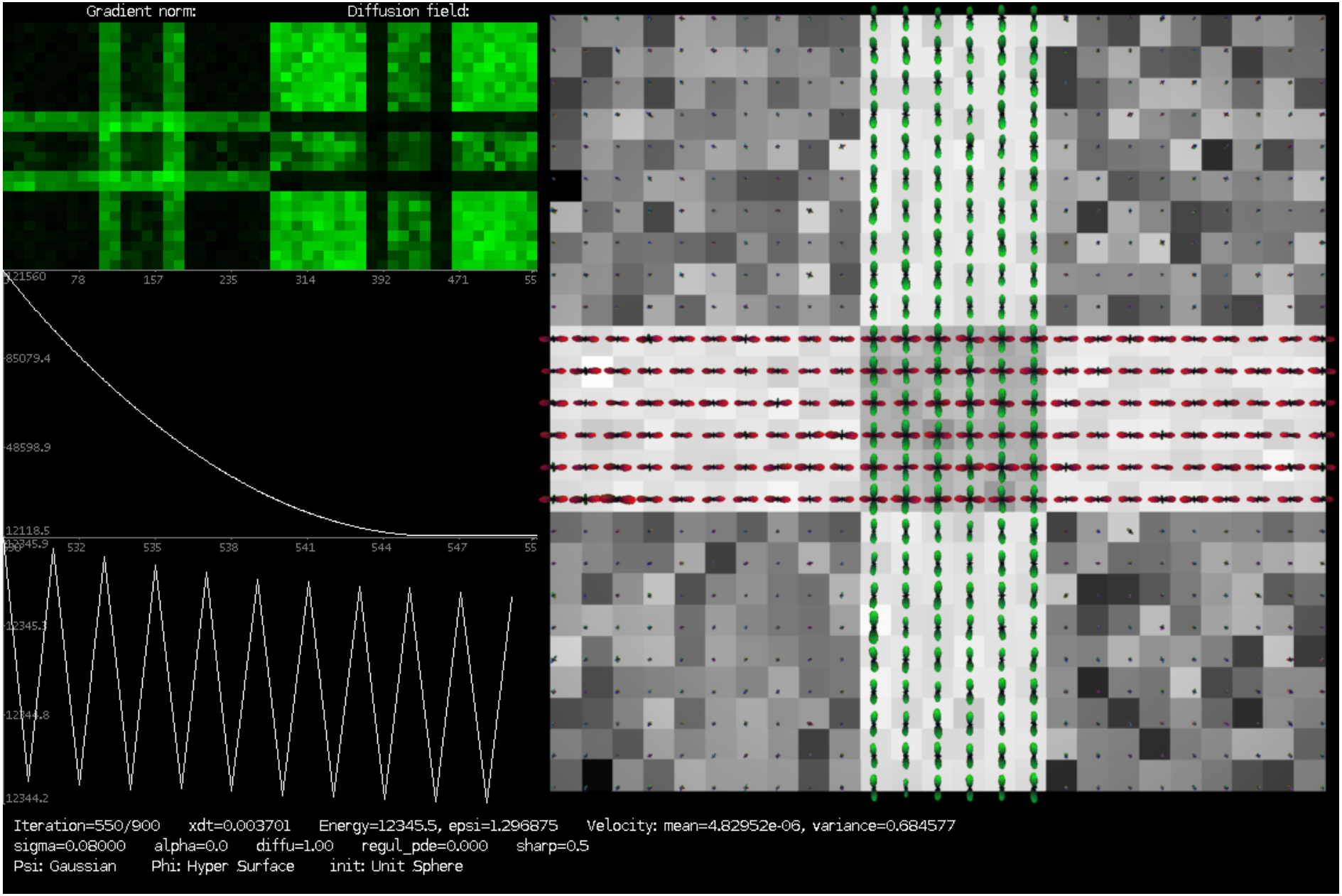

Results of *in-vivo* experiences

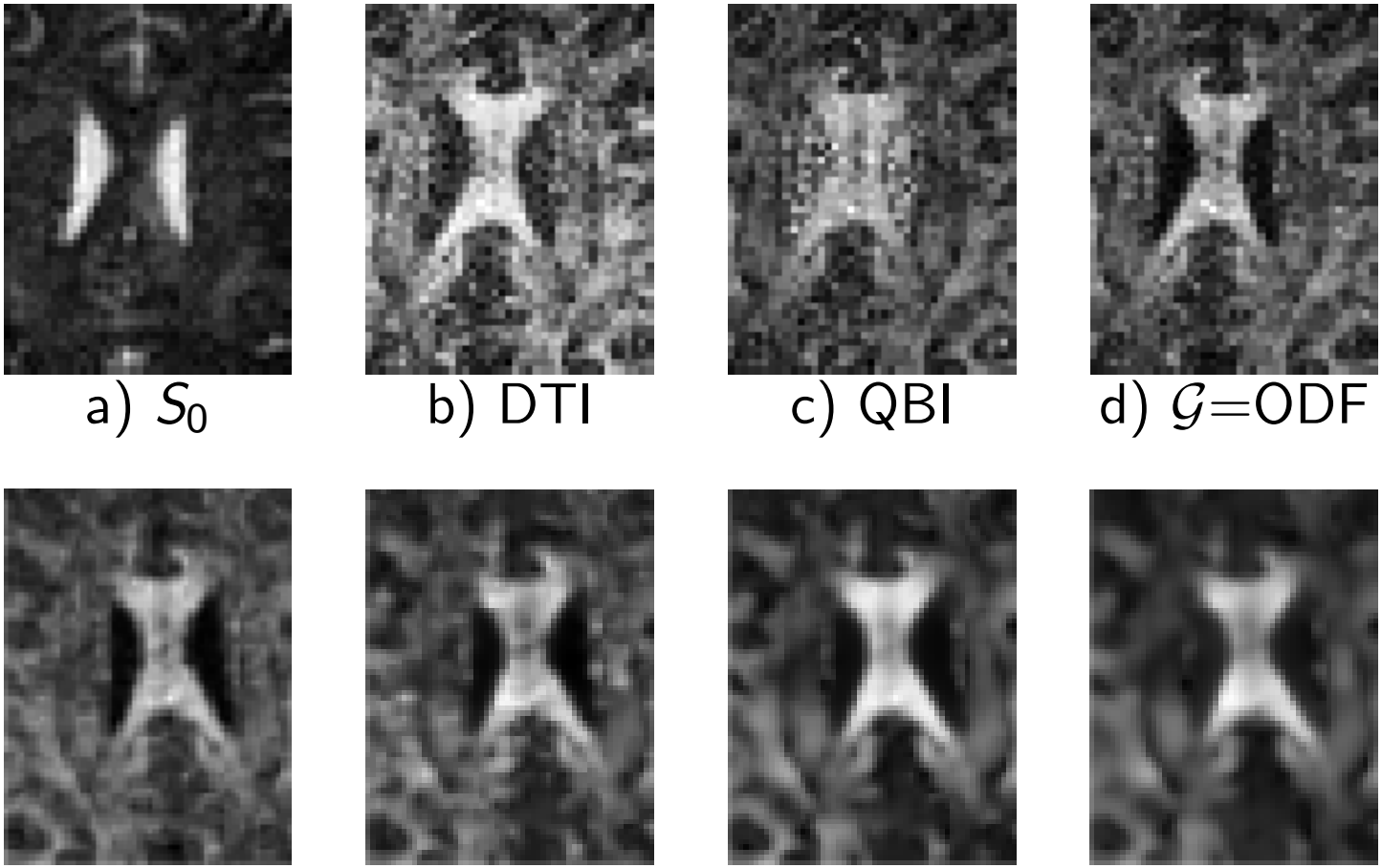

a) S_0 b) DTI c) QBI d) $\mathcal{G}$=ODF

e) Rice f) Soft Reg. g) Med. Reg. h) Strong Reg.

Figure: Comparison of GFA on region of corpus callosum and lateral ventricles.

Fiber-tracking

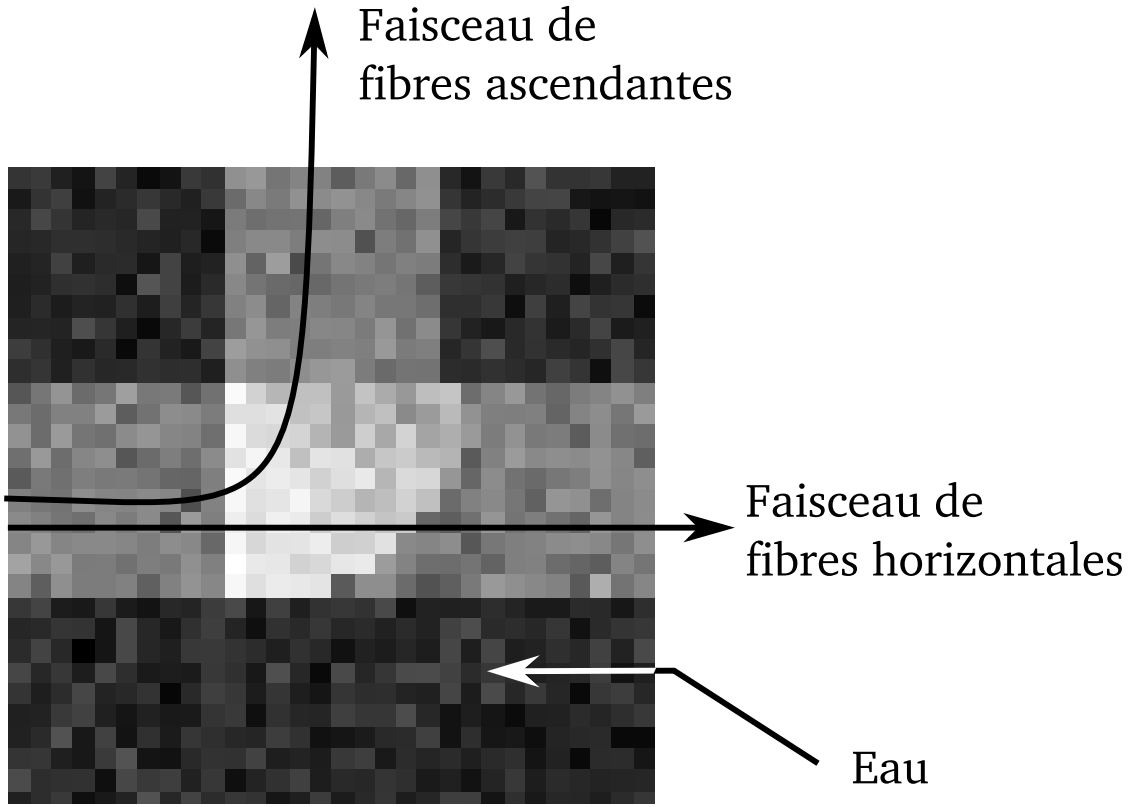

Fiber-tracking

GFA

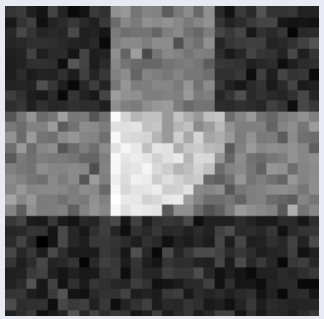

DTI

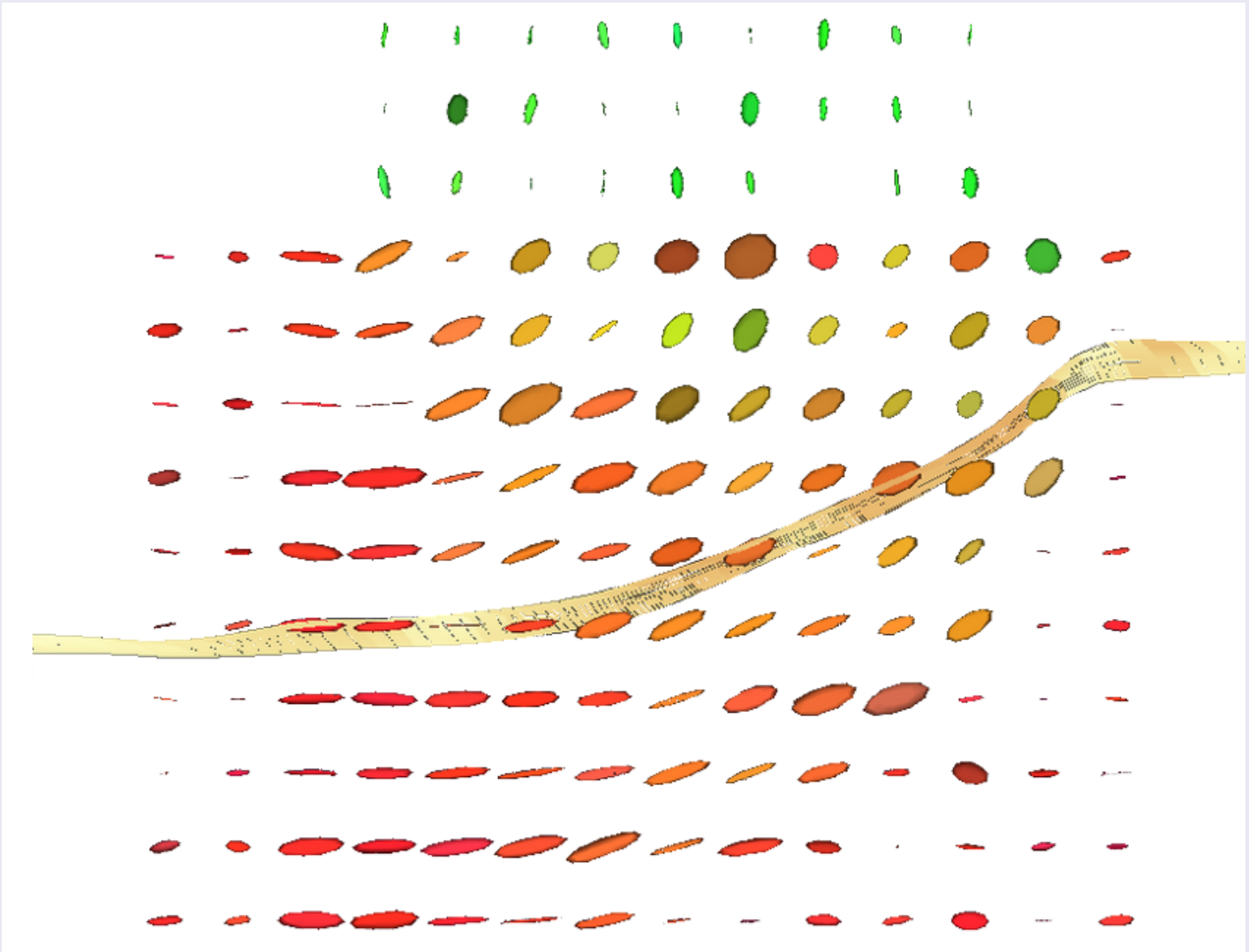

Fiber-tracking

GFA

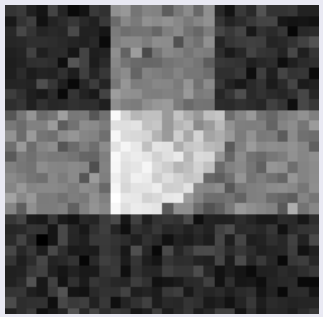

Linear Least Square

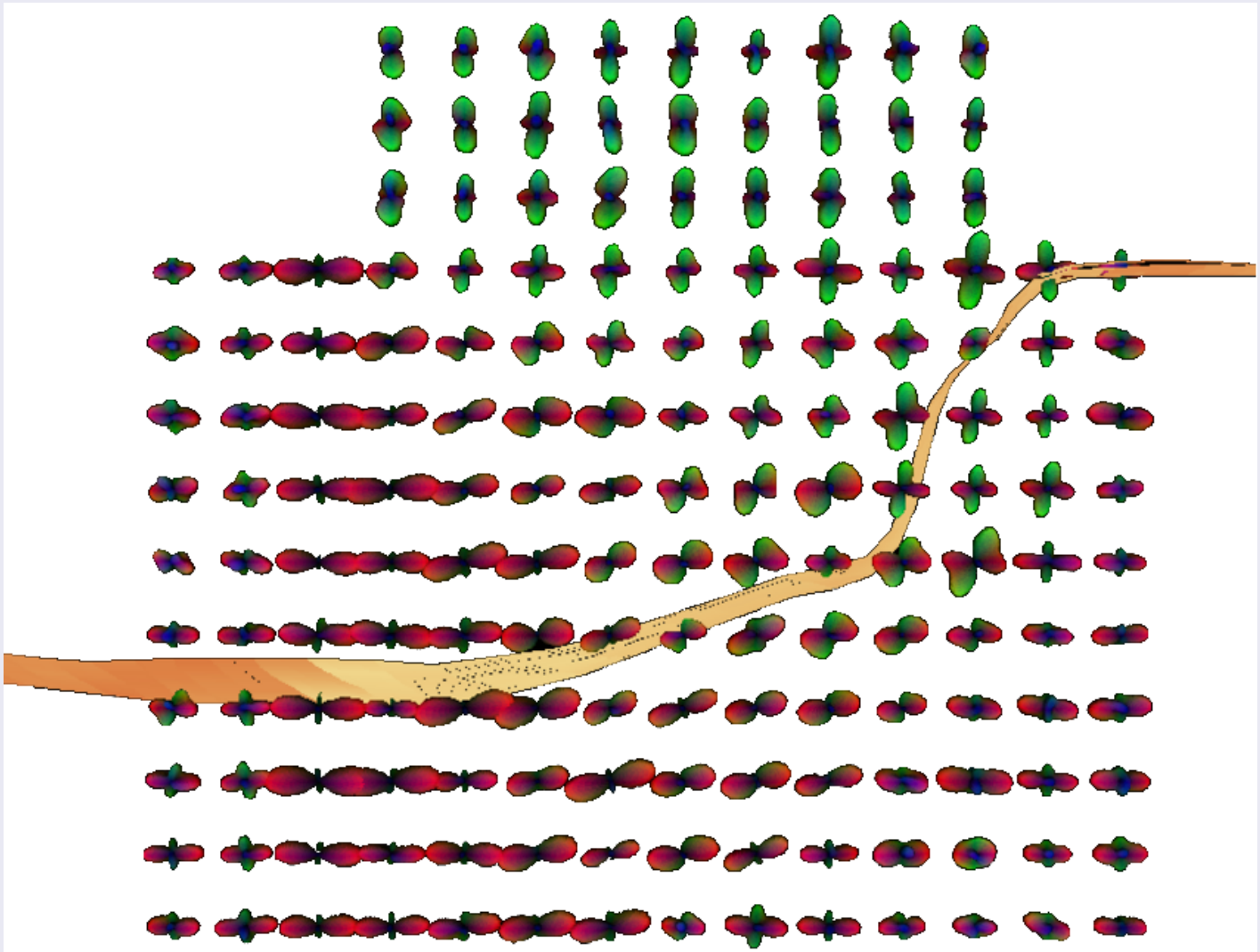

Fiber-tracking

GFA

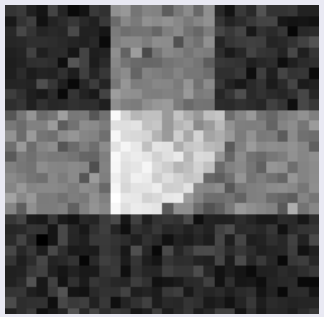

Linear Least Square

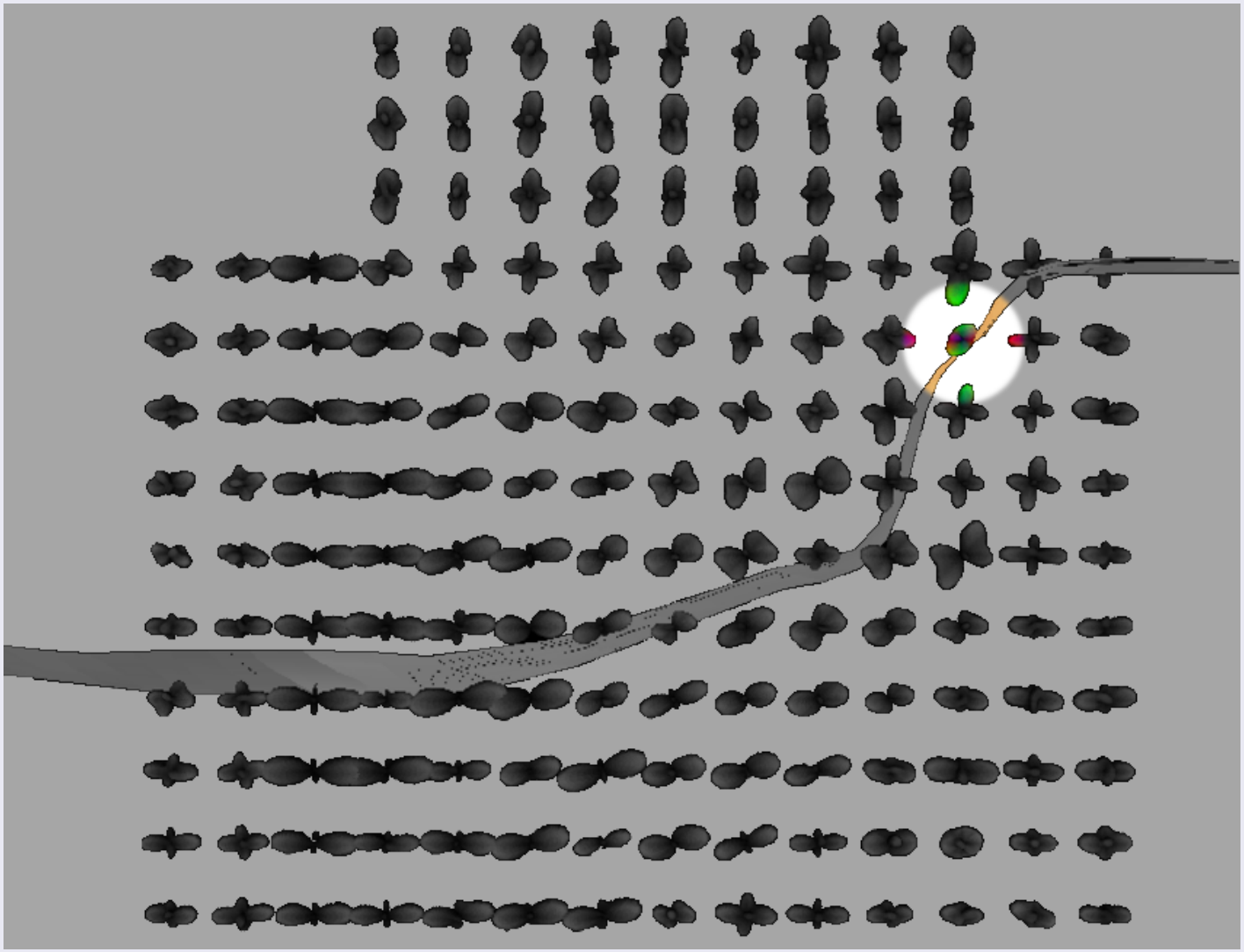

Fiber-tracking

GFA

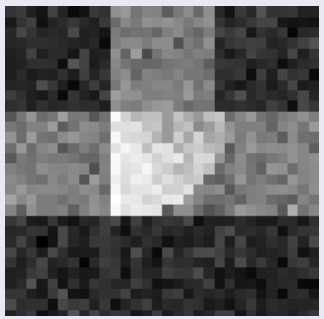

PDE

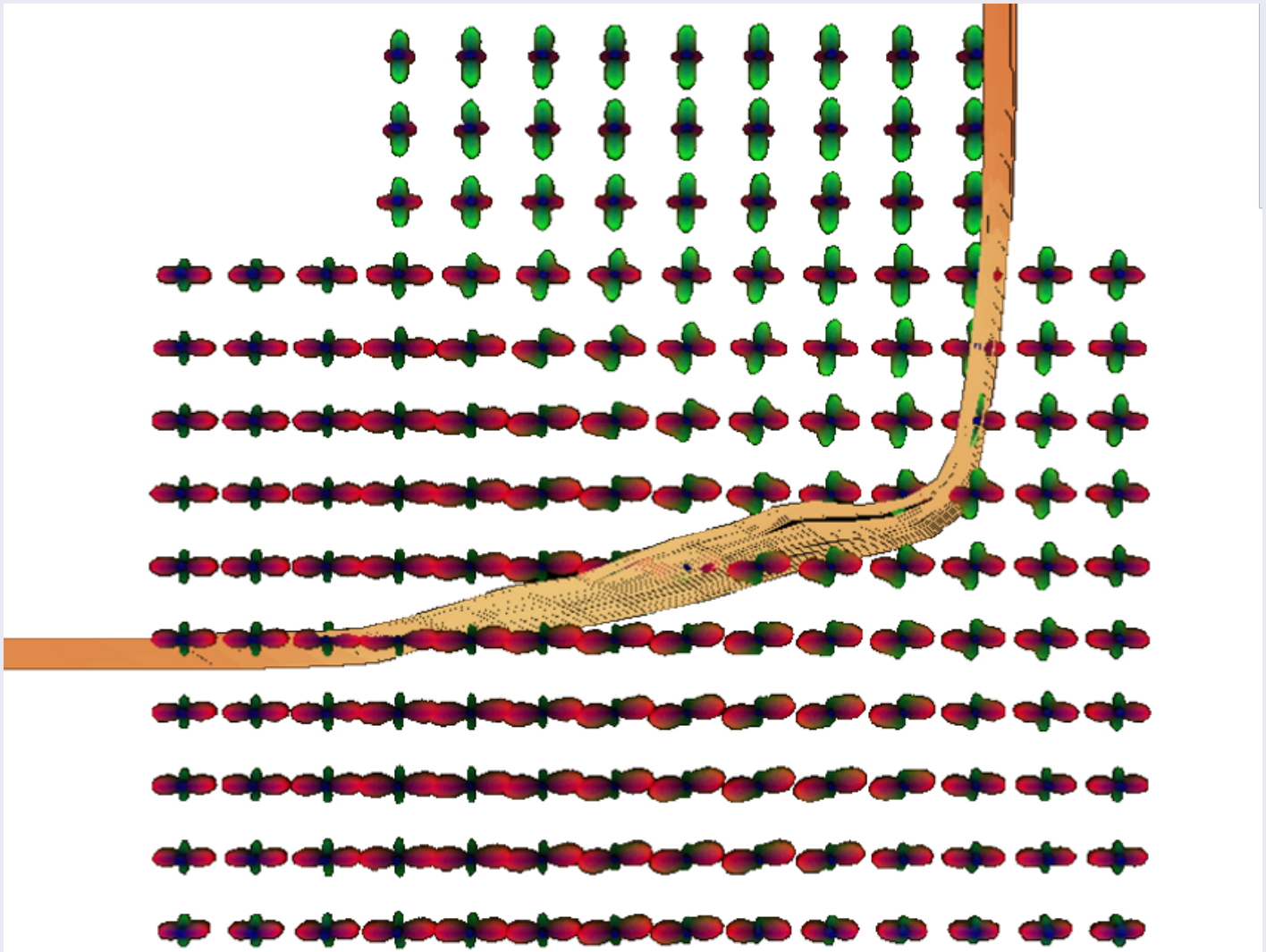

1. Diffusion signal estimation
   - Continuous representation of the signal
2. Extraction of various features of the PDF
   - Algorithm
   - Overview of proposed features
3. Robust extraction of diffusion features
   - Robustness to noise
   - Robustness to q-space sampling

q-space Sampling Distribution

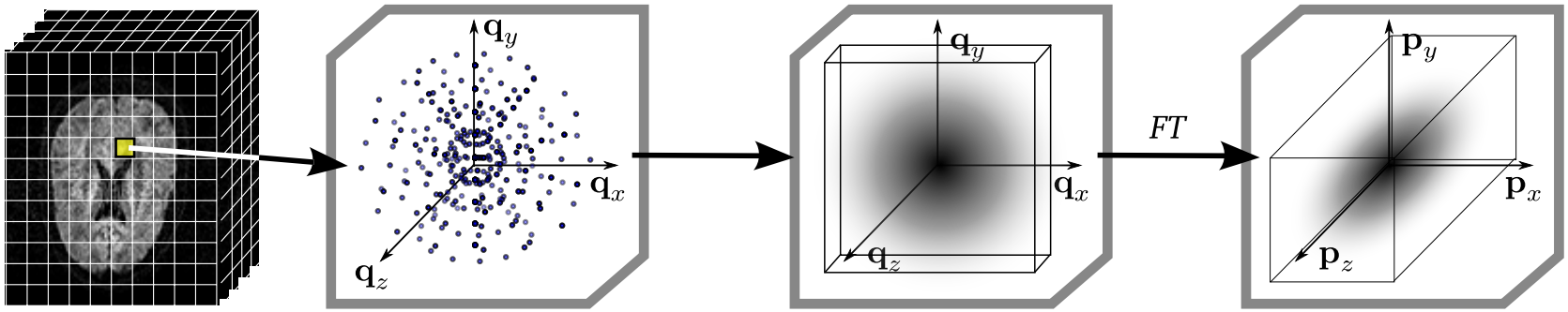

a) diffusion MRI of brain

b) q-space sampling

c) Approximation of diffusion profile E

d) Computation of diffusion propagator P

Questions

q-space Sampling Distribution

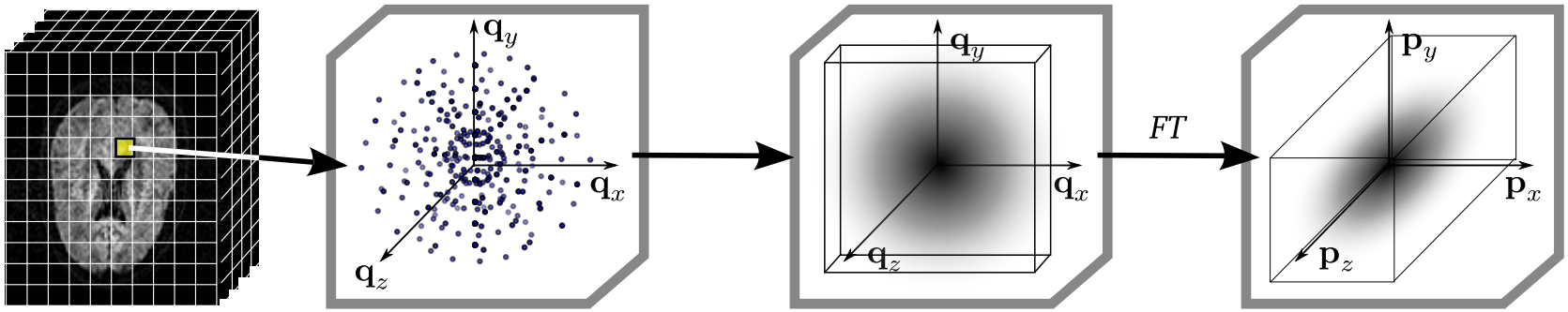

a) diffusion MRI of brain

b) q-space sampling

c) Approximation of diffusion profile E

d) Computation of diffusion propagator P

Questions

- Which sampling distribution gives the best results ?

q-space Sampling Distribution

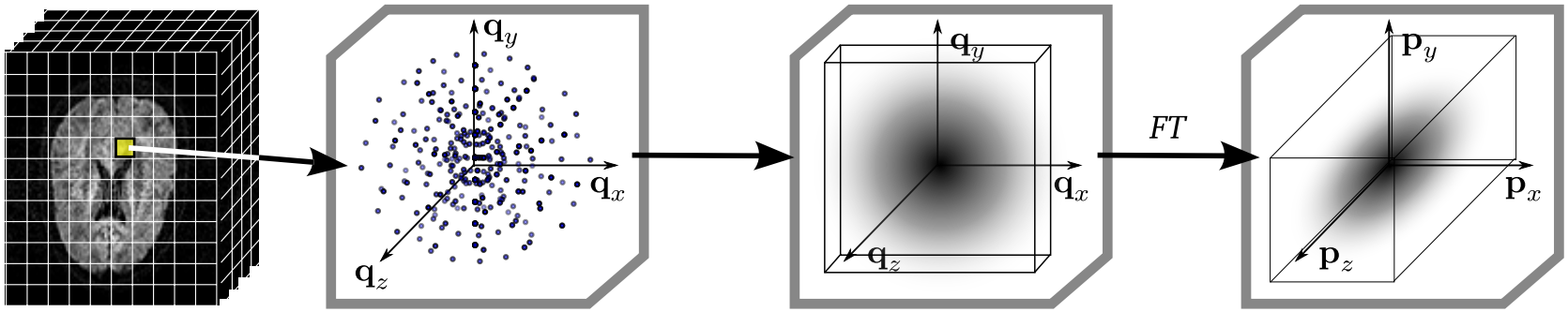

a) diffusion MRI of brain

b) q-space sampling

c) Approximation of diffusion profile E

d) Computation of diffusion propagator P

Questions

- Which sampling distribution gives the best results ?
- Is it possible to unify the sparse sampling in the literature in one model ? [Assaf05, Özarslan06, Wu07, Khachaturian07, Assemlal-et.al08, Assemlal-et.al09]

q-space Sampling Distribution

$$f_x(\eta) = \frac{q_x^\eta}{\sum_{i=1}^{n_b} q_i^\eta} n_s, \quad \text{and} \quad q_i(\beta) = \left(\frac{i-1}{n_b - 1}\right)^\beta (q_{max} - q_{min}) + q_{min}$$

q-space Sampling Distribution

$$f_x(\eta) = \frac{q_x^{\eta}}{\sum_{i=1}^{n_b} q_i^{\eta}} n_s, \quad \text{and} \quad q_i(\beta) = \left(\frac{i-1}{n_b - 1}\right)^{\beta} (q_{max} - q_{min}) + q_{min}$$

	$\eta = -2$	$\eta = -1$	$\eta = 0$	$\eta = 1$	$\eta = 2$	$\eta = 3$
$n_b = 2$	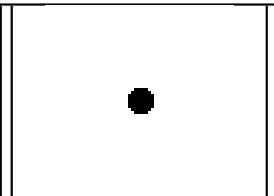	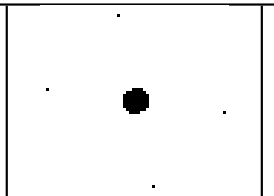	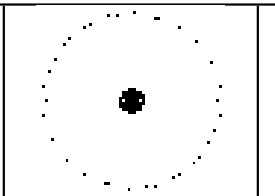	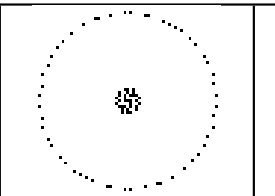	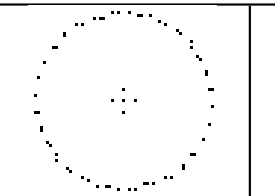	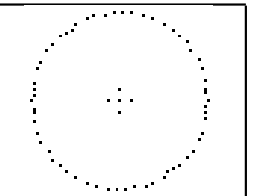
$n_b = 5$	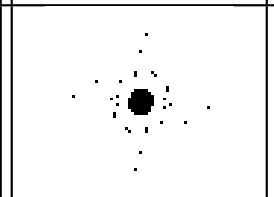	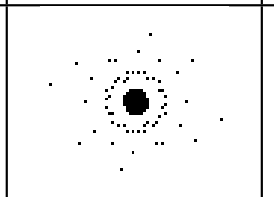	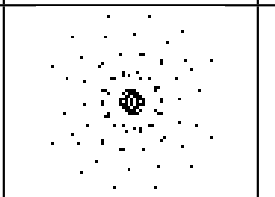	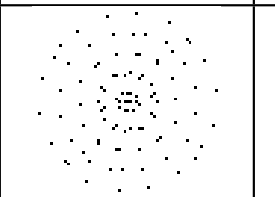	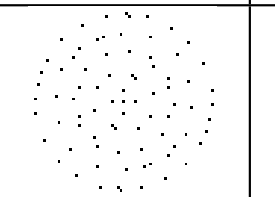	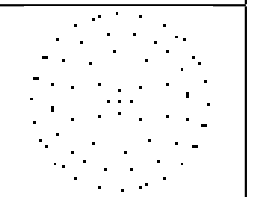
$n_b = 10$	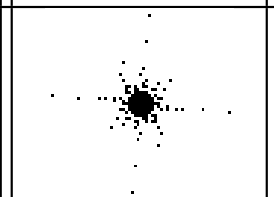	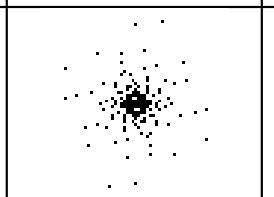	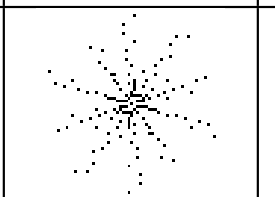	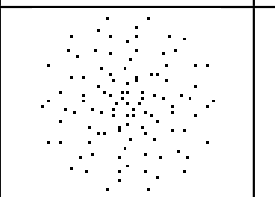	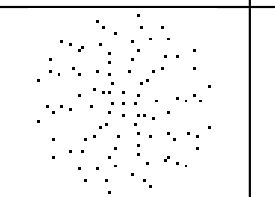	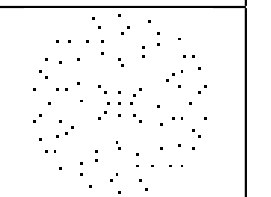

Simulation: q-space Sampling Distribution

Figure: *Condition number* $C = ||\mathbf{M}_{reg}||_\infty ||\mathbf{M}_{reg}^{-1}||_\infty$. The lower C is, the more stable the reconstruction is. Data simulates crossing fibers diffusion signal.
$L = 4, N = 3,\ n_b \geq 3$. (d) $\lambda_n = 10^{-4}$, $\lambda_l = 10^{-6}$.

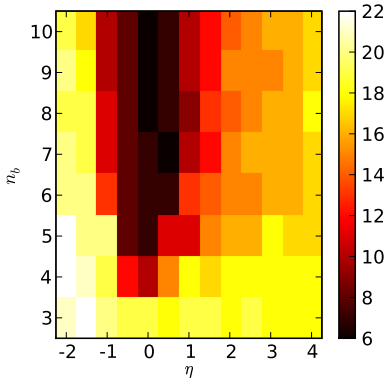

(a) $n_s = 300$
No regularization.

Simulation: q-space Sampling Distribution

Figure: *Condition number* $C = ||\mathbf{M}_{reg}||_\infty ||\mathbf{M}_{reg}^{-1}||_\infty$. The lower C is, the more stable the reconstruction is. Data simulates crossing fibers diffusion signal.
$L = 4, N = 3, n_b \geq 3$. (d) $\lambda_n = 10^{-4}$, $\lambda_l = 10^{-6}$.

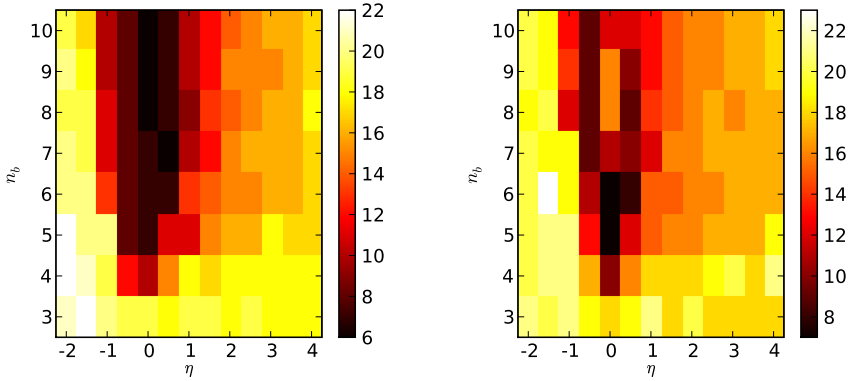

(a) $n_s = 300$
No regularization.

(b) $n_s = 200$
No regularization.

Simulation: q-space Sampling Distribution

Figure: *Condition number* $C = ||\mathbf{M}_{reg}||_\infty ||\mathbf{M}_{reg}^{-1}||_\infty$. The lower C is, the more stable the reconstruction is. Data simulates crossing fibers diffusion signal.
$L = 4, N = 3, n_b \geq 3$. (d) $\lambda_n = 10^{-4}$, $\lambda_l = 10^{-6}$.

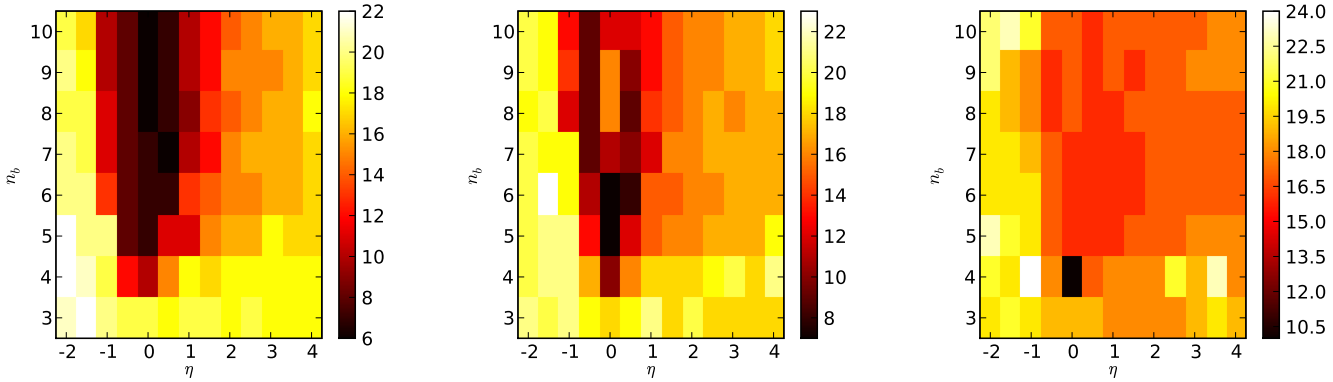

(a) $n_s = 300$
No regularization.

(b) $n_s = 200$
No regularization.

(c) n_s=120
No regularization.

Simulation: q-space Sampling Distribution

Figure: *Condition number* $C = ||\mathbf{M}_{reg}||_\infty ||\mathbf{M}_{reg}^{-1}||_\infty$. The lower C is, the more stable the reconstruction is. Data simulates crossing fibers diffusion signal.
$L = 4, N = 3, n_b \geq 3$. (d) $\lambda_n = 10^{-4}$, $\lambda_l = 10^{-6}$.

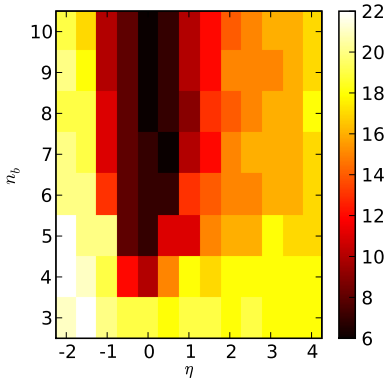

(a) $n_s = 300$
No regularization.

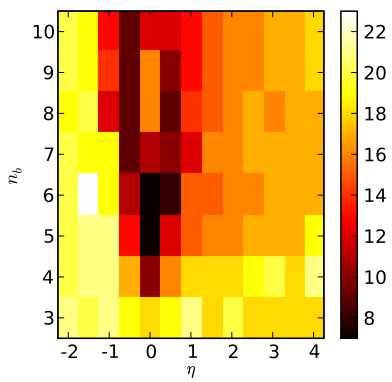

(b) $n_s = 200$
No regularization.

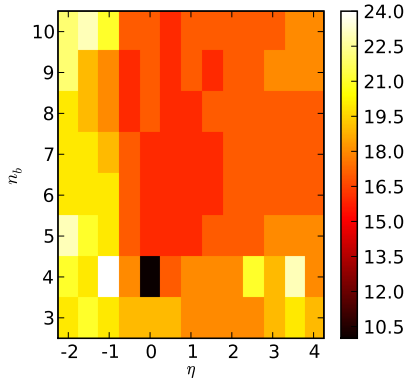

(c) n_s=120
No regularization.

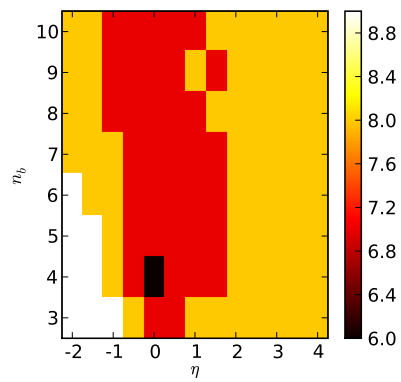

(d) n_s=120.
With regularization.

Simulation: q-space Sampling Distribution

Figure: *Condition number* $C = ||\mathbf{M}_{reg}||_\infty ||\mathbf{M}_{reg}^{-1}||_\infty$. The lower C is, the more stable the reconstruction is. Data simulates crossing fibers diffusion signal.
$L = 4, N = 3, n_b \geq 3$. (d) $\lambda_n = 10^{-4}$, $\lambda_l = 10^{-6}$.

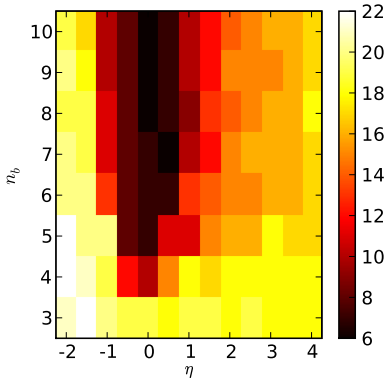

(a) $n_s = 300$
No regularization.

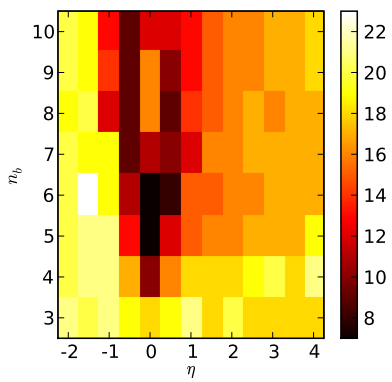

(b) $n_s = 200$
No regularization.

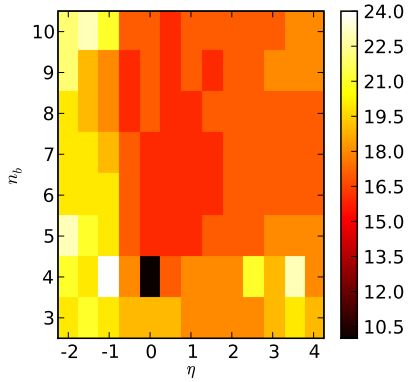

(c) n_s=120
No regularization.

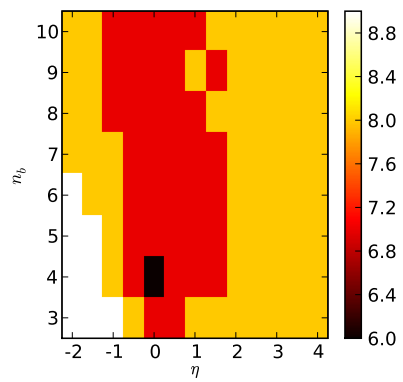

(d) n_s=120.
With regularization.

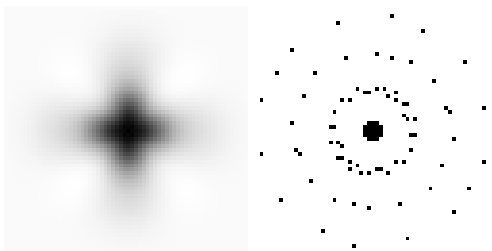

(e) PSNR=40.23 dB

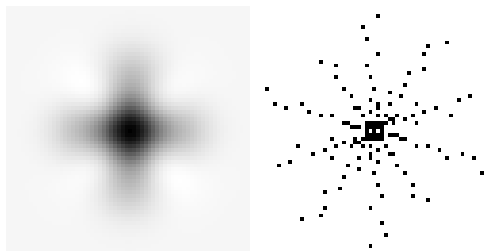

(f) PSNR=39.98 dB

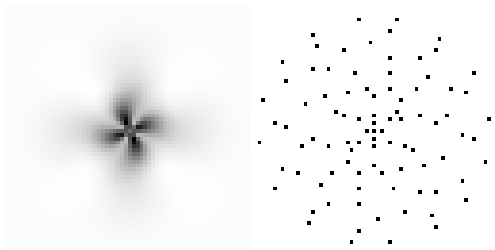

(g) PSNR=27.54 dB

1. Diffusion signal estimation
   - Continuous representation of the signal
2. Extraction of various features of the PDF
   - Algorithm
   - Overview of proposed features
3. Robust extraction of diffusion features
   - Robustness to noise
   - Robustness to q-space sampling

Conclusion: 1-MR signal approximation

	DTI	HARDI	DSI	SPF
Acquisition time	☺	☺	☹	☺
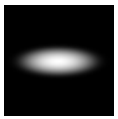 One fibers bundle	☺	☺	☺	☺
Cross fibers bundles	☹	☺	☺	☺
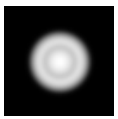 Diffusion-diffraction	☹	☹	☺	☺

Conclusion: 2-PDF features

Features $\mathcal{G}$	Domain $\mathcal{M}$
Moments	–
Return to zero	–
Anisotropy	–
Mean radial diffusion	$\mathbb{R}$
Funk-Radon Transform (FRT)	$\mathcal{S}^2$
Orientation Density Function (ODF)	$\mathcal{S}^2$
Isoradius (ISO)	$\mathcal{S}^2$
Displacement PDF	$\mathbb{R}^3$
Diffusion signal E	$\mathbb{R}^3$

Table: Overview of proposed features $\mathcal{G}$ of the PDF.

Conclusion: 3-Robustness

Robustness to noise

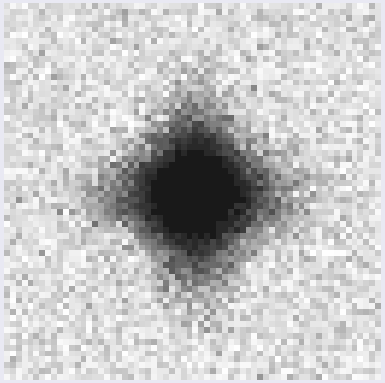

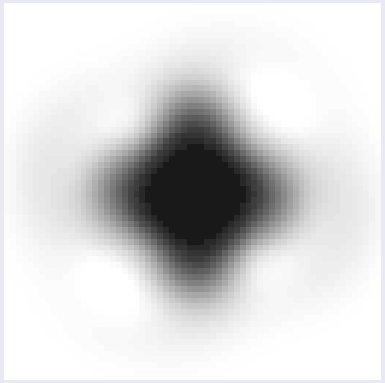

Robustness to sampling distribution

	$\eta = -2$	$\eta = -1$	$\eta = 0$	$\eta = 1$	$\eta = 2$	$\eta = 3$
$n_b = 2$	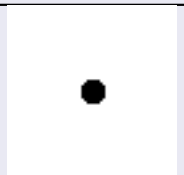	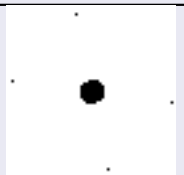	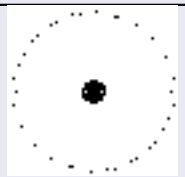	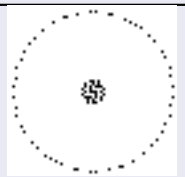	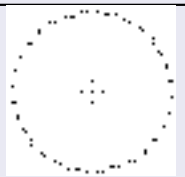	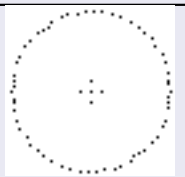
$n_b = 5$	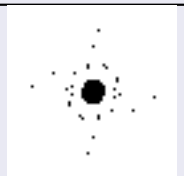	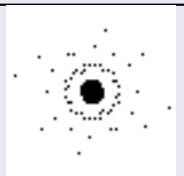	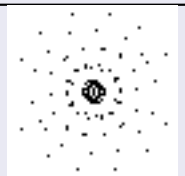	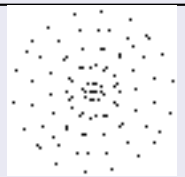	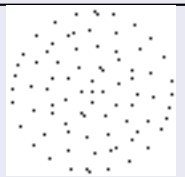	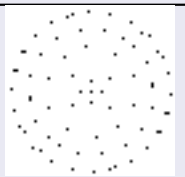

Final slide

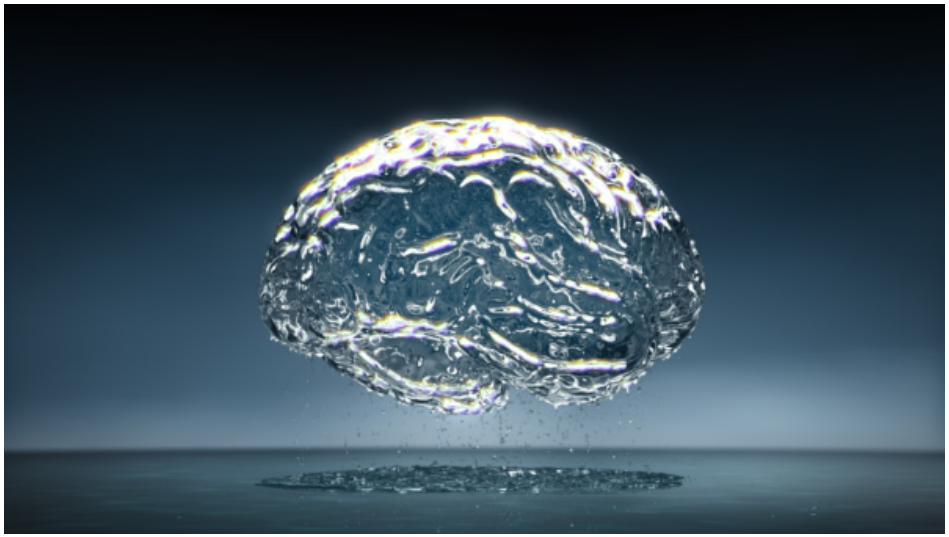

Thank you for your attention.

Radial eigenfunctions

Proposition

We propose the use of Gauss-Laguerre functions:

$$R_n(||\mathbf{q}||) = \left[\frac{2}{\gamma^{3/2}}\frac{n!}{\Gamma(n+3/2)}\right]^{1/2} \exp\left(-\frac{||\mathbf{q}||^2}{2\gamma}\right) L_n^{1/2}\left(\frac{||\mathbf{q}||^2}{\gamma}\right), \quad (10)$$

where γ is the scale factor.
Let L_n^k be a generalized Laguerre polynomial:

$$L_n^k = \frac{1}{n!}\sum_{i=0}^{n}\frac{n!}{i!}\binom{k+n}{n-i}(-x)^i \quad (11)$$

The Gauss attenuation comes from the normalization of these polynomials:

$$\int_0^\infty e^{-k}x^k L_n^k(x)L_{n'}^k(x)dx = \frac{(n+k)!}{n!}\delta_{nn'} \quad (12)$$

Results: radial truncation order

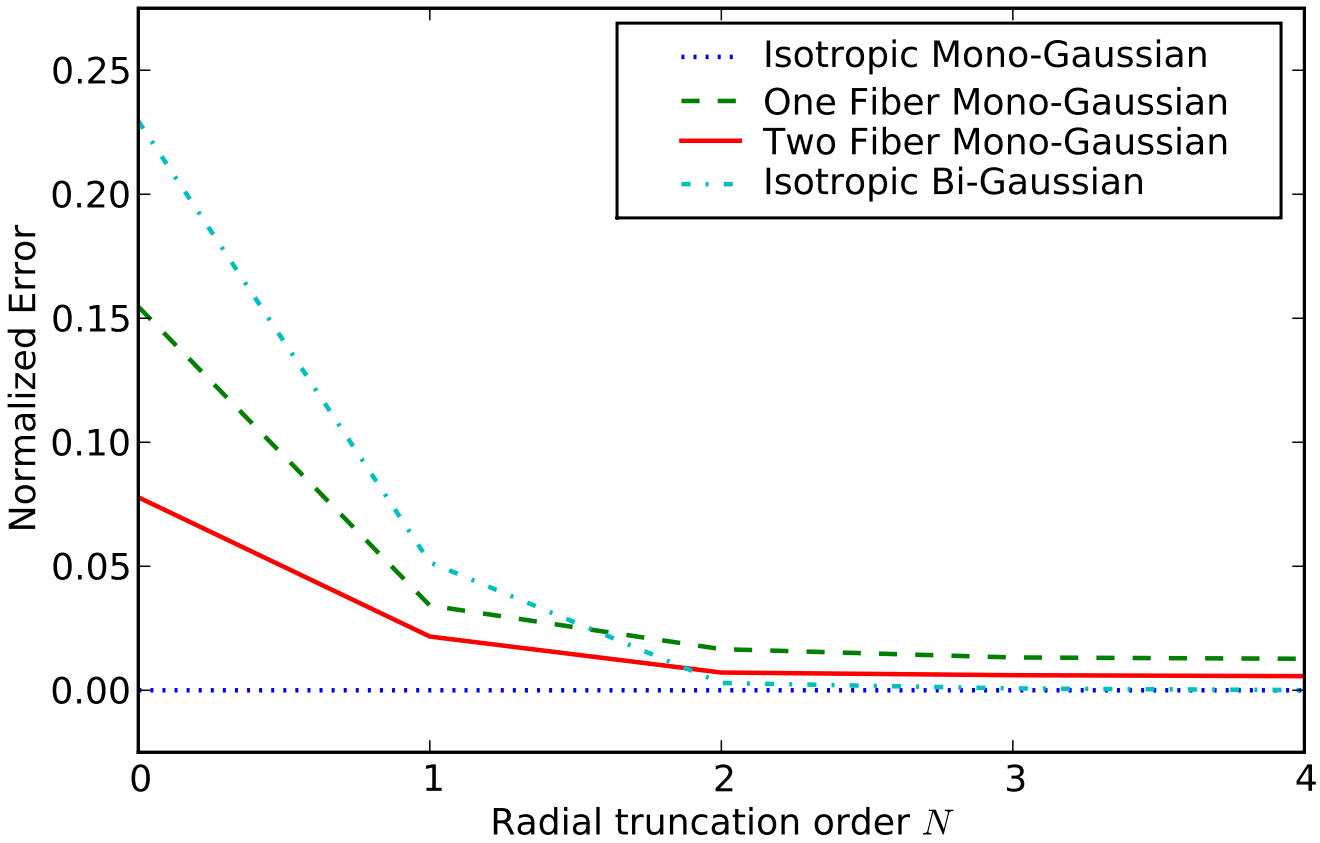

Figure: Power spectrum along with increasing radial truncation order.

Runge-Kutta

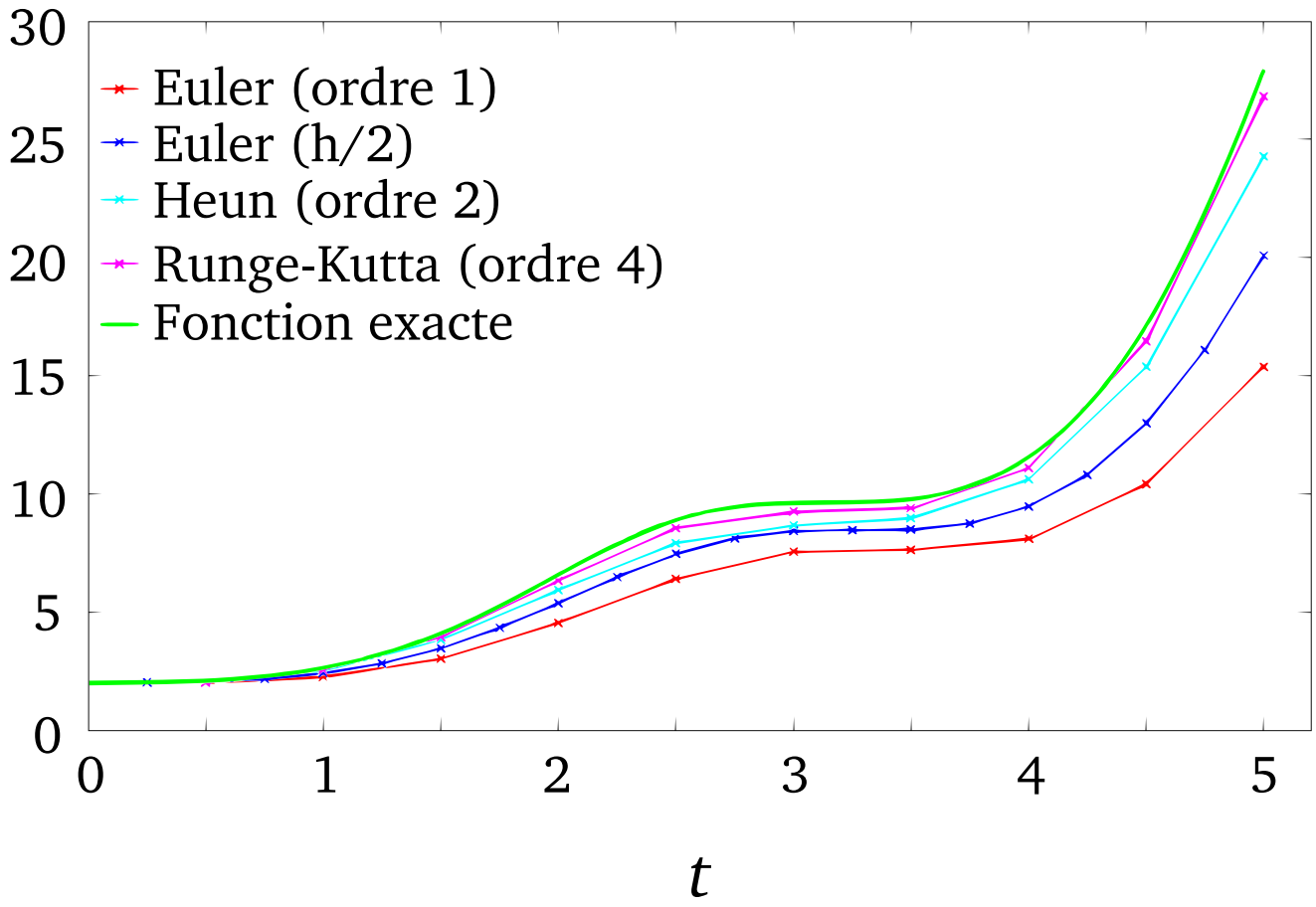

Figure: Comparaison de méthodes de suivi de fibres $\mathcal{C}$, définie par $y' = \sin(t)^2 * y$.

PDE initialization

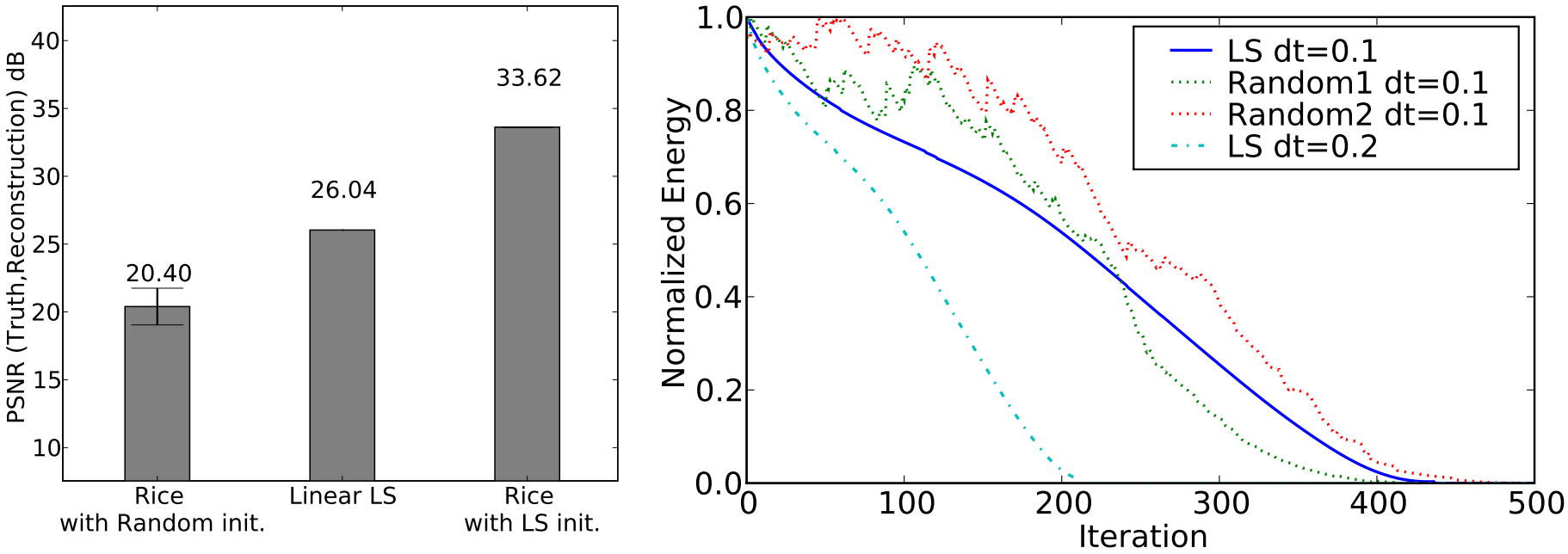

Figure: Influence de l'initialisation A_0 sur la convergence de la méthode de descente du gradient. Les données sont bruités telles que PSNR(Originale,Bruité)=19.5 dB.

Regularization functions φ

Nom de la fonction	$s \to \varphi(s)$, $s \in \mathbb{R}$
Tikhonov	s^2
Perona-Malik	$1 - \exp(-s^2/\kappa^2)$
Surfaces minimales	$2\sqrt{1+s^2} - 2$
German-McClure	$s^2/(1+s^2)$
Variation totale	s
Green	$2\log(\cosh(s))$

Table: Liste de quelques fonctions de régularisation φ possibles. Tableau adapté de [Tschumperlé02].

Noise histogram

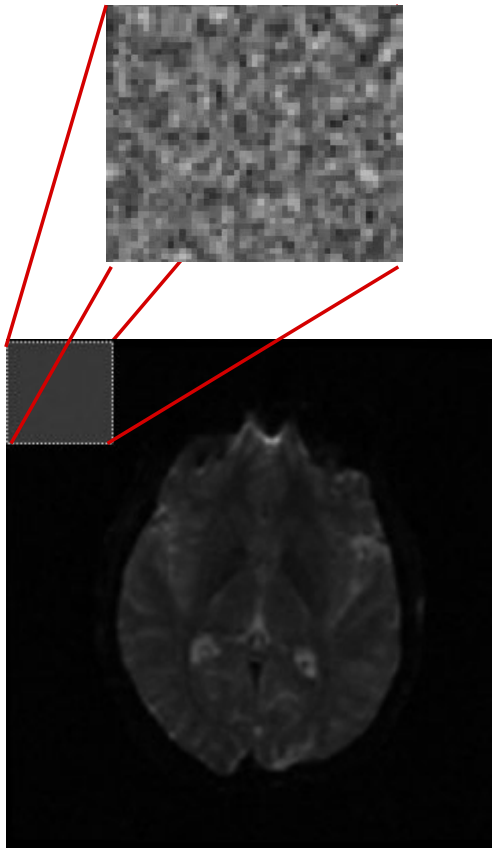

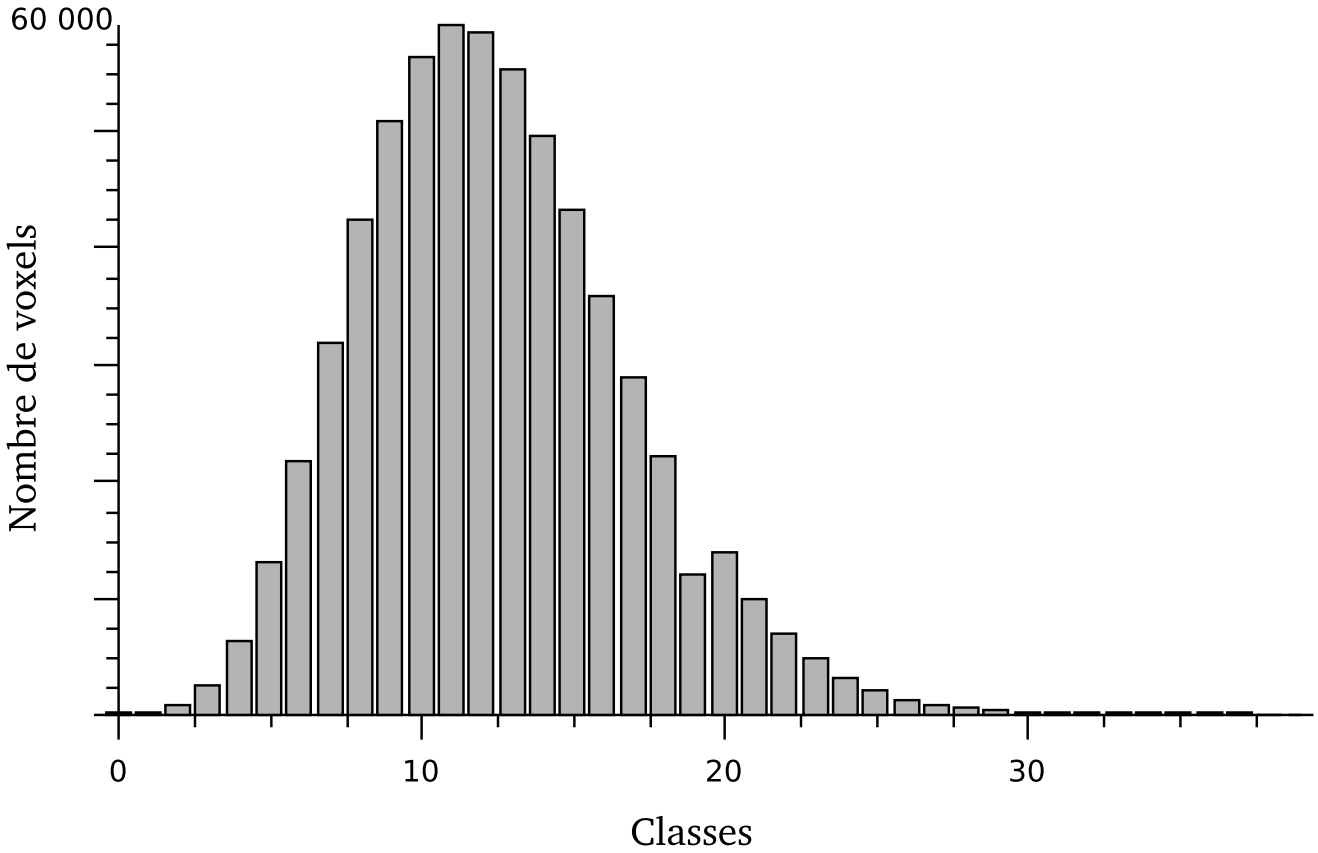

Figure: Histogramme du bruit dans les images d'IRM de diffusion.

Execution time

Domaine $\mathcal{M}$	$\mathbb{R}$	$\mathbb{R}^3$	$\mathcal{S}^2$
Tps d'exécution	9 s	$\sim$ 360 h	22 s

Table: Temps d'exécution de la construction d'une caractéristique dans l'ensemble de son domaine $\{h^{\mathbf{k}}_{nlm}, \forall \mathbf{k} \in \mathcal{M}\}$.

Nombre de valeurs de ζ	1	16	224
Tps d'exécution	12 s	21 s	5 min

Table: Temps d'exécution pour l'estimation du signal de diffusion dans la base SPF.

Domaine $\mathcal{M}$	$\mathbb{R}$	$\mathbb{R}^3$	$\mathcal{S}^2$
Tps d'exécution	5 s	21 s	9 s

Table: Temps d'exécution pour l'extraction d'une caractéristique.

Return to zero probability

Scalar feature of free / restriction diffusion.

$$\mathcal{G} = P(0) = \int_{\mathbf{p}\in\mathbb{R}^3} P(\mathbf{p})H(\mathbf{p})\mathrm{d}\mathbf{p} \quad \text{avec} \quad H(\mathbf{p}) = \delta(\mathbf{p})$$

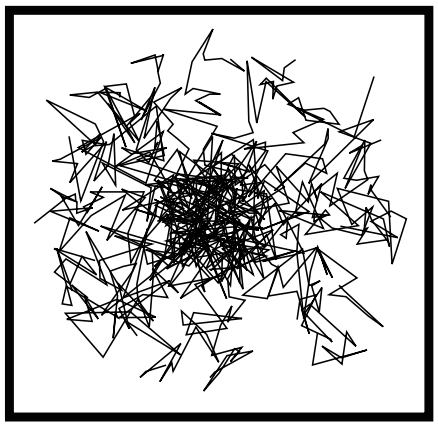

(a)

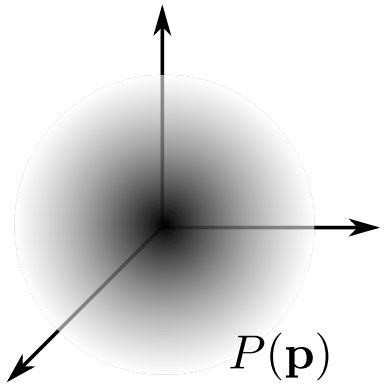

(b)

Return to zero probability

Scalar feature of free / restriction diffusion.

$$\mathcal{G} = P(0) = \int_{\mathbf{p}\in\mathbb{R}^3} P(\mathbf{p})H(\mathbf{p})\mathrm{d}\mathbf{p} \quad \text{avec} \quad H(\mathbf{p}) = \delta(\mathbf{p})$$

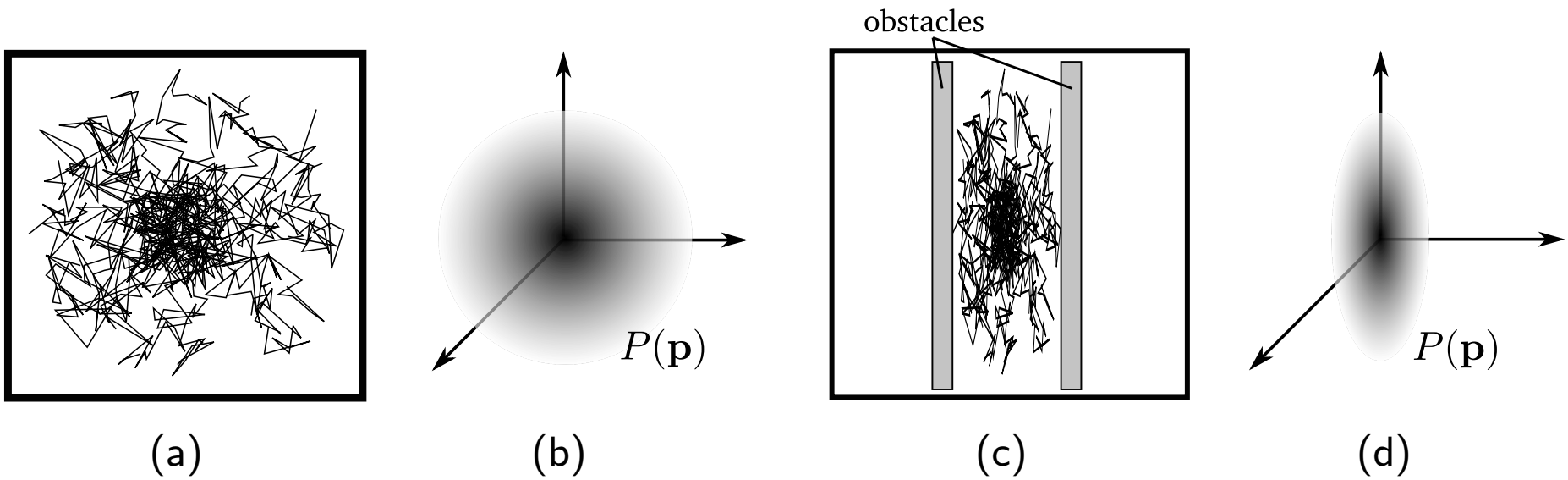

Figure: Free diffusion (a-b) and restricted (c-d) in a voxel.

Average radial diffusion

Radial diffusion robust to anisotropy.

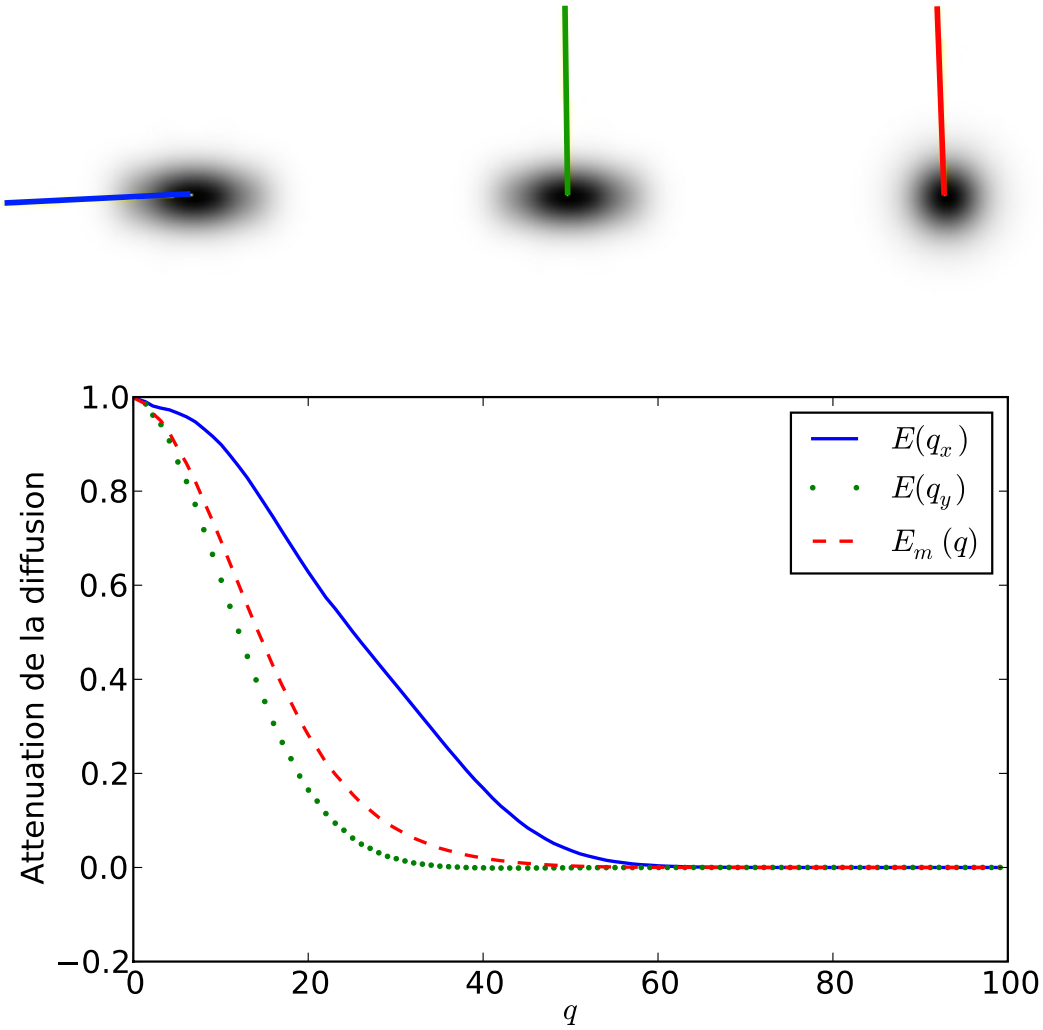

Isoradius

Feature which reproduces the results of the DOT method [Özarslan06].

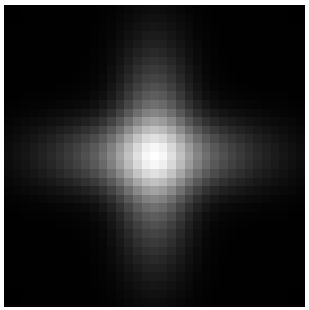

(a) PDF

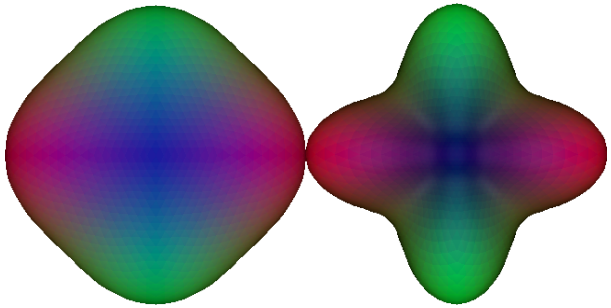

(b) DOT

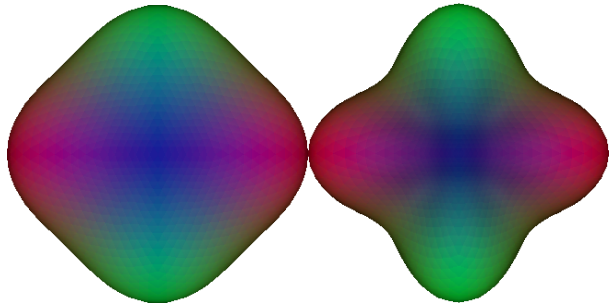

(c) $\mathcal{G} = \text{ISO}$